

# Results from measurements on the PV-VENT systems at Sundevedsgade/Tøndergade



# **Results from measurements on the PV-VENT systems at Sundevedsgade/Tøndergade**

**Søren Østergaard Jensen**

**Solar Energy Centre Denmark  
Danish Technological Institute**

**April 2001**

## Preface

The present report concludes together with (Jensen, 2001) Solar Energy Centre Denmark's (Danish Technological Institute) measuring work in the PV-VENT project. The measuring project was partly financed by EU via the JOULE project "PV-VENT – Low cost energy efficient PV-ventilation in retrofit housing", contract no. JOR3-CT97-0160 and partly by the Danish Ministry of Environment and Energy via the project "PV-VENT", journal no. 51181/97-0021.

The project group behind the project was:

Cenergia Energy Consultants, DK  
Fortum Energy (former NESTE-NAPS), SF  
AirVex Danmark (former Temovex Denmark), DK  
FSB, DK  
Danish Technological Institute, DK  
Ecofys, NL  
PA-Energy, DK  
NTNU, N  
Copenhagen Energy, DK

The following persons have participated in the measuring project:

Søren Østergaard Jensen. M.Sc., Solar Energy Centre Denmark  
William Otto, laboratory technician, Solar Energy Centre Denmark  
Ole Larsen, laboratory technician, Solar Energy Centre Denmark  
Lars Molnit, student (B.Sc.), Solar Energy Centre Denmark  
Bertel Jensen, B.Sc., Solar Energy Centre Denmark  
Ulrik Mehr, M.Sc., Solar Energy Centre Denmark  
Hans Olsen. B.Sc., Ventilation and Environment, Technological Institute of Denmark  
Jens Heidelbach Andersen, B.Sc., Cenergia Energy Consultants  
Lisbet Michaelsen, B.Sc., Cenergia Energy Consultants

Results from measurements on the PV-Vent systems at Sundevedsgade/Tøndergade  
1<sup>st</sup> printing, 1<sup>st</sup> edition  
© Danish Technological Institute  
Energy division

ISBN: 87-7756-614-9  
ISSN: 1600-3780

## List of content

1.	Introduction .....	3
1.1.	The PV-VENT systems .....	6
1.1.1.	Control of the systems .....	13
1.1.2.	PV-mixer .....	15
2.	Measuring system .....	17
2.1.	Air temperature measurements in the solar wall .....	17
2.2.	Weather measurements .....	19
2.3.	Temperature and flow measurements in the ventilation system .....	19
2.4.	Electrical measurements .....	20
2.5.	Data collection .....	23
2.6.	Treatment of measured data .....	24
3.	Measurements .....	25
3.1.	Measurements from week 5 and 6, 2001 .....	25
3.1.1.	Thermal part of the system .....	25
3.1.2.	PV-part of the system .....	27
3.2.	Measurements from specific weeks .....	38
3.2.1.	Air flows .....	38
3.2.2.	PV-mixer .....	38
3.3.	Calculations based on the measurements and more general conclusions .....	40
3.3.1.	The efficiency of the air to air heat exchanger .....	40
3.3.2.	Fan power .....	51
3.3.3.	Temperatures in the solar wall .....	52
3.3.4.	The PV-mixer .....	57
3.4.	Obtained and obtainable savings of the system .....	60
3.4.1.	Obtained savings .....	60
3.4.2.	Obtainable savings .....	64
4.	Conclusions .....	70
4.1.	Aims of the PV-VENT project .....	70
4.2.	Results from the PV-VENT project .....	70
4.2.1.	Architectural results .....	70
4.2.2.	Pre-heating of fresh air – cooling of PV-panels .....	71
4.2.3.	Air to air heat exchanger .....	72
4.2.4.	Low fan power .....	72
4.2.5.	Direct coupling of PV-panels and fans .....	72
4.2.6.	Total systems .....	73
4.2.7.	General conclusions .....	73
5.	References .....	74
Appendix A	Data sheets for the heat exchangers and fans .....	75
Appendix B	Data sheets for the PV-panels .....	78

# 1. Introduction

The objective of the project was to research, develop and test low cost, high efficiency PV-powered ventilation systems for retrofitting of apartment blocks. Systems where the fans are powered directly by the PV-panels and where the waste heat from the PV-panels is utilized to pre-heat fresh air to the apartments.

The present report describes the obtained experience from measurements on the PV-VENT systems installed in an apartment building in the area Vesterbro of Copenhagen, Denmark. The building is situated Sundevedsgade 14/Tøndergade 1. The building is part of the Hedebygade block – a site plan of this block is shown in figure 1.1. The Hedebygade block has during the late 90'ies been exposed to a major renovation project including extensive utilisation of solar energy.

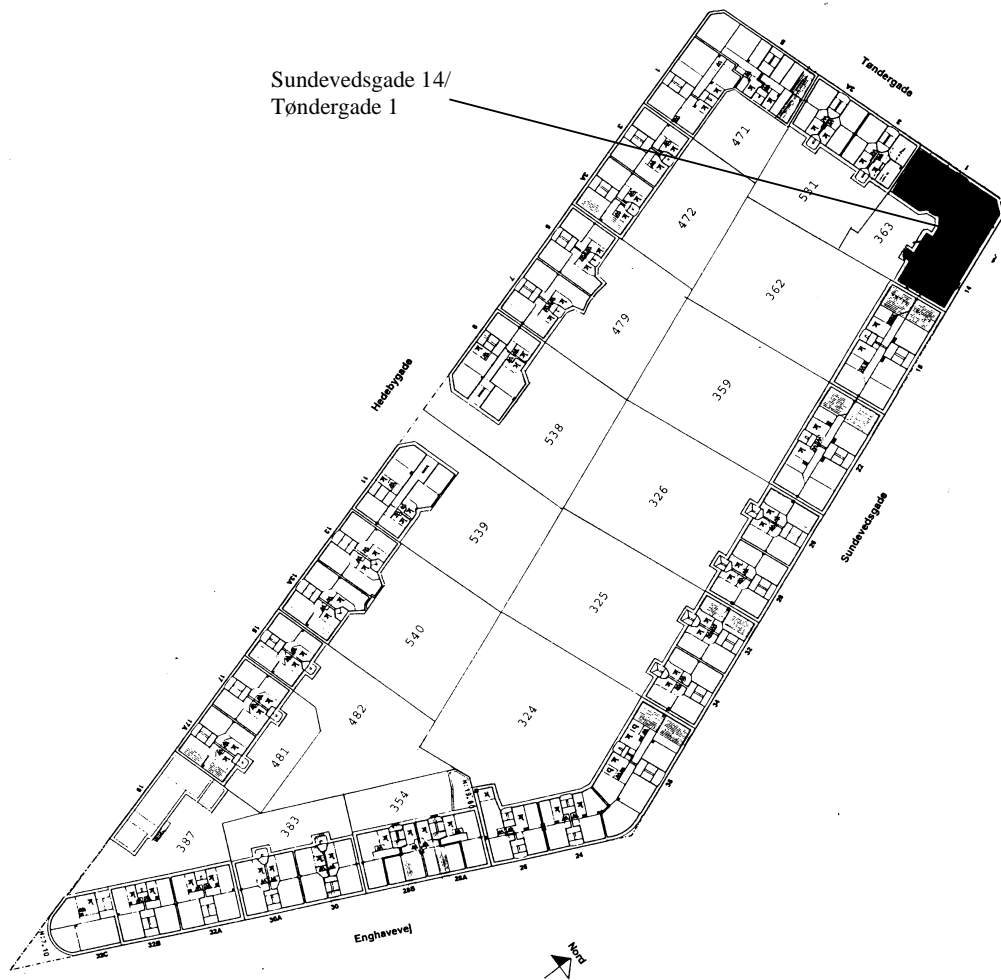


Figure 1.1. The site plan for the Hedebygade block and the location of Sundevedsgade 14/Tøndergade 1.

The five-storied building was erected in 1884 and is typical for that period. The building contains 20 apartments and has a net floor area of 1137 m<sup>2</sup>. Figure 1.2 shows the facades of the building facing the streets after the renovation. The original appearance of the facade has not been changed.



Figure 1.2. The facades of the building after the renovation.

The dwellings had before the renovation no bathrooms or central heating, and the piping system for domestic water and the sewer system were of a poor quality. The flats were poorly insulated and the heating system was old-fashioned – e.g. wood-burning stoves, electric heating panels or gas heating furnaces. The windows were not tight and there was no ventilation system in the building. A renovation of the building was thus badly needed.

The renovation contained the following items:

- total renovation of the interior including new kitchens and bathrooms,
- new piping and plumbing,
- low-energy windows,
- insulation – especially against the attic and roof,
- new heating system with radiators,
- sun spaces in 8 of the dwellings,
- balanced ventilation system including the PV-VENT systems with solar walls,
- solar air heating system for pre-heating domestic hot water and space heating

Figure 1.3 shows the facades of the building facing the courtyard after the renovation. The appearance of these facades is changed considerably compared to the facades facing the streets. The photo shows the solar walls with PV-panels and the sun spaces.



Figure 1.3. The facades facing the courtyard after renovation.

A more detailed description of the ideas behind the renovation may be found in (Lien and Hestness, 1999 and Cenergia, 1999). Here will only the PV-VENT systems briefly be described.

## 1.1. The PV-VENT systems

Figure 1.4 gives a schematically overview of the ventilation system in the building.

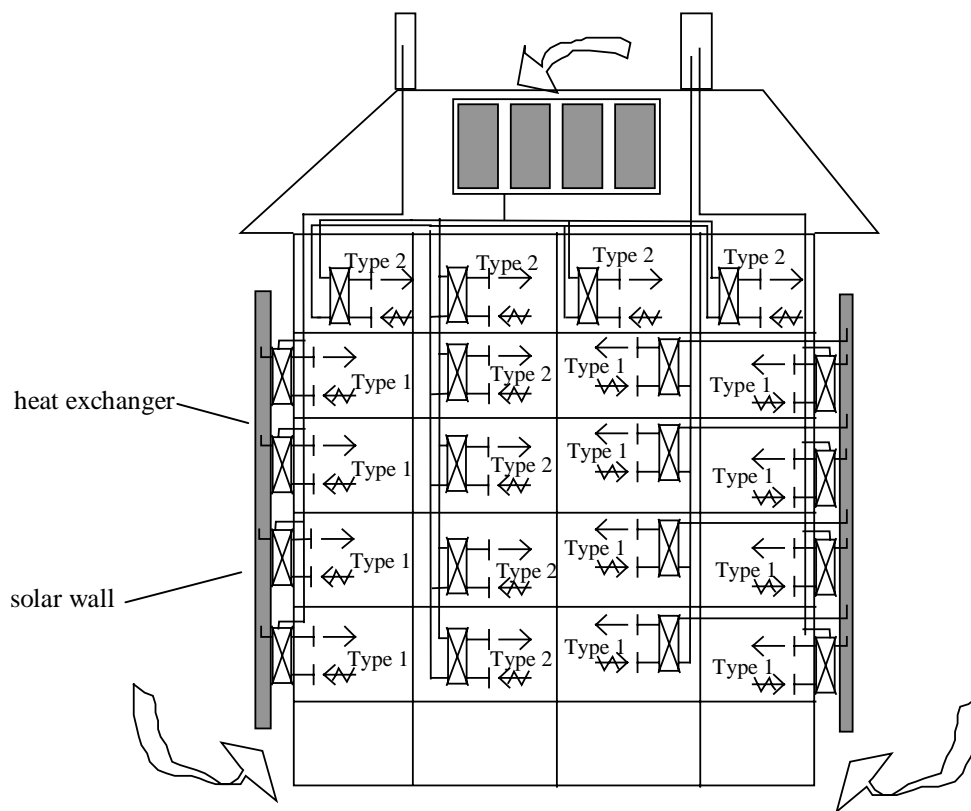


Figure 1.4. Principle of the ventilation system in the building.

The ventilation system consists basically of two types of ventilation systems:

Type 1: Individual PV-VENT systems with a heat exchanger JoVex 175 and fans type 175 (56 V dc) (developed by AirVex as part of the project (Jensen and Pedersen, 1999) and appendix A) in each apartment are installed in 12 dwellings: the 8 lowest dwellings in Sundevedsgade 14 and the 4 lowest apartment to the right in Tøndergade 1. The heat exchangers are located on the outside of the exterior wall behind the glazing of the solar walls – the spacing between the exterior walls and the cover of the solar walls is 40 cm. The area of the solar wall per dwelling is  $3 \cdot 1 \text{ m}^2$  in Tøndergade 1 and  $3 \cdot 1.25 \text{ m}^2$  in Sundevedsgade 14 (height  $\cdot$  width). In Sundevedsgade 14 two heat exchangers are located site by site at each floor (see figure 1.8), while in Tøndergade 1 only one heat exchanger is located at each floor (see figure 1.9). The fresh air to the heat exchangers is taken from the solar wall. The fresh air is thus pre-heated by the solar wall/excess heat from the PV-panels and by the heat loss through the walls of the building. The fresh air to the solar wall is drawn in through a grill at the bottom of the solar wall as shown in figure 1.4-5. The cover of the solar wall consist partly of the PV-panels and partly of opal glazing (as seen in figure 1.3) in order to hide the heat exchangers behind the glazing and still let solar radiation into the solar walls. During warm days the solar walls may be vented by opening dampers in the solar walls.





Figure 1.5. The inlet to one of the solar walls.

Figures 1.6-7 show drawings of the solar walls and the sun spaces, while figures 1.8-9 show the location of the heat exchangers in the solar walls. Figure 1.10 shows a photo of one of the heat exchangers in the solar wall and an entrance door to one of the solar walls. Figure 1.11 shows the floor plans before and after the renovation. The total ventilation system of Tøndergade 1 to the right is shown in figure 2.5.

The ventilation system consists of efficient counter flow heat exchangers and DC fans with a very low electricity demand developed within the project by AirVex (Jensen and Pedersen, 1999) (see also appendix A).

The PV-array for each dwelling consists of three PV-panels of two different sizes (A1 and A2) in the front of the solar walls as shown in figures 1.3, 1.12 and Appendix B and two other sizes (B1 and B2) in the gable of the solar wall on Sundevedsgade 14 as seen in figure 1.13 (Leppänen, 2000). The dimensions of the panels are A1: 490 x 723 mm<sup>2</sup>, A2: 490 x 1122 mm<sup>2</sup>, B1: 907 x 723 mm<sup>2</sup> and B2: 907 x 1122 mm<sup>2</sup> (see appendix B). The total peak power per three panels (ie per PV-mixer – see later) is either 121 or 242 W<sub>p</sub>. The polycrystalline (c-Si) cells of the PV-panels are located with an spacing of 3-4 mm with a translucent lamination film in-between the cells allowing solar radiation to penetrate into the solar wall. The PV-panels were developed by Fortum Energy as part of the project (Leppänen, 1999). The electricity produced by the PV- panels is directly used to power the fans. However, the PV-panels are not able to power the fans all 24 hours of the day, so a so-called PV-mixer is installed to mix PV-power with grid power in order to maintain the necessary power level for the fans. The PV-mixer is further described in section 1.1.2.

Three of the top floor apartments are not as shown in figure 1.4 connected to the solar air collector at the roof but obtain the fresh air from the solar walls. Apart from this the ventilation systems are type 2 as described below. The three apartments are: the two top floor dwellings in Sundevedsgade 14 and the top floor to the right in Tøndergade 1.



Figure 1.6. Drawing of the solar wall and sun spaces at Sundevedsgade 14.



Figure 1.7. Drawing of the solar wall and sun spaces at Tøndergade 1.

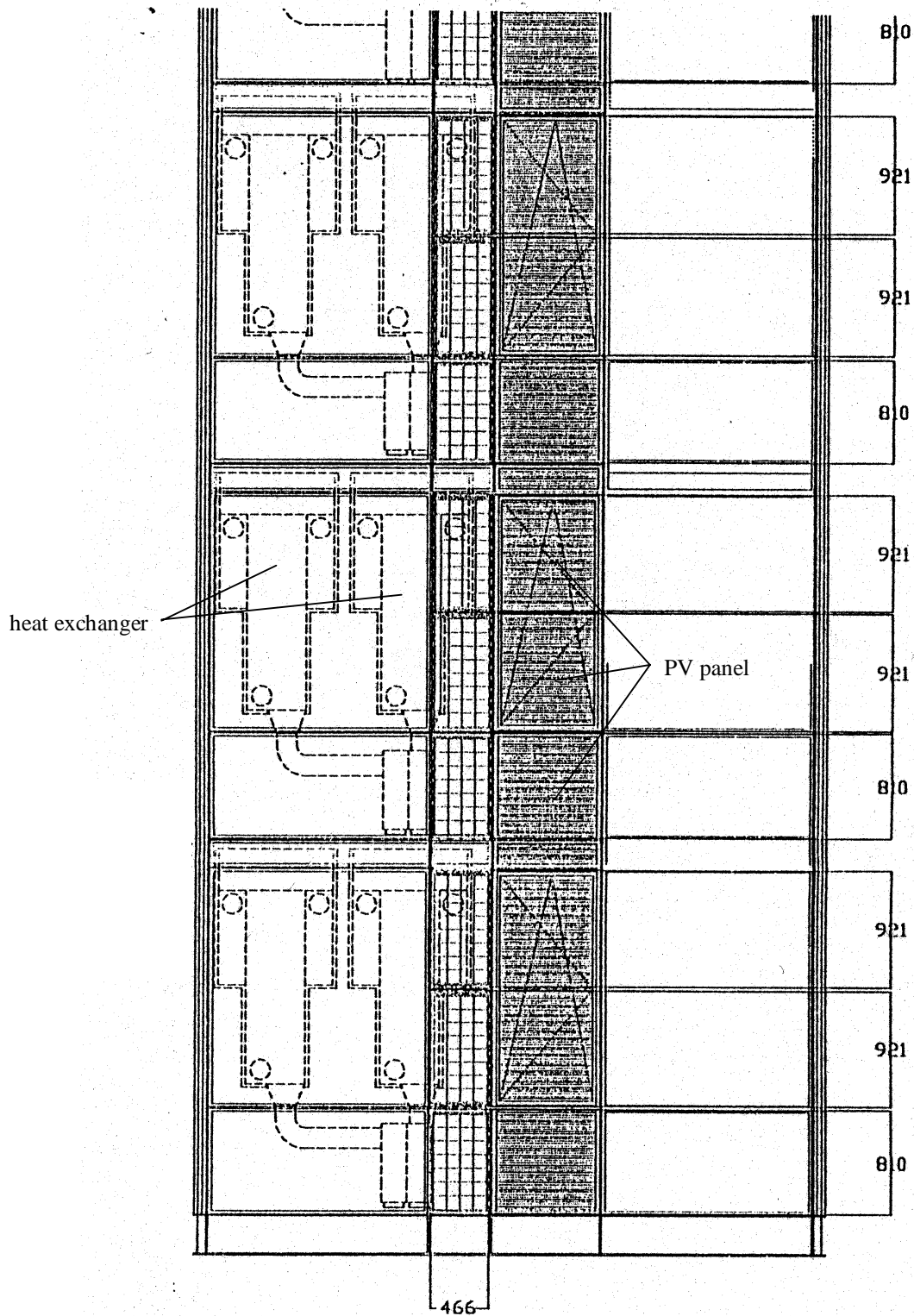


Figure 1.8. Location of the heat exchangers in the solar wall at Sundevedsgade 14.

The solar wall of Sundevedsgade 14 has mainly a westerly orientation ( $20^\circ$  from west towards south), while the solar wall of Tøndergade 1 has an orientation of  $20^\circ$  from south towards east.

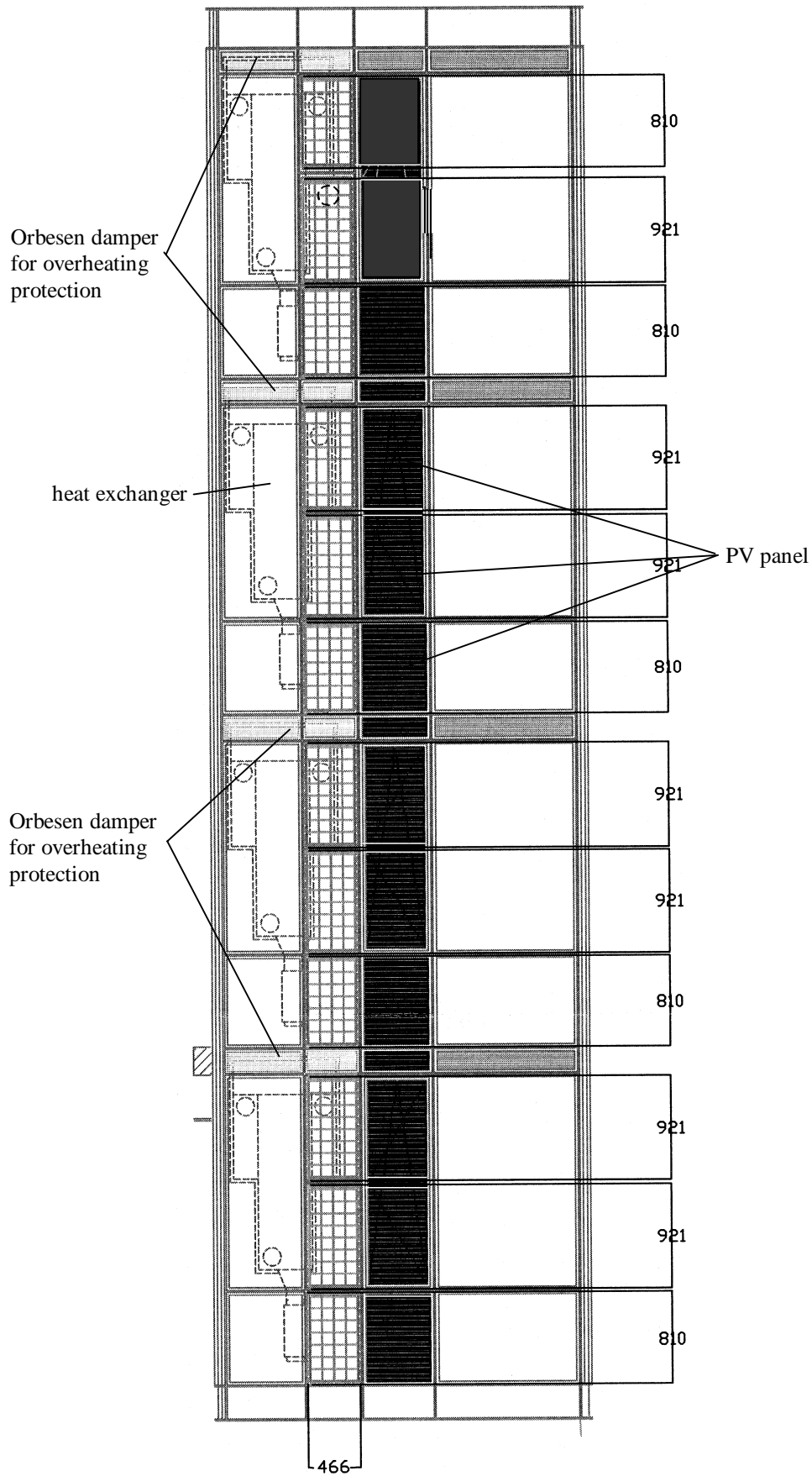


Figure 1.9. Location of the heat exchangers in the solar wall at Tøndergade 1.

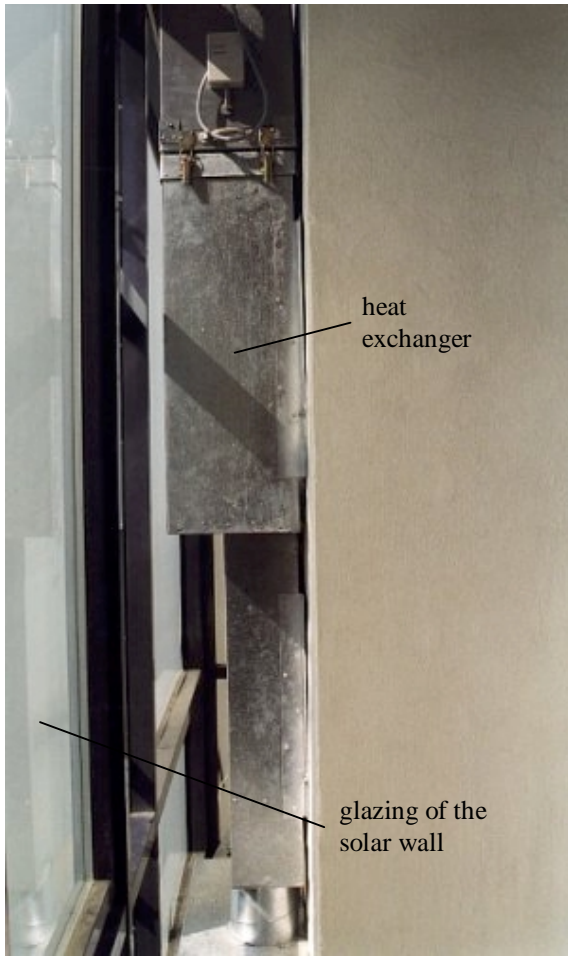


Figure 1.10. Photo of one of the heat exchangers in the solar walls and an entrance door to a solar wall.

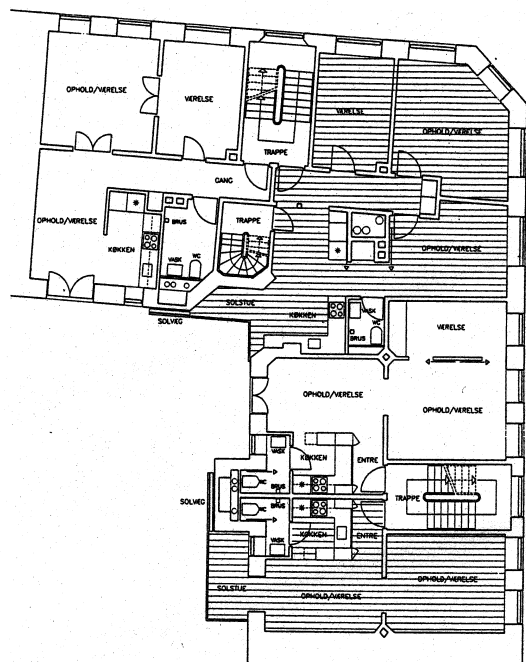
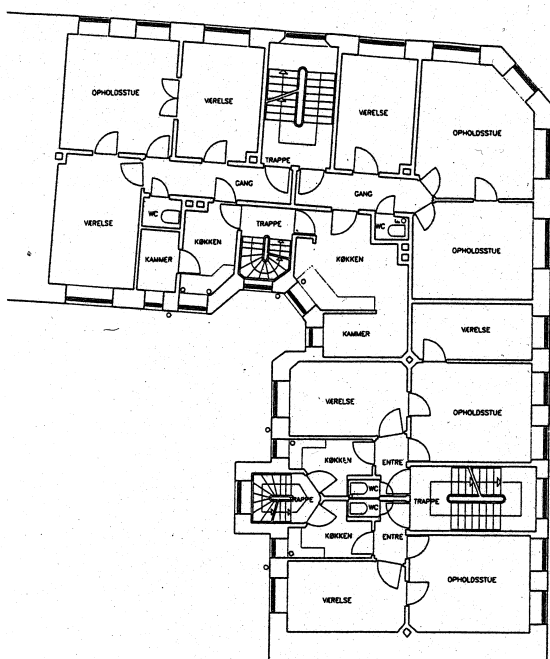


Figure 1.11. Typical floor plan before (to the left) and after (to the right) the renovation.

Damper for over-  
heating protection



Figure 1.12. Close up of the PV-panels for one dwelling.

Type 2: The ventilation systems of the remaining 8 dwellings have also individual heat exchangers JoVex H300 and fans type 175 (56 V dc) from AirVex (Jensen and Pedersen, 1999) – see also appendix A. These system is not part of the PV-VENT project. The efficiency of the heat exchanger in the type 2 systems has been evaluated in the project at Lundebjerg (Jensen, 2001). The heat exchangers are situated inside the dwellings except for the top floor apartments where the heat exchangers are located in the attic. These three dwellings are as earlier mentioned connected to the solar walls.

Solar air collector: A solar air collector of 19 m<sup>2</sup> is located on the roof of Tøndergade 1 as seen in figure 1.13. The solar air collector covers via an air to water heat exchanger part of the domestic hot water and space heating of the building.

This system is nor part of the PV-VENT project.



Figure 1.13. The grid connected PV-panels on the south gable of the solar wall on Sundevedsgade 14 and the solar air collector array on the roof of Tøndergade 1.

### 1.1.1. Control of the systems

The occupants of the apartments are able to control their ventilation systems via a control panel located in the dwelling – figure 1.14 shows a photo of the control panel. According to the Danish building code the flow rate of exhaust air from a dwelling should be 126 m<sup>3</sup>/h. The tenants may, however, choose between normal, max and min flow rate and between winter and summer mode as shown in table 1.1. Table 1.1 shows the intended/pre-set air flow rates in the apartments. The flow rate of exhaust air should always be higher than the flow rate of fresh air in order to create a small under pressure in the apartments, which will prevent humid air in being forced into the constructions. It is as shown in table 1.1 possible to run the ventilation systems as purely exhaust ventilation (summer mode) in order to prevent pre-heated air from the solar wall to enter the dwellings during periods with no heat demand.

The max power consumption of the two fans per dwelling is 45 W each.



Figure 1.14. The control panel from which the occupants of the dwellings may control their ventilation systems.

Mode	Winter		Summer	
	Exhaust m <sup>3</sup> /h	Fresh air m <sup>3</sup> /h	Exhaust m <sup>3</sup> /h	Fresh air m <sup>3</sup> /h
Max	198	116	198	0
Normal	126	116	126	0
Min	45-85*	40-77*	45-85*	0

Table 1.1. Ventilation modes, which can be chosen via the control panel in the apartments.  
\* the minimum ventilation is not identical for the apartments.

The systems can during warm periods be run in summer mode which means that no air will be drawn from the solar walls to the dwellings. The air gap behind the PV-panels may, therefore, overheat which will reduce the electricity production of the PV-panels. So in order to cool the PV-panels during these periods Orbesen dampers driven by wax motors are installed in the top of each of the two solar walls. One damper is further installed at each floor as seen in figure 1.3, 1.9 and 1.12. The dampers start to open at a temperature of 23°C and is fully open at a temperature of 27°C – the dampers starts to close again at a temperature of 24°C and are closed a 21°C. When the dampers start to open the PV-panels will be cooled by a buoyancy driven air stream in the air gab.



### 1.1.2. PV-mixer

The dc fans of the ventilation systems are directly connected to the PV-panels. However, the PV-panels are not during the night and during overcast conditions able to run the fans at the required speed. A so-called PV-mixer has, therefore, been developed as part of the project. The function of the PV-mixer is to ensure that as much electricity from the PV-panels as possible is used for running the fans. If the PV-power is too low to run the fans the PV-mixer top up with electricity from the grid via a transformer.

The development of the PV-mixer was unfortunately delayed. The first company chosen for the development came up with a solution as late as in January 2000. The Danish Technological Institute obtained one sample for evaluation (Mehr, 2000). It was judged that the principle chosen for controlling the power from the PV-panels and the grid didn't give enough credit to the PV-panels leading to too high power consumption from the grid even if enough power could be delivered by the PV-panels. The PV-mixers was further of a very poor quality. The soldering of the components looked to be made by a plumber rather than by a electrotechnician.

The PV-mixer was, therefore, rejected and a new firm for developing the PV-mixer was found. They came up with a new design in August 2000 which also was evaluated and further tested by the Danish Technological Institute (Jensen, 2000). This concept was approved. The test results are shown in tables 1.2-4.

Supply from PV and grid		test 1	test 2	test 3	unit
Measured	U pv	12.11	12.20	48.10	Volt
	I pv	5.00	8.00	3.50	Ampere
	U grid	54.60	54.70	55.20	Volt
	I grid	4.10	3.55	2.35	Ampere
	U consumption fans	53.40	53.70	54.20	Volt
	I consumption fans	5.10	5.15	5.10	Ampere
Calculated	P1 pv + grid	284.4	291.8	298.1	Watt
	P2 consumption fans	272.3	276.6	276.4	Watt
	Efficiency	95.8	94.8	92.7	%
	PV ratio	22.2	35.3	60.9	%

Table 1.2. Results from tests of the PV-mixer in mixed mode.

Only supply from grid		test 1	unit
Measured	U grid	56.10	Volt
	I grid	5.20	Ampere
	U consumption fans	54.90	Volt
	I consumption fans	5.10	Ampere
Calculated	P1 grid	291.7	Watt
	P2 consumption fans	280.0	Watt
	Efficiency	96.0	%

Table 1.3. Results from tests of the PV-mixer in grid mode.

Only supply from PV		test 1	test 2	test 3	unit
Measured	U pv	12.24	12.30	47.90	Volt
	I pv	7.97	10.05	7.08	Ampere
	U consumption fans	25.35	27.80	57.80	Volt
	I consumption fans	3.10	3.49	5.30	Ampere
Calculated	P1 pv	97.6	123.6	339.1	Watt
	P2 consumption fans	78.6	97.0	306.3	Watt
	Efficiency	80.6	78.5	90.3	%

Table 1.4. Results from tests of the PV-mixer in PV mode.

The tests showed an efficiency of the PV-mixer of between 93 and 96% for mixed PV and grid mode, which is in the same area of the efficiency of inverters. In purely grid mode the efficiency of the PV-mixer is 96% which is the max efficiency that can be expected for this concept based on the switch mode technology. For the purely PV mode the efficiency lay in the tests between 81 and 90% depending on the power needed for the fans. Table 1.4 indicates that the efficiency of the PV-mixer in only PV mode may get lower at lower fan power than shown in table 1.4.

The first PV-mixers of the final concept were delivered and installed in December 2000.

## 2. Measuring system

The PV-VENT system in Sundevedsgade/Tøndergade consists of several ventilation systems where most are more or less identical consisting of individual heat exchanger units for each dwelling located in common solar walls. Main difference is the orientation of the solar wall and if there is one or two heat exchanger units per floor in the solar wall.

For this reason measurements have only been performed for one of the solar walls and detailed measurements for one apartment.

The chosen solar wall is the most south facing solar wall located on the wall of Tøndergade 1. The apartment for detailed measurements was chosen to be the dwelling on the fourth floor to the right as pointed out on figure 2.1.



Figure 2.1. The solar wall and apartment where the measurements have been carried out on.

### 2.1. Temperature measurements in the solar wall

Figure 2.2 shows the location of the air temperature sensors in the solar wall together with the location of the sensor for surface temperature on one of the PV-panels. Figure 2.2 further shows the location of the sensors for measuring the solar radiation and ambient temperature.

The used air temperature sensors were PT100 class A sensors. The air temperature sensors in the solar wall were located at the fresh air inlet to the heat exchangers as shown in figure 2.3. The sensors were thus well vented and shielded from direct sun light.

The sensor in the fresh air inlet to the fifth floor was located about 20 cm inside the fresh air duct to this system in order to shield it from the sun as seen on figure 2.5.

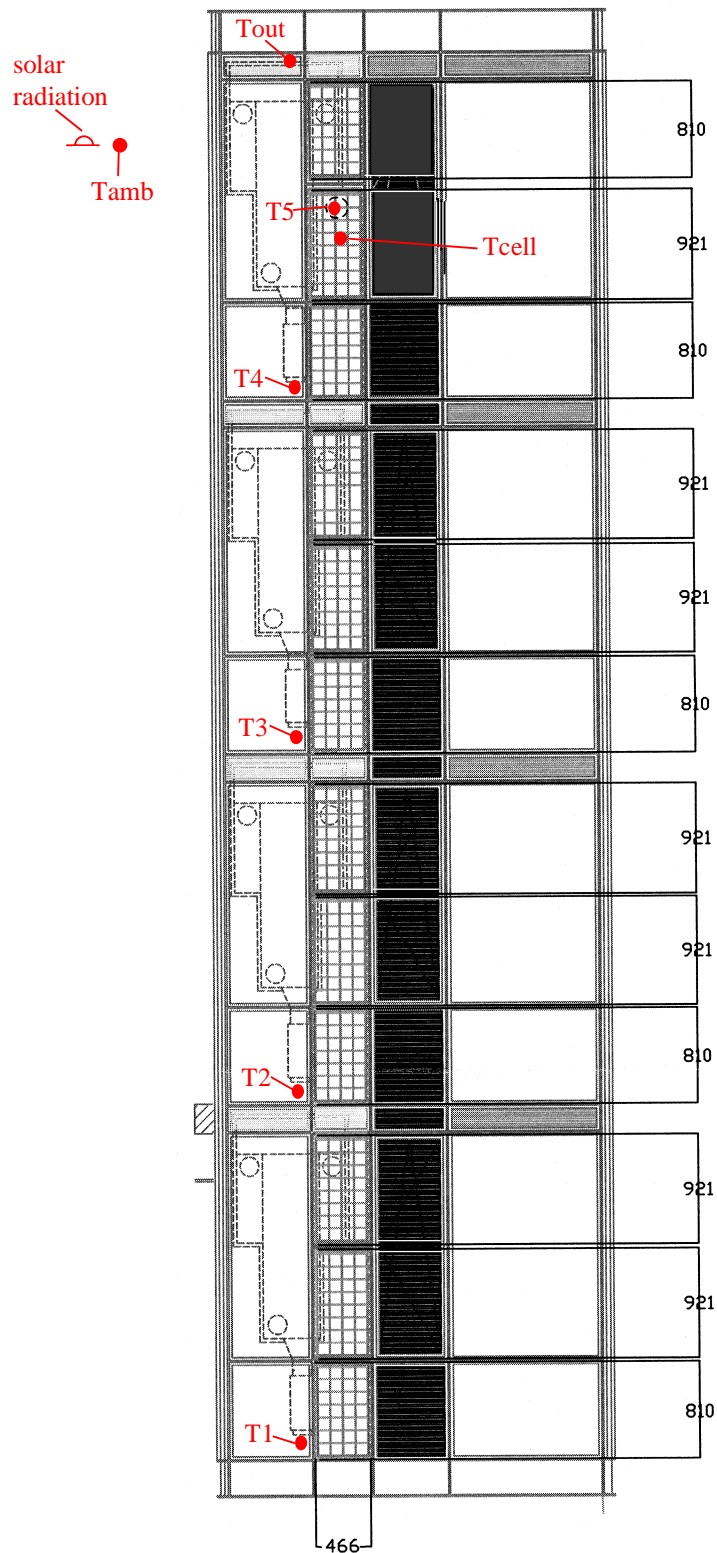


Figure 2.2. The location of temperature sensors in the solar wall and location of pyranometer and ambient temperature sensor.

One more air temperature sensor (also a PT100 class A sensor) was located at the top of the solar wall (Tout in figure 2.2) – at the outlet for summer venting of the solar wall.

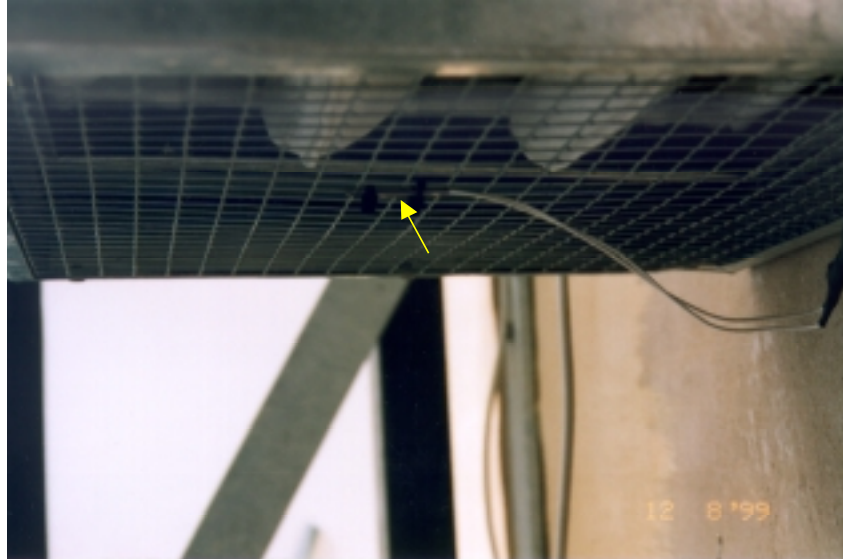


Figure 2.3. The location of the air temperature sensor in the solar wall – mounted at the grid of the fresh air inlet to the heat exchanger units.

The surface temperature sensor at the back of the PV-panel at the fourth floor was located in the middle of the middle panel behind a solar cell. This sensor was a PT100 class A sensor mounted by means of aluminium tape. Thermo pasta was located between the PV-panel and the sensor in order to obtain a good thermal connection.

## 2.2. Weather measurements

The used pyranometer was a calibrated SolData Pyranometer type 80-HD for measuring of total radiation. The instrument for measuring of ambient temperature was a PT100 class A temperature sensor located in a shield consisting of two concentric tubes in order to screen it from the sun. Figure 2.1 shows the location of the pyranometer while figure 2.4. shows the ambient temperature sensor and the back of the pyranometer.

## 2.3. Temperature and flow measurements in the ventilation system

Figure 2.5 shows the ventilation system of Tøndergade 1. The figure further shows the location of the air temperature sensors and air flow measuring devices in the ventilation system in the apartment at the fourth floor.

Besides the temperature of the fresh air (figure 2.2) three other air temperatures were measured in the ventilation system of the apartment at the fourth floor to the right – as seen in figure 2.5: the temperature of the outlet from the apartment, the exhaust air from the heat exchanger and the inlet air to the apartment from the heat exchanger. The sensors were PT100 class A sensors.

The air flow rate of fresh air and exhaust air was determined by measuring the pressure drop across a calibrated orifice or a calibrated bending. For the fresh air a calibrated bending (Lindab MBU 90°-100) was used while the exhaust air was measured using a calibrated ori-

face (Lindab FMU-100). The pressure drops were measured using calibrated pressure transmitters (Huba Control type 694) – see figure 2.9.



Figure 2.4. The shielded ambient temperature sensor and the back of the pyranometer.

The calibrated orifice was located in a small shaft between the solar wall and the bathroom as shown on figure 2.6 while the calibrated bending was located above the suspended ceiling of the bathroom. The calibrated orifice and calibrated bending are shown in figures 2.7-8. In order to determine any heat losses from the ventilation ducts in the shaft a PT100 class A temperature sensor was located in the shaft to measure the air temperature – see figure 2.6.

#### **2.4. Electrical measurements**

The fans of the system are partly powered by the PV-panels in the solar wall. At low or no PV-power the fans run partly or only on power from the grid. A PV-mixer is in charge of assuring that the fans are supplied with as much PV-power as possible.

The PV-mixer is one of the new parts developed in the project. It is, therefore, important to establish knowledge of the function of the PV-mixer.

It is, however, a non-trivial task to determine the performance of the PV-mixer as it has two power inputs and one power output. Especially the inputs may change rapidly over time e.g. if a cloud gets in front of the sun. It is, thus, extremely important that the voltage and current is measured at the same time – even a small time shift between the measuring of the two values for all in and outputs may lead to a wrong picture of the performance of the PV-mixer and the PV-panels.

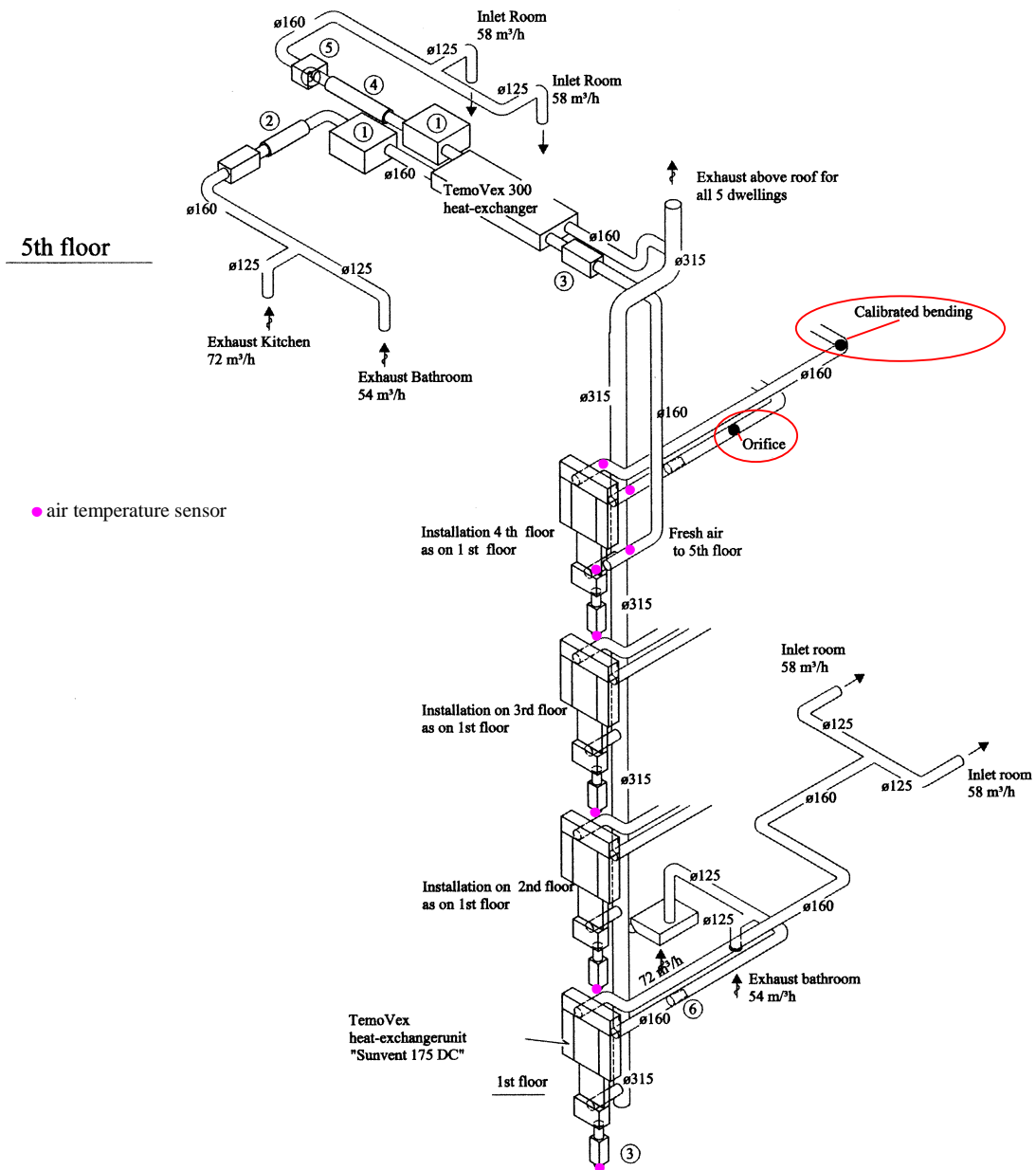


Figure 2.5. The ventilation system of Tøndergade 1 to the right.

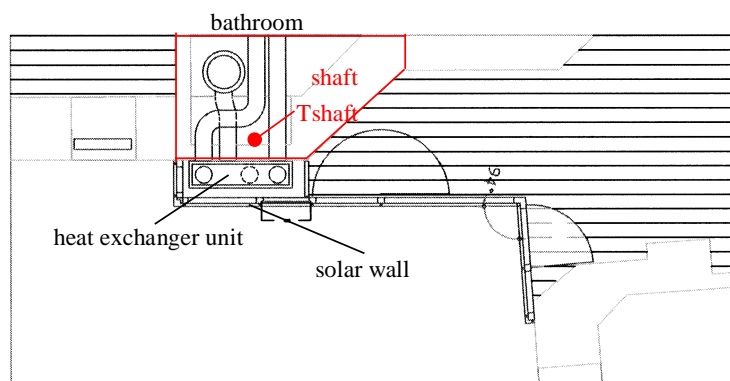


Figure 2.6. The installation shaft.



Figure 2.7. The calibrated orifice.



Figure 2.8. The calibrated bending.

At first it was tried to find an existing sensor/meter that was able to perform the measurements with the necessary accuracy on the first version of the PV-mixer. However, no such was found as it was very difficult to measure connected values of voltage and current to and from the PV-mixer in order to get a true picture of the power to and from the first version of



the PV-mixer. Finally Solar Energy Centre Denmark decided to develop the sensor. The sensor consisted basically of a 4-quadrant analogue multiplier, which at a high frequency measure the voltage and current going either in or out of the PV-mixer and multiply the two values in order to obtain the power. The measuring frequency is higher than the fastest variation of either in or output of the PV-mixer – this ensures precise and correct measurements of the power. This design of the sensor was maintained although the new version of the PV-mixer made it much easier to measure connected values of voltage and current to and from the PV-mixer. The developed sensors was installed and calibrated by the end of 2000. However, it was discovered that the readings from the sensors unfortunately didn't give much meaning. After a careful investigation it was discovered that the 4-quadrant analogue multiplier is rather temperature dependent (not mentioned in the data sheet for the chip). This means that the calibration equation changes with the temperature meaning that the readings cannot be transferred to meaningful measurements.

The new version of the PV-mixer makes it fortunately easier to measure connected values of voltage and current to and from the PV-mixer. A new marked survey showed that signal calculators from PRelectronics type 2289 could measure connected voltage and current to and from the PV-mixers. The new sensors were installed and calibrated by the end of January 2001.



Figure 2.9. The pressure transducers for measuring the pressure drop across a calibrated orifice and a calibrated bending.

## 2.5. Data collection

All sensors were connected to a data logger system with modules from Analog Devices. Each sensor were scanned each 10<sup>th</sup> second and averaged into 10 minutes mean values and stored on the hard disk of a PC.

The PC via the software Labteck Control controlled the data logger system. Spot values of the sensor readings were continuously shown on the screen of the PC. The PC/data logger system was located in the attic at Tøndergade 1 as shown in figure 2.10.



Figure 2.10. The attic at Tøndergade 1 with the PC/data logger system located at the back wall.

## 2.6. Treatment of measured data

Using the data logger system/PC the measured values were directly translated into physical understandable values like temperatures and solar radiation.

Using the calibration equations other measured values were later transformed to air flow rates and power. The thermal performance of the heat exchanger and solar wall were likewise later calculated using the measured temperatures and air flow rates.

### 3. Measurements

Measurements have been carried out at Sundevedsgade/Tøndergade for more than one year from the beginning of February 2000 to end March 2001. Some sensors have, however, not been in place for the whole period – e.g. the measurements on the PV-mixer were first started on February 1, 2001 as mentioned earlier. One other sensor – the pressure transducer for determination of the air flow rate of exhaust air was malfunctioning until March 15, 2000 and the temperature sensor for measuring the air temperature in the shaft was first installed on March 15, 2000.

Data has unfortunately been lost due to what is believed to be power cuts to the measuring PC. These holes in the measurements are mainly a few hours to one day. However, 18 days was unfortunately lost in May 2000 (May 8-26).

The first section of this chapter contains graphs showing the measurements from two weeks in order to illustrate the function of the PV-VENT system – the two chosen weeks are week 5 and 6 of 2001 (January 29 – February 11), after this is a section with graphs showing different details from the one year of measurements. The third section contains more general conclusions on the different components of the system, while in the fourth section the savings of the system is calculated.

#### 3.1. Measurements from week 5 and 6, 2001

Figures 3.1-2 show the weather conditions during these specific weeks – i.e. total solar radiation on the wall at the fourth floor – see figure 2.1 – and ambient temperature at the same location. The two weeks are characterised by days with clear sky conditions and days with cloudy conditions. The ambient temperature was between  $-9$  and  $12^{\circ}\text{C}$ .

##### 3.1.1. Thermal part of the system

Figures 3.3-4 show the temperatures in the solar wall at the points shown in figure 2.2 including the ambient temperature. The figures show an increase of the fresh air temperature to the ventilation system at Tøndergade 1, 4, to the right (T4) of up to 20 K, while the temperature at the top of the solar wall (T<sub>out</sub>) is up to 28 K higher than the ambient temperature. A strange phenomenon is seen for the fresh air temperature to the fifth floor (T5) – regularly the temperature at this point doesn't follow the behaviour of the other temperatures. This is because the temperature sensor as seen in figure 2.5 is located 20 cm inside the duct in order to avoid the solar radiation hitting the sensor. However, when the fresh air fan to the fifth floor is stopped, the temperature at this point will as seen increase due to the heat gain from the shaft at the fourth floor, where this duct is situated – see figure 2.5. The temperature of the shaft is as seen in figure 3.9-10 rather high.

Figures 3.5-6 show the temperature of the PV-panel together with the ambient temperature and the temperature at the top of the solar wall (T<sub>out</sub>). The temperature of the PV-panel is of course lower than T<sub>out</sub> during periods without solar radiation, but during clear sky conditions the temperature of the PV-panel obtained during the two weeks an excess temperature compared to ambient of up to 37 K, while this temperature difference is 28 K at the top of the solar wall.

Figures 3.7-8 show the air flow rates of fresh air to and exhaust air from the apartment (Tøndergade 1, 4 to the right). The occupant operates the ventilation system in order to run it at normal mode during the day and at min. mode during the night. This is because although rather silent the noise from the system still irritates the occupants during the night. The flow rate during normal mode is: exhaust  $\approx 113 \text{ m}^3/\text{h}$  and fresh air  $\approx 107 \text{ m}^3/\text{h}$  which is close to the values given by the Danish building code (126 and  $113 \text{ m}^3/\text{h}$ ). During min. mode the flow rates are: exhaust air  $\approx 76$  and fresh air  $\approx 80 \text{ m}^3/\text{h}$ . During year 2000 the flow rate of fresh air and exhaust air at min. flow rate has further been almost identical – see section 3.2.1. The shift to a higher air flow rate of fresh air is because only the filter for the fresh air has been changed prior to figures 3.7-8. The peak values of exhaust air of up to  $170 \text{ m}^3/\text{h}$  are created by the kitchen hood which on/off contact control the max. mode of the ventilation system. By the start of the measurements the max. air flow rate of exhaust air was  $\approx 190 \text{ m}^3/\text{h}$ . This illustrates the influence of a dirty filter in the system. Figures 3.7-8 show a well operated ventilation system. However, during most of year 2000 the system was only run in min. mode (and max. mode when cooking) – see section 3.2.1.

Figures 3.9-10 show the temperatures around the air to air heat exchanger located in the solar wall and the air temperature in the shaft. The fresh air temperature shown in figures 3.9-10 is identical to  $T_4$  in figures 3.3-4. Solar radiation at clear conditions brings the fresh air temperature to the heat exchanger above the exhaust temperature. Figure 3.9-10 further show that the air temperature of the shaft is rather high  $23\text{-}24^\circ\text{C}$ . This is because the tubing of the heating system is located here and further not insulated as seen at the lower left corner of figure 2.7.

Figures 3.9-10 give together with figures 3.7-8 the efficiency of the heat exchanger. Figures 3.11-12 show the efficiency of the heat exchanger calculated in the following way:

$$\eta = q_{\text{in}} / q_{\text{out}} \quad (3.1)$$

where:  $q_{\text{in}}$  is the heat transferred to the fresh air in the heat exchanger

$q_{\text{out}}$  is the energy in the exhaust air calculated based on the temperature of the exhaust air from the apartment and the temperature of the fresh air to the heat exchanger

However, the efficiency shown in figures 3.11-12 is not the real efficiency for the heat exchanger as the heat from the fans are not considered. Figure 3.21 shows the principle of the heat exchanger incl. fans and the locations of the temperature measurements. If the efficiency from figures 3.11-12 is compensated for the energy to the fans figures 3.13-14 appears. The compensation for the fan energy is based on the measured fan power – see figures 3.42.

The peak values in figures 3.11-14 are created by the excess exhaust by the kitchen hood and by solar radiation. Two levels of efficiencies appear. One for min. flow rates and one for normal flow rates. It would be expected, that the efficiency increases with increasing air flow rates. But figures 3.13-14 show the opposite situation – around 80 % at min. flow rate and around 70 % at normal flow rate. This is because the air flow rate of fresh air at min. flow rate is higher than the flow rate of exhaust air. A more thorough investigation of the efficiency of the heat exchanger is carried out in section 3.3 also including condensation and heat losses – please see this.

### 3.1.2. PV part of the system

Figures 3.15-16 show the electrical power to and from the PV-mixer. From the figures is seen that when solar power is available an immediate drop occurs in the power consumption from the grid. When the PV-panels can supply all the power to the fan no power is taken from the grid – i.e. the power demand of the PV-mixer itself is in these situations taken from the PV-panel. The difference between fan and grid power at no solar power gives the efficiency of the PV-mixer in grid mode, which according to table 1.3 should be 96 %. In pure PV mode the necessary PV power is higher than the fan power – the difference gives the efficiency of the PV-mixer in pure PV mode. From figures 3.15-16 it is seen that the efficiency in pure PV mode is lower than in pure grid mode. This is dealt with in table 1.4 and further in section 3.3.

Figures 3.17-18 show the utilized PV power and the potential power from the PV-panels (the loss in the wiring is not considered as it is in the order of 2-3% and thus far less than the uncertainty of the measurements). The potential power from the PV-panel is the power the PV-panel would have been able to deliver, if a higher demand had been present. The potential power is calculated in the following way:

$$P_{\text{potential}} = P_p \cdot E_{\text{useful}} / E_p \cdot (1 - (T_{\text{actual}} - T_p) \cdot 0.004) \text{ [W]} \quad (3.2)$$

where  $P_p$  is the peak power found with a solar radiation  $E_p$  of 1000 W/m<sup>2</sup> and a cell temperature  $T_p$  of 25°C

$E_{\text{useful}}$  is the useful solar radiation calculated as described below

$T_{\text{actual}}$  is the temperature measured at the backside of the PV-panel – see figures 3.5-6.

0.004 is the temperature dependence of the PV-panels

- The total radiation on the PV-panel is transformed to useful radiation by taking into account the reflection of the solar radiation in the glazing of the PV-panels at periods with a non zero incidence angle for the solar radiation. In order to correct for the reflections it is necessary to calculate the split between direct and diffuse radiation based on the measured total radiation. This was done using the equations in (Duffie and Beckman, 1991). The calculated split introduces a small uncertainty compared to a case where both total and diffuse radiation are measured. The following correction factor has been applied to account for the reflection in the cover:

$$k = 1 - \tan^a(\theta/2) \quad (3.3)$$

where  $\theta$  is the incidence angle for the radiation: the actual incidence angle for the direct radiation and 60° for the diffuse radiation.  $a$  is 3.7 (Nielsen, 1995).

Figures 3.17-18 show that the utilization of the potential PV power is very dependent on the actual demand as seen when comparing figures 3.17-18 with figures 3.15-16. How large a fraction - that actually is utilized - is shown in figures 3.19-20. Between 30 and 90 % (30 % on day 33 with a very low power demand of the fans) has been utilized during the shown period. At low radiation levels the utilization should have been 100 % as the potential power from the PV-panels is lower than the demand of the fans. The reason for not being 100 % is the large uncertainty of the model (3.2) at low radiation levels and the uncertainty of the measuring equipment -  $\pm 1$  W, which at low power leads to high uncertainties. The yearly saving and waste are dealt with in section 3.4. However, from figures 3.17-20 it can be stated

that the peak power of the PV-panels should not be higher than the demand divided with the efficiency of the PV-mixer at that specific demand.

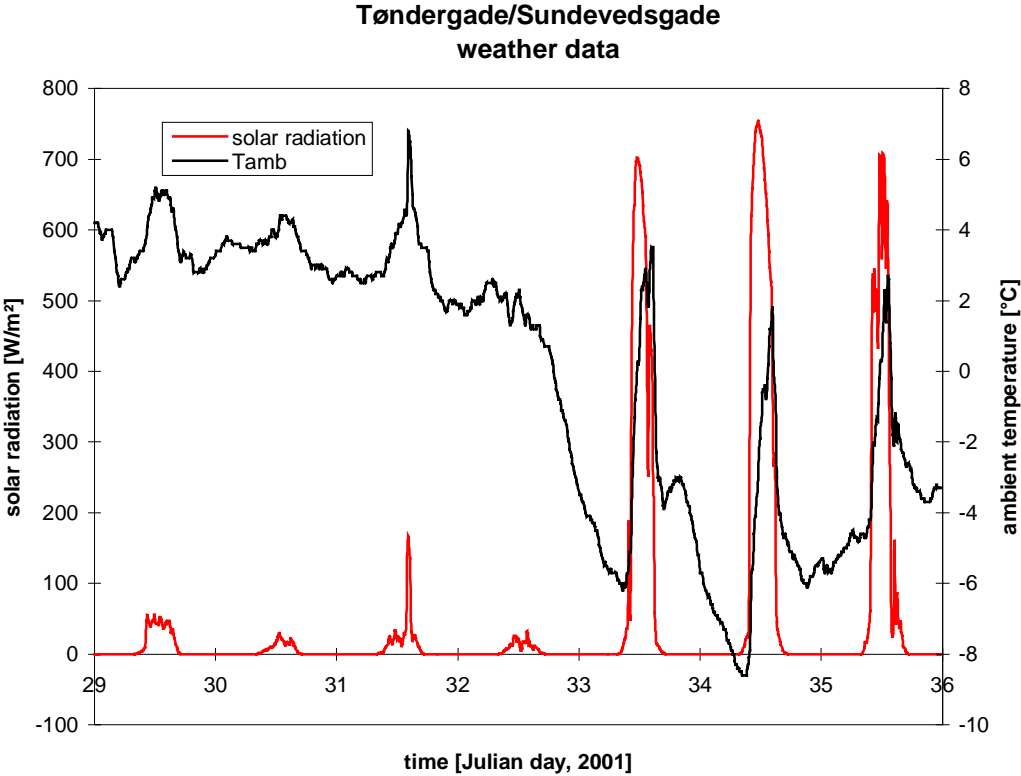


Figure 3.1. The weather conditions during week 5, 2001 (January 29 – February 4).

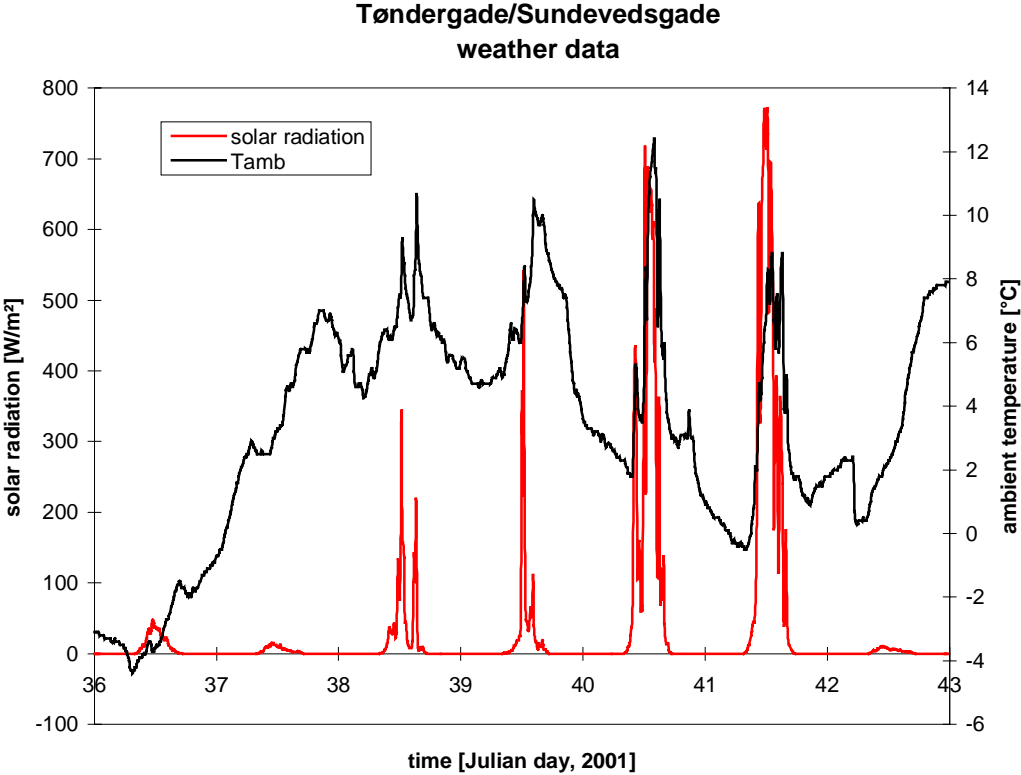


Figure 3.2. The weather conditions during week 6, 2001 (February 5 – February 11).

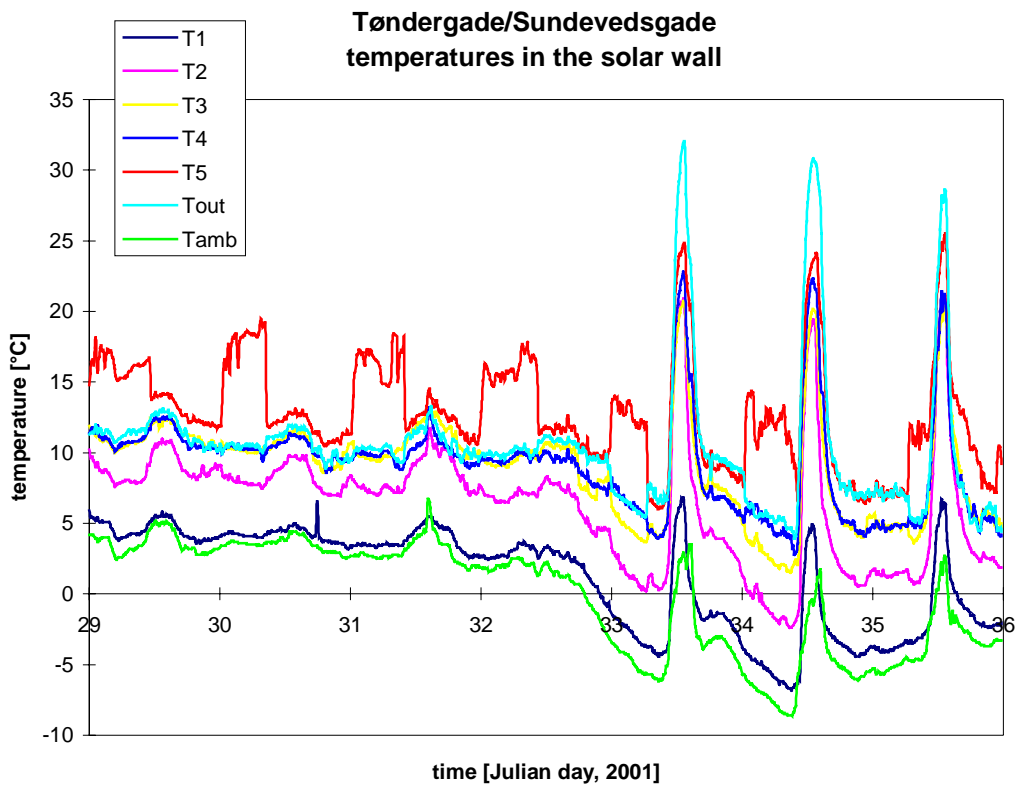


Figure 3.3. Temperatures in the solar wall during week 5, 2001 (January 29 – February 4).

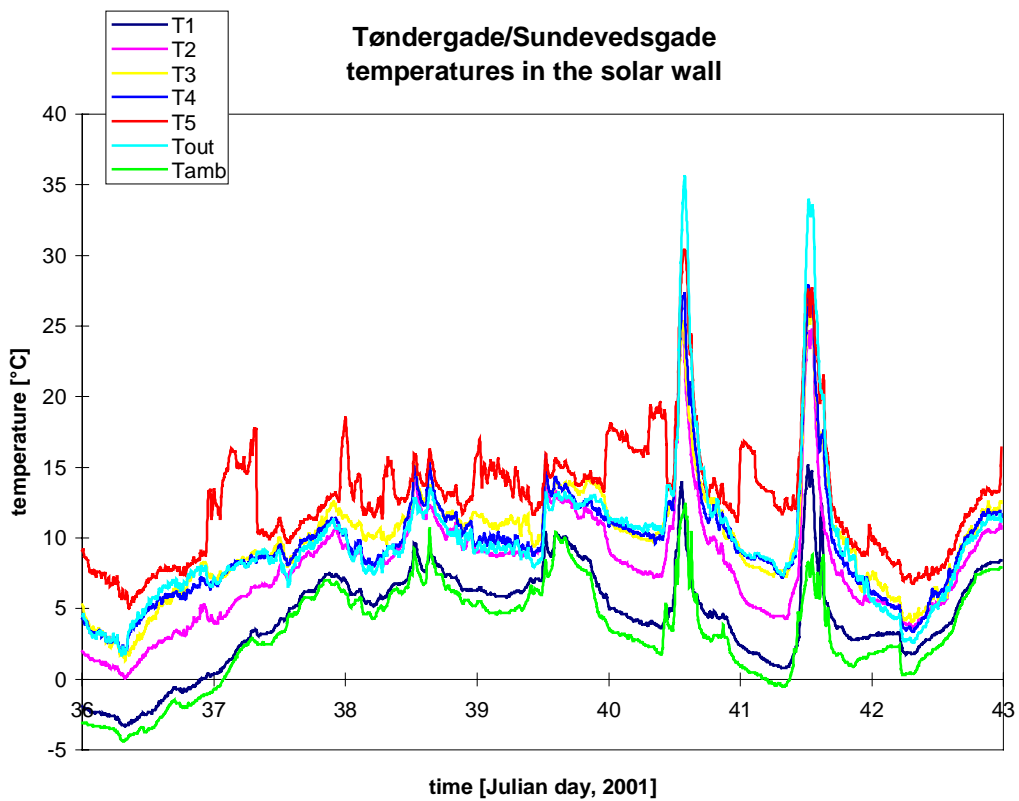


Figure 3.4. Temperatures in the solar wall during week 6, 2001 (February 5 – February 11).

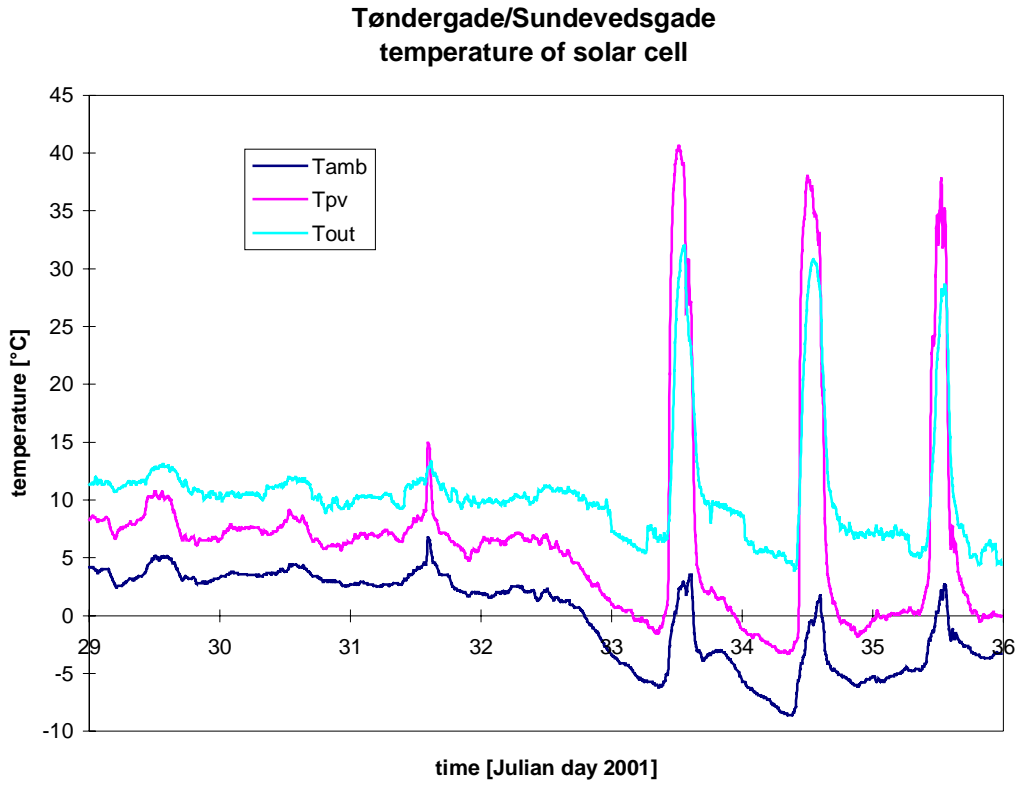


Figure 3.5. Temperatures of the PV-panel during week 5, 2001 (January 29 – February 4).

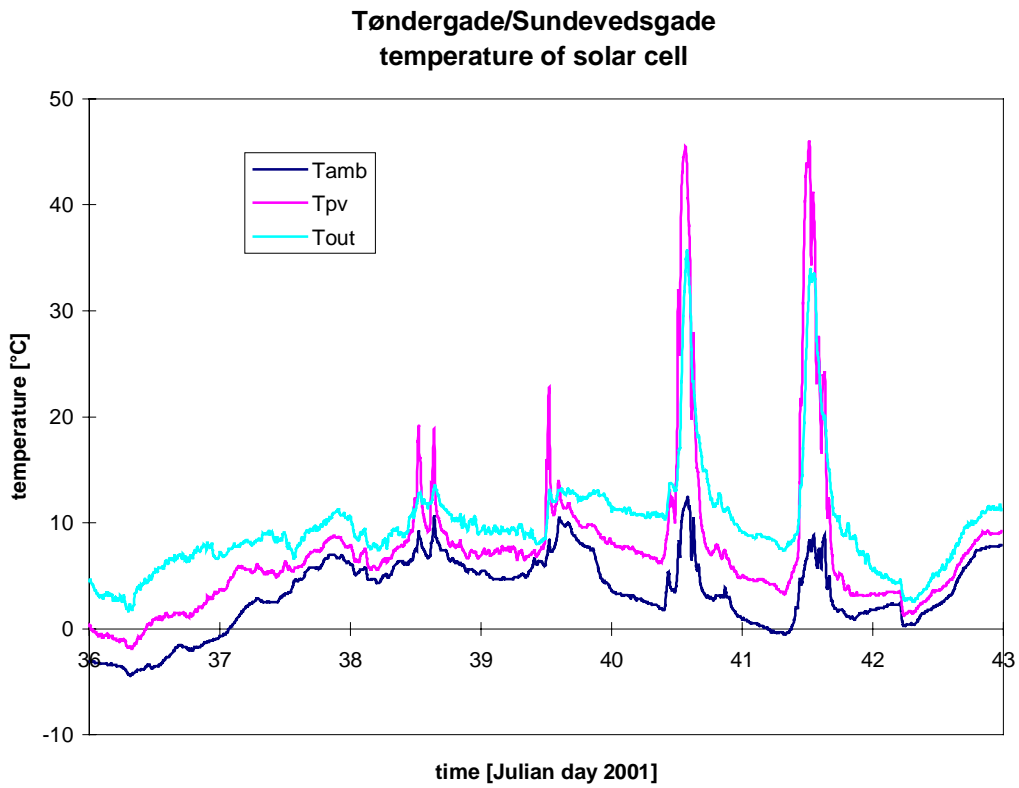


Figure 3.6. Temperatures of the PV-panel during week 6, 2001 (February 5 – February 11).



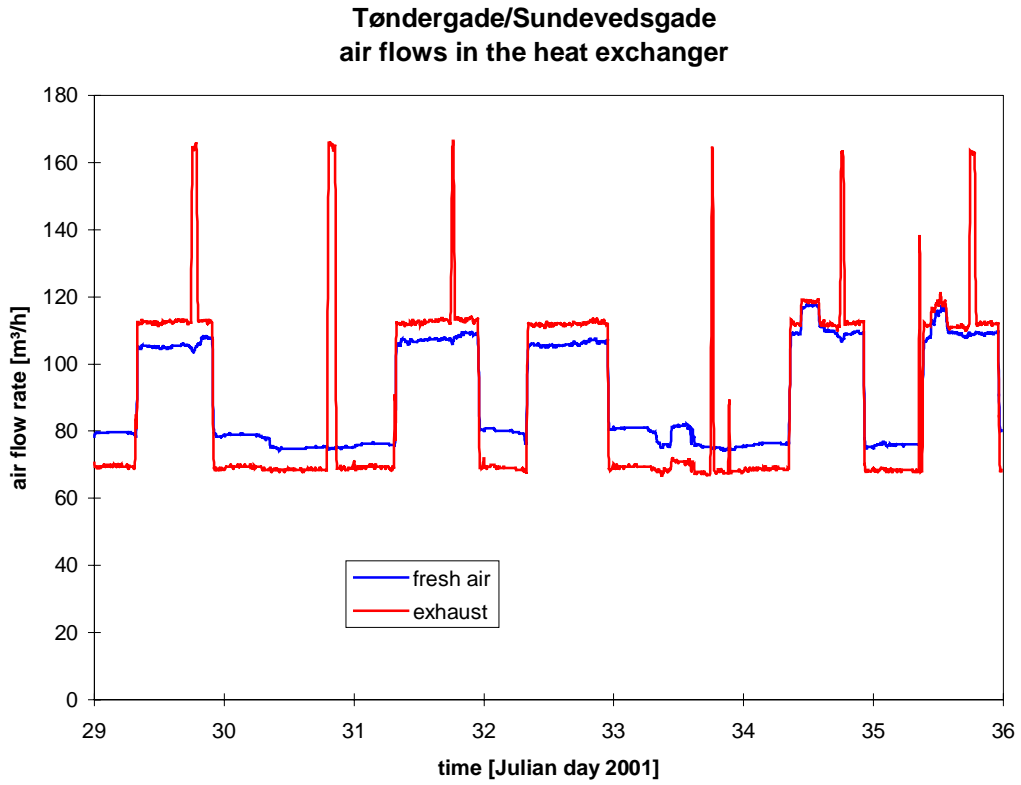


Figure 3.7. Air flow rates in the system during week 5, 2001 (January 29 – February 4).

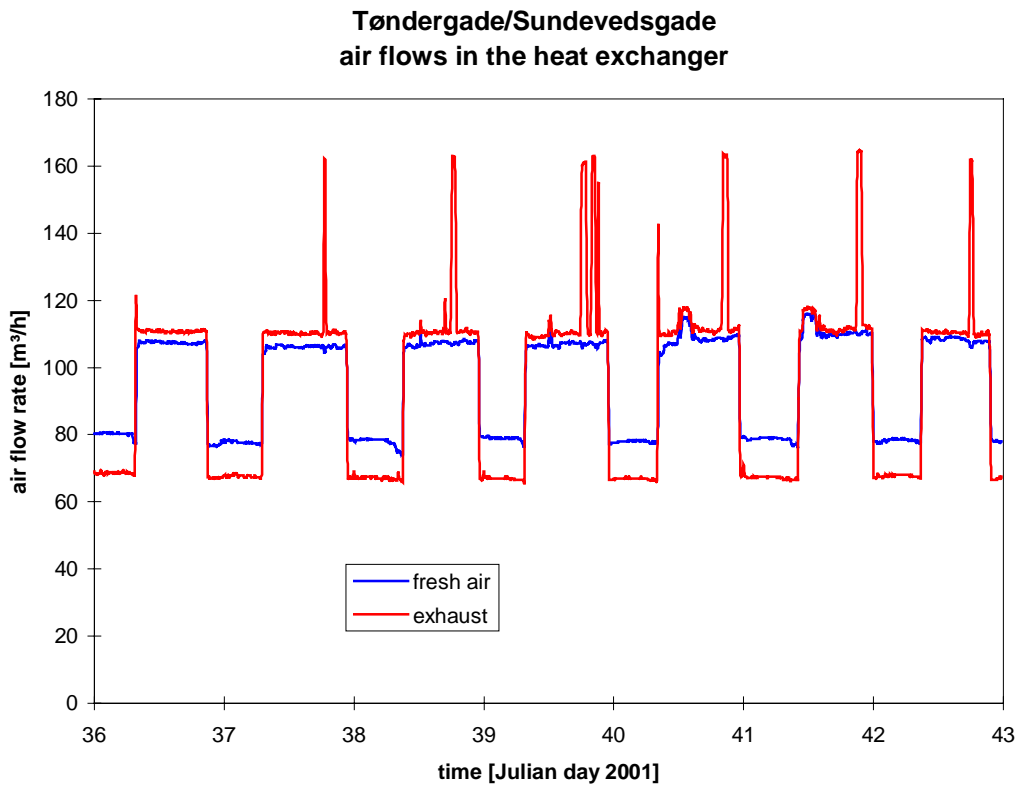


Figure 3.8. Air flow rates in the system during week 6, 2001 (February 5 – February 11).

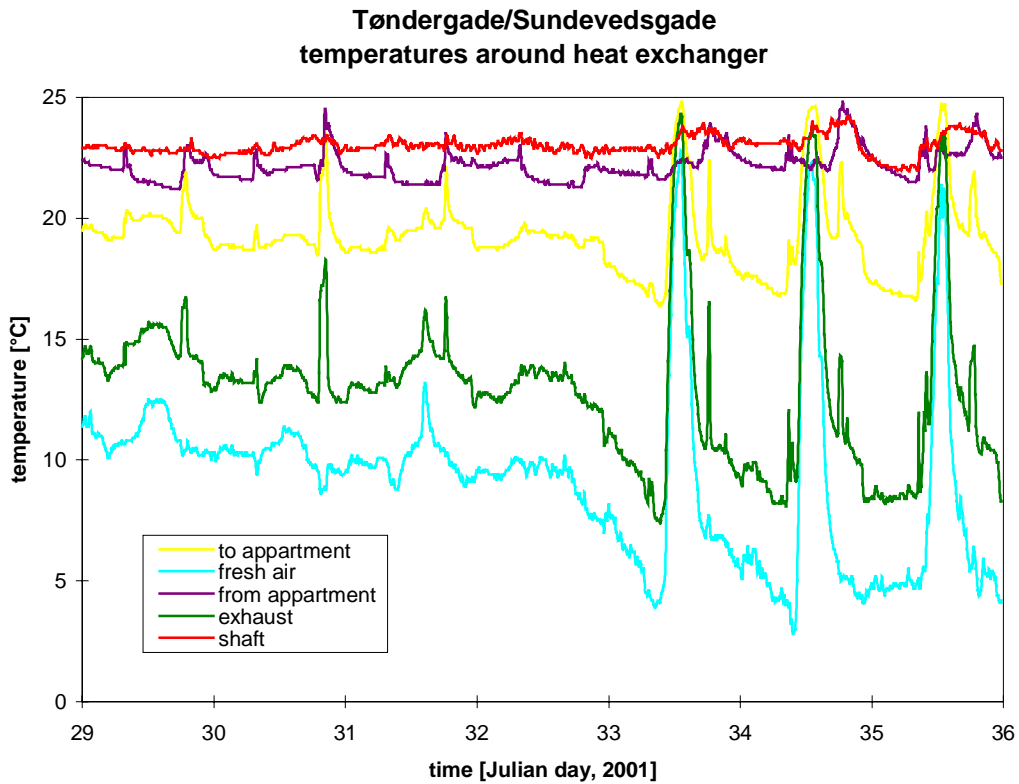


Figure 3.9. Temperatures of air to and from the heat exchanger during week 5, 2001 (January 29 – February 4).

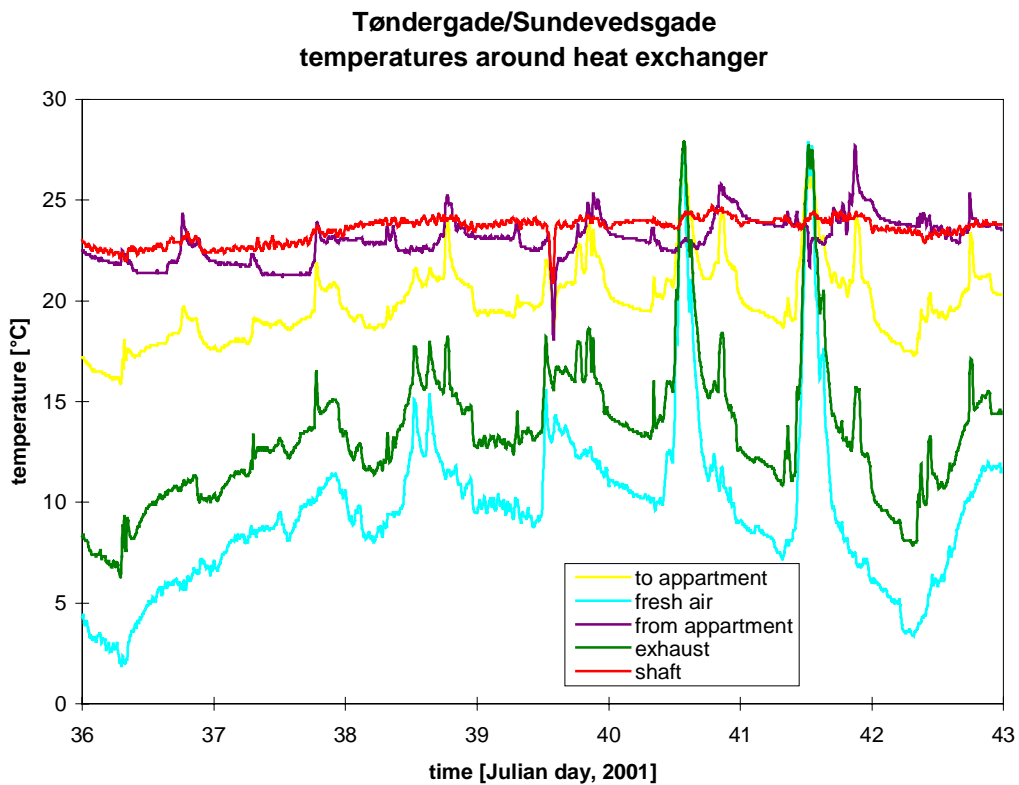


Figure 3.10. Temperatures of air to and from the heat exchanger during week 6, 2001 (February 5 – February 11).

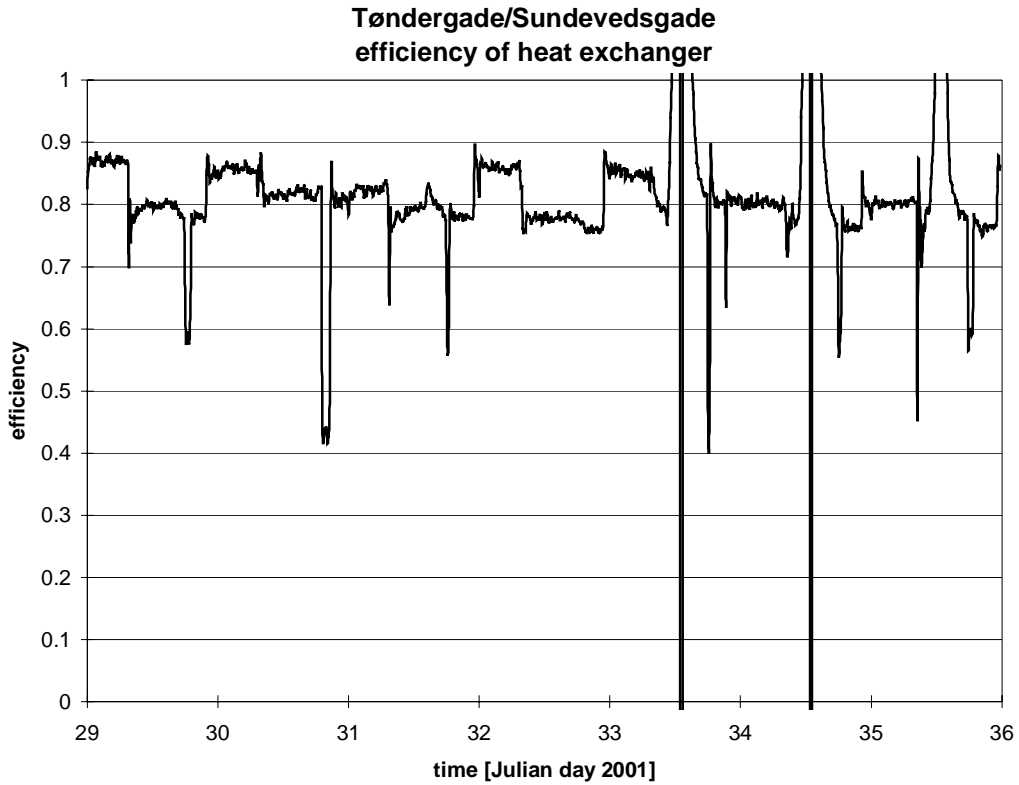


Figure 3.11. The efficiency of the heat exchanger incl. fans during week 5, 2001 (January 29 – February 4).

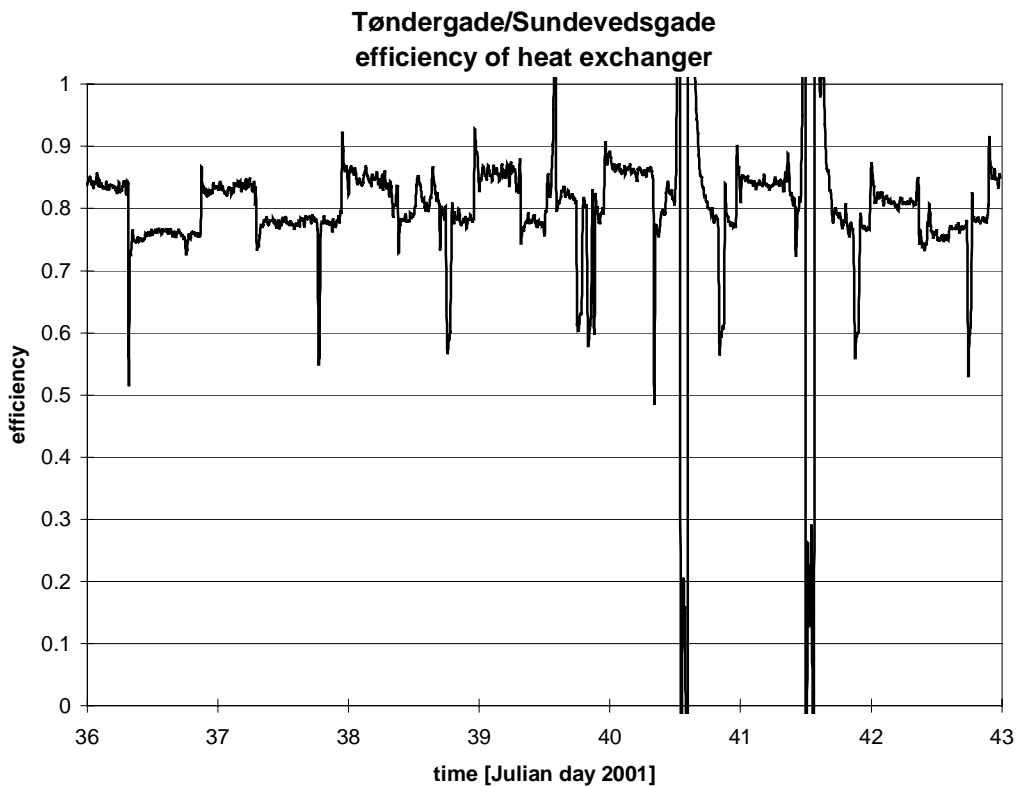


Figure 3.12. The efficiency of the heat exchanger incl. fans during week 6, 2001 (February 5 – February 11).

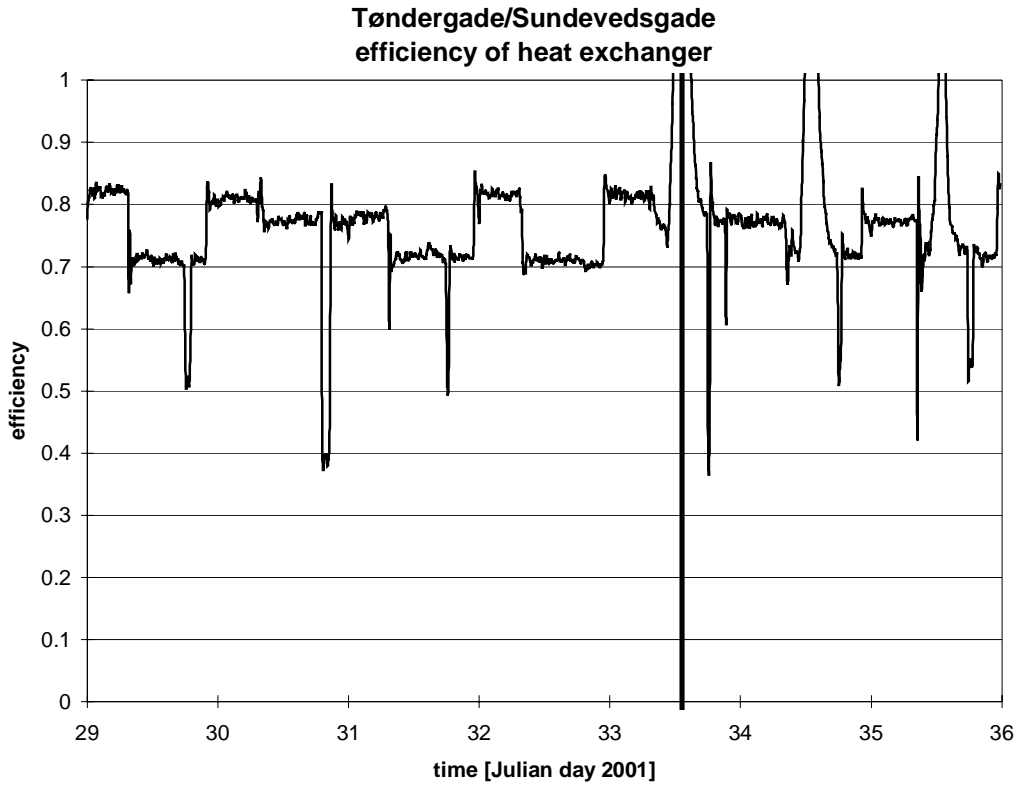


Figure 3.13. The efficiency of the heat exchanger excl. fans during week 5, 2001 (January 29 – February 4).

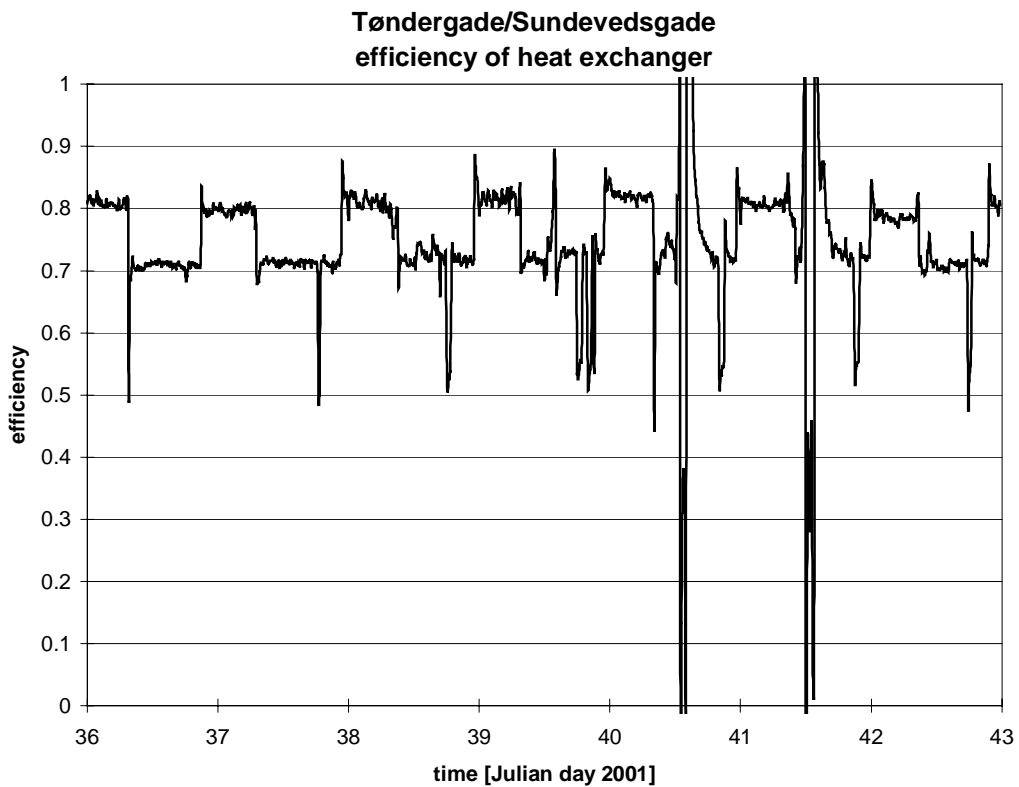


Figure 3.14. The efficiency of the heat exchanger excl. fans during week 6, 2001 (February 5 – February 11).

**Tøndergade/Sundevedsgade  
power to and from PV-mixer**

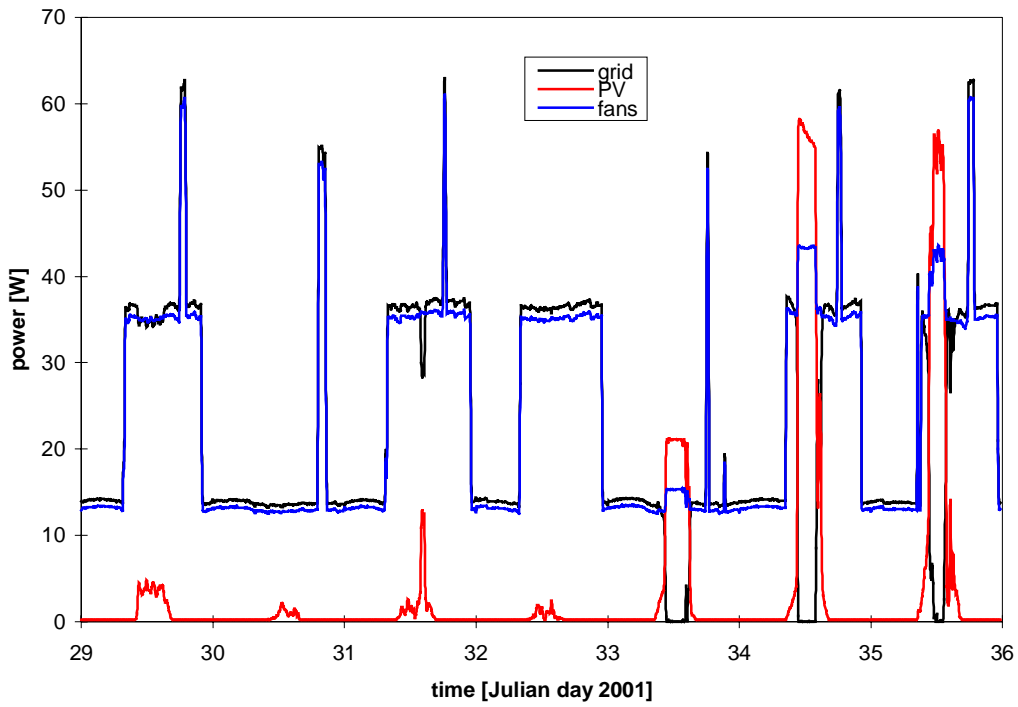


Figure 3.15. Power to and from the PV-mixer during week 5, 2001 (January 29 – February 4).

**Tøndergade/Sundevedsgade  
power to and from PV-mixer**

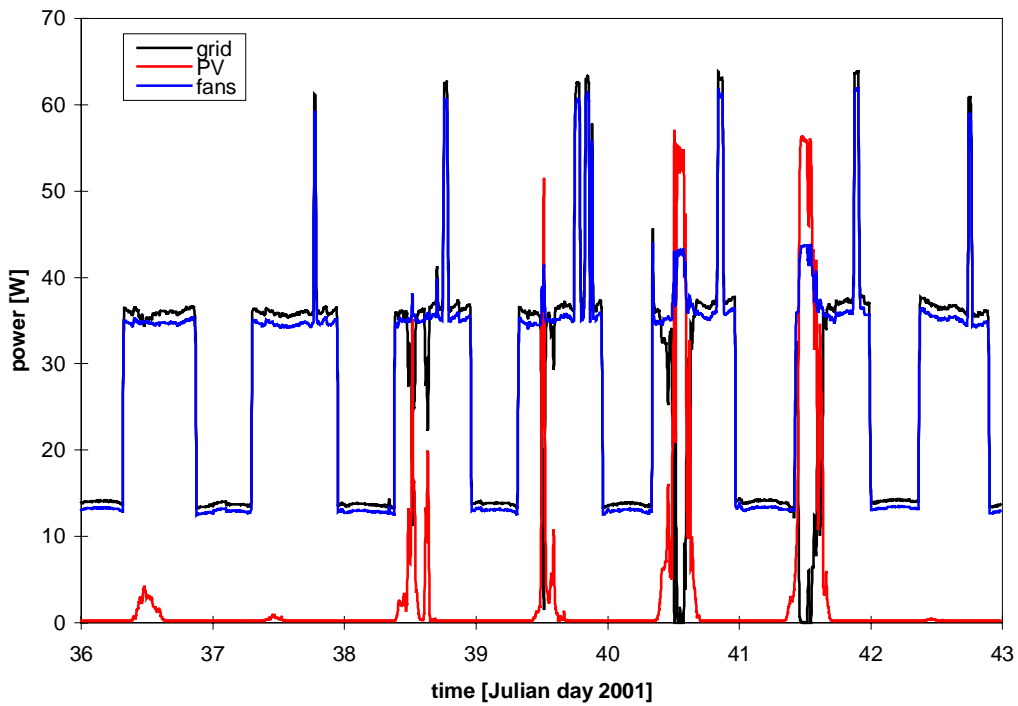


Figure 3.16. Power to and from the PV-mixer during week 6, 2001 (February 5 – February 11).

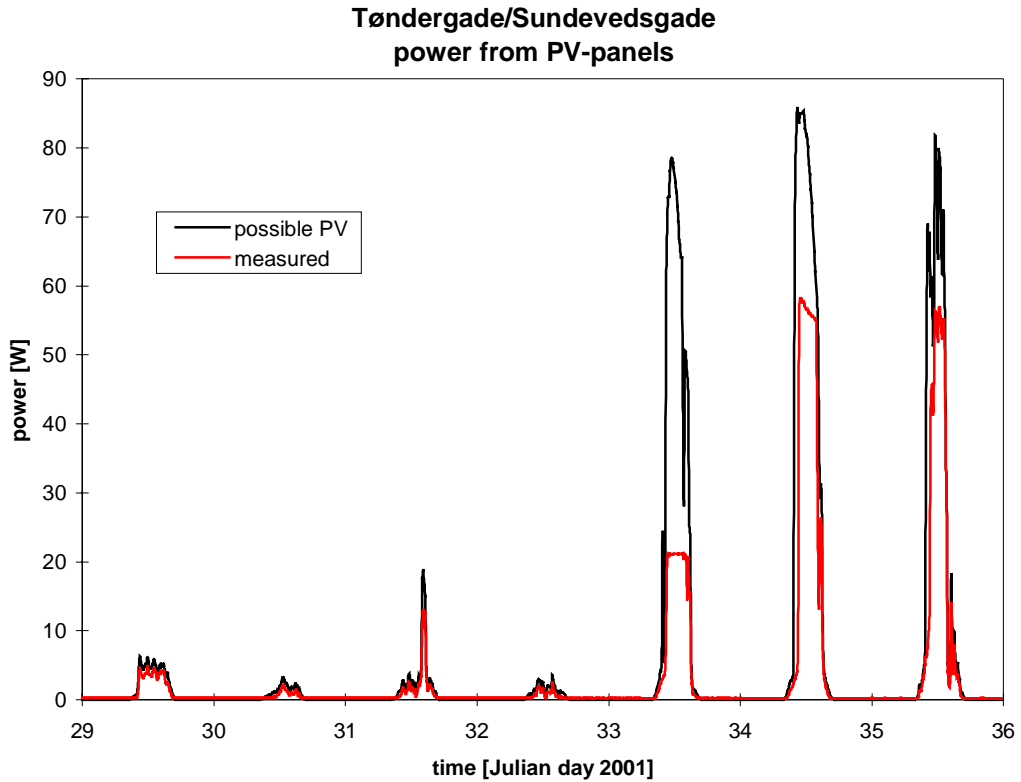


Figure 3.17. Actual power and potential power from the PV-panel during week 5, 2001 (January 29 – February 4).

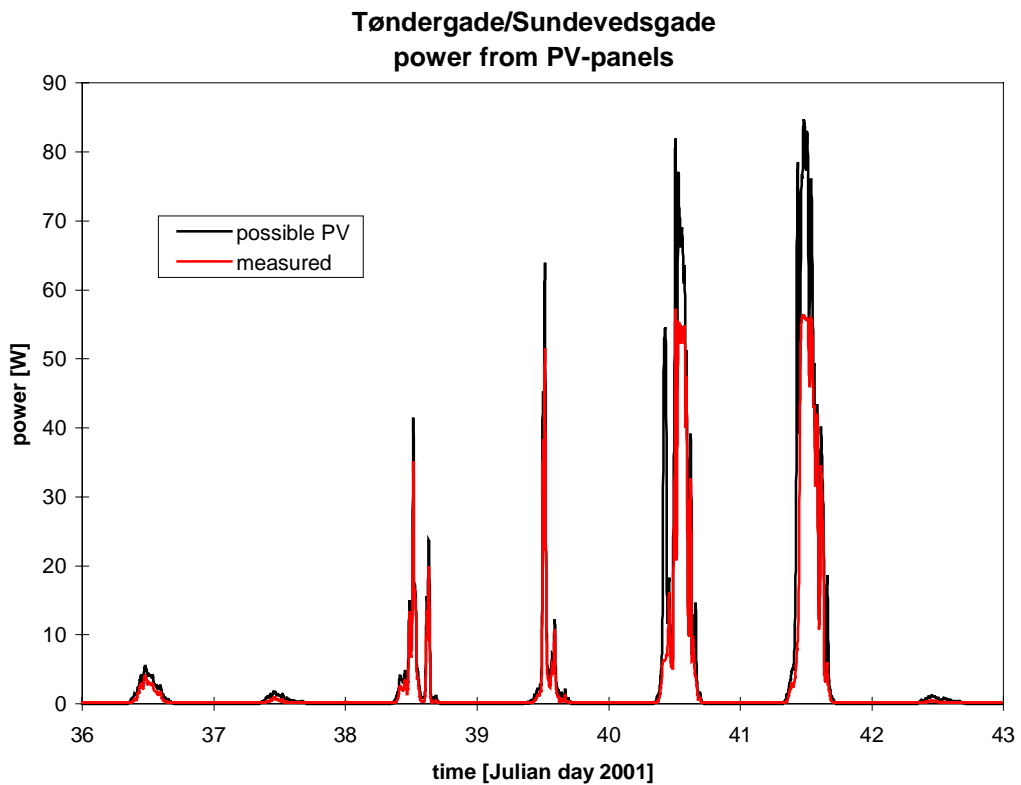


Figure 3.18. Actual power and potential power from the PV-panel during week 6, 2001 (February 5 – February 11).

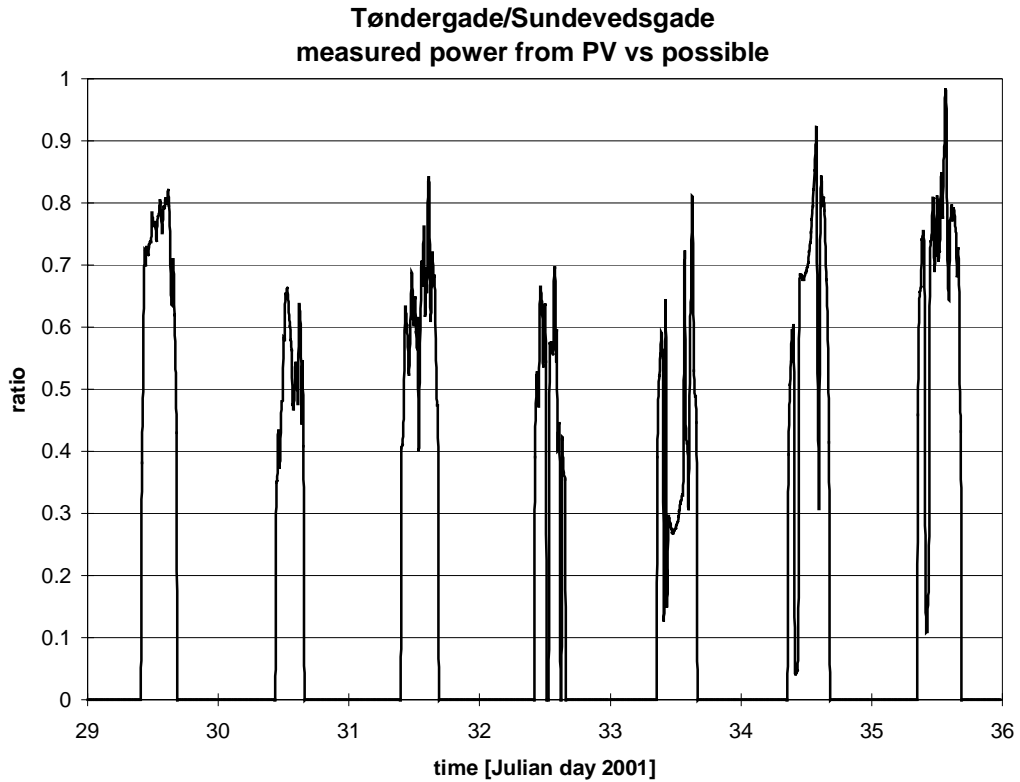


Figure 3.19. Actual power divided with potential power from the PV-panel during week 5, 2001 (January 29 – February 4).

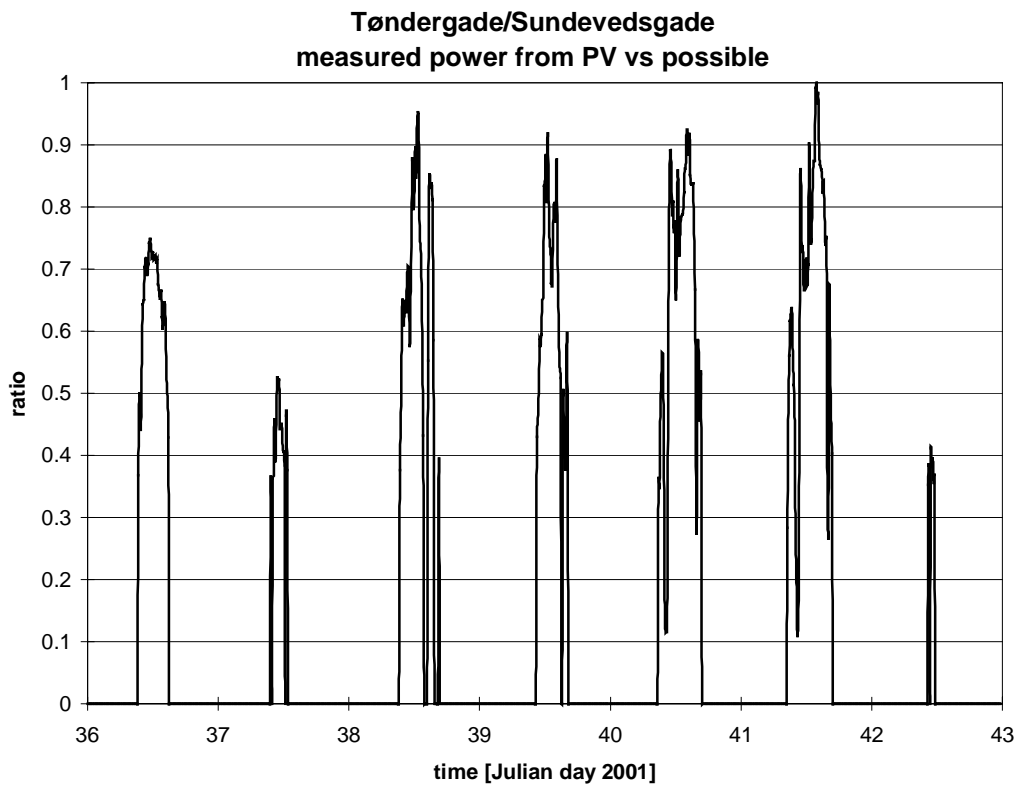


Figure 3.20. Actual power divided with potential power from the PV-panel during week 6, 2001 (February 5 – February 11).

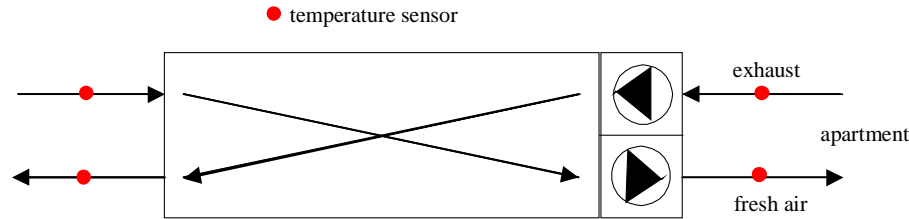


Figure 3.21. The principle of the air to air heat exchanger and the location of the temperatures sensors.

When comparing figures 3.7-8 with 3.15-16 it is seen that the air flow rates increase when the PV-panels are able to cover the demand. This is because the voltage to the fans increases.

### 3.2. Measurements from specific weeks

In this section graphs are shown for specific weeks in order to show features/problems not shown in the graphs in section 3.1.

#### 3.2.1. Airflows

Figures 3.7-8 show a very well controlled system with respect to the air flow rate. However, the figures also show the risk of this way of manually controlling the system. The system was not switched to normal mode on day number 30 and 33 even if it can be seen that the occupants were at home – i.e. the max. flow rate created by the kitchen hood.

During main part of year 2000 the system was run at min. mode as e.g. seen in figure 3.22. The efficiency of the heat exchanger and the utilized PV-power are lower in this mode and there is a risk of getting a too humid indoor climate in the apartment. The latter is the reason for the “better” operation of the system in year 2001 because the occupants got aware that drying of cloth in the living room leads to high relative humidity in the dwelling if not ventilated well.

The reason for the min. mode during year 2000 and during the nights of year 2001 is as already mentioned the noise from the system during the night.

Figure 3.22 further shows that the two air flows by the start of the system was almost identical.

From end of April 2000 to beginning of October 2000 the ventilation system was mainly run in summer mode - i.e. the fresh air fan was switched off. The exhaust was run in min. flow rate mode.

#### 3.2.2. PV-mixer

It was in chapter 2 mentioned that the first PV-mixer installed in the system didn't work. This is shown in figures 3.23-24, where it is seen that although able to maintain the power to the fresh air fan the air flow of exhaust air fluctuated extremely much. Figure 3.24 shows that after installing the new PV-mixer everything functioned again. The figure further shows that the



PV-mixer was installed on December 13 leaving very little time to perform measurements on the system with all components working.

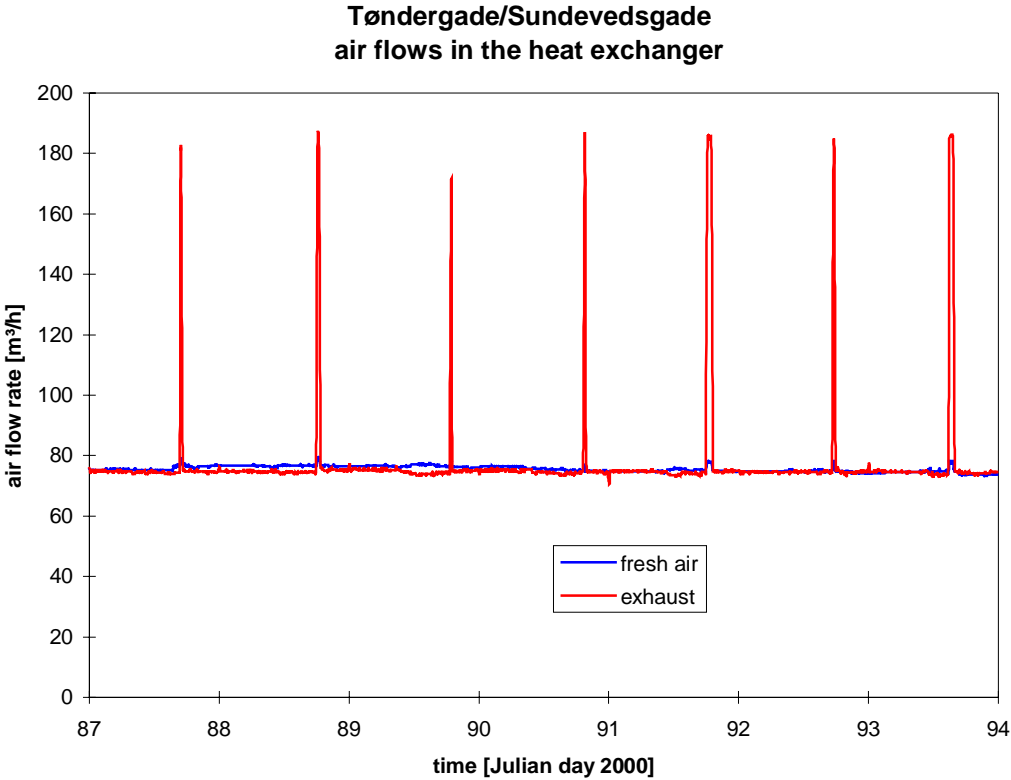


Figure 3.22. Air flow rates during the week March 28 – April 2, 2000.

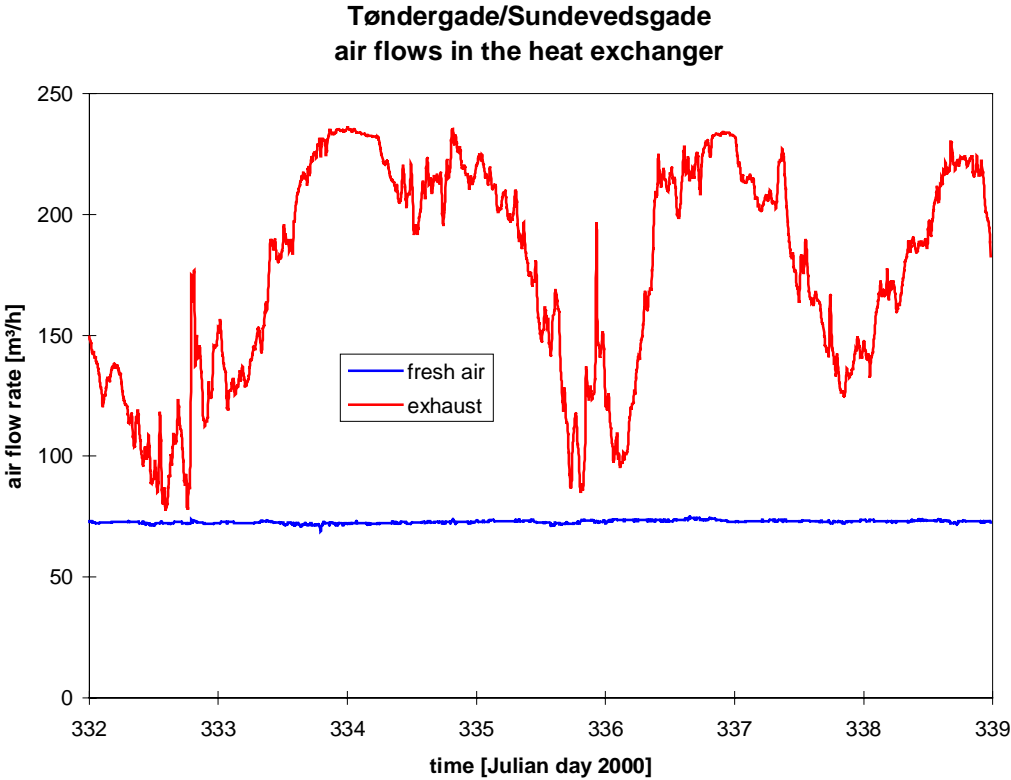


Figure 3.23. Air flow rates during the week November 27 – December 3, 2000.

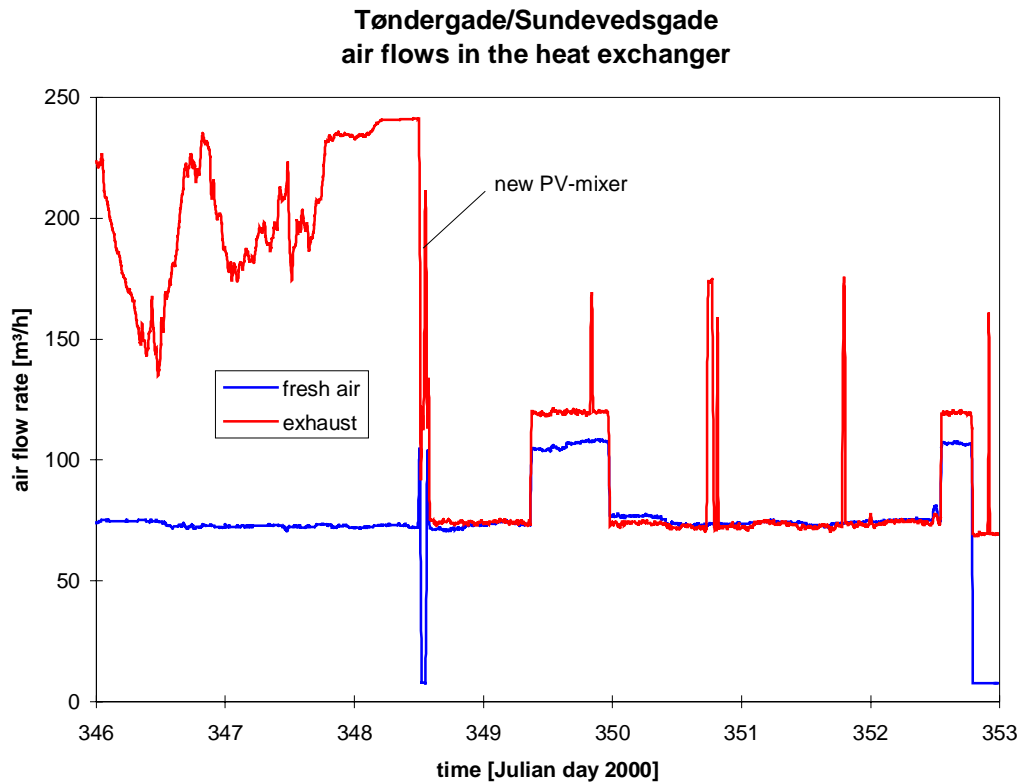


Figure 3.24. Air flow rates during the week December 11 – December 17, 2000.

### 3.3. Calculations based on the measurements and more general conclusions

The section deals with the function of the air to air heat exchanger, the fan power, the temperatures in the solar wall and the PV-mixer, while the next section deals with the actual savings due to these components.

#### 3.3.1. The efficiency of the air to air heat exchanger

Figures 3.11-14 show the efficiency of the heat exchanger incl./excl. fan power for two weeks in the beginning of year 2001. The shown efficiencies don't necessarily show a correct picture of the efficiency of the heat exchanger. In the following the efficiency is evaluated based on the whole set of data rather than on only two weeks.

Determination of the efficiency of the heat exchanger is not an easy task as condensation may occur and as the heat exchanger is located outside the heated indoor space the heat loss further plays a role.

First of all is determined if the calculations of the heat flows (based on dry temperatures) on both sides of the heat exchanger are correct – they should be identical when no condensation occurs. Figures 3.25-28 show the calculated heating of the fresh air divided with the calculated cooling (based on dry temperatures) of the exhaust air in the heat exchanger for year 2000 and January-March 2001 respectively and further for min. and normal mode. The ratio is shown as a function of the inlet temperature to the heat exchanger, however, only for inlet temperatures below 17°C in order to avoid periods with high inlet temperatures due to the

sun, as the function of the heat exchanger here is opposite – when the inlet temperature gets higher than the exhaust temperature. High inlet temperatures further leads to small temperature differences across the heat exchanger, which again increase the uncertainty of the calculations.

Be aware of different y-axes in figures 3.25-28.

Figures 3.25-28 show not as expected an increase in the ratio between the two heat flows when going towards lower inlet temperatures to the heat exchanger. At low inlet temperatures to the heat exchanger condensation should occur in the heat exchanger leading to a higher heating of the fresh air than cooling of the exhaust air when the heat flows are calculated based on dry temperatures. A reason for this has not been found. It could be that the heat exchanger couldn't get rid of the water from the condensation leading to a decrease in heat transfer area. But the heat exchanger is vertical as seen in figure 1.10 and even if the water outlet is blocked, the water will just drain down the exhaust duct. Another reason, which seems more likely, is that the heat loss of the heat exchanger has a major influence of the efficiency of the heat exchanger. The increase of the efficiency due to condensation at decreasing inlet temperature is compensated due to an equal increase in the heat loss, as the inlet temperature to the heat exchanger also is the surrounding temperature for the heat exchanger. This may also be the reason why the ration in figures 3.26-27 increases going towards higher inlet temperatures. The increase may be due to solar radiation actually hitting the surface of the heat exchanger leading to a surface temperature above the inlet temperature.

Figures 3.29-36 show the calculated “dry” efficiencies for normal and min. flow mode, with and without the fan power included and for the year 2000 and January-March 2001.

Most parts for the values in 3.29-36 lay nicely together on a line.

The heat exchanger has hardly been run in normal flow mode during year 2000. The values are thus limited here, which makes figures 3.29-3.30 less conclusive.

In order to compensate for condensation and the heat loss the efficiency of the heat exchanger should be found at the axis to the right in the graphs. However, figures 3.31 and 3.33 show an unrealistic increase of the efficiency at inlet temperatures above 13°C. The efficiencies are instead found by extrapolation a regression line for the values between inlet temperatures of 6 and 13°C to the axis to the right of the graphs. Doing this the following information are obtained – however, the stated efficiencies are rather uncertain do to the way they are determined:

Year	ventilation mode	approx. flow rate m <sup>3</sup> /h	efficiency %
2000	normal	120	69
2001	normal	120	70
2000	min.	80	77
2001	min.	80	83

Table 3.1. The efficiency of the heat exchanger found from figures 3.29, 3.31, 3.33 and 3.35.

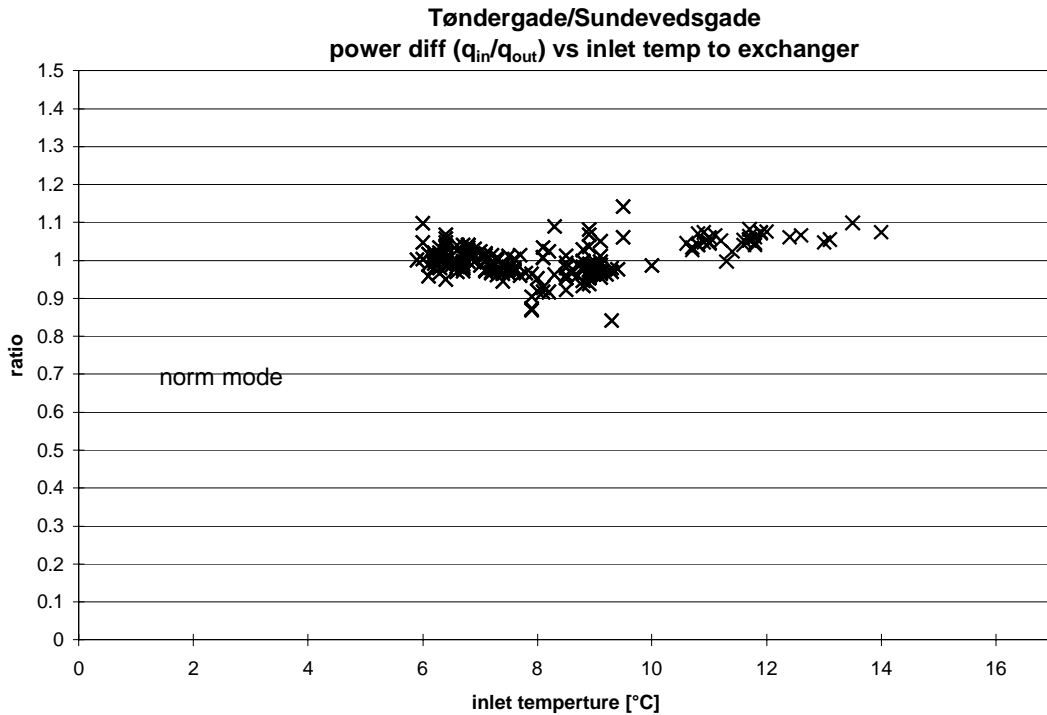


Figure 3.25. The calculated heating of the fresh air divided with the calculated cooling of the exhaust air (based on dry temperatures) in the heat exchanger for year 2000 at normal flow rate.

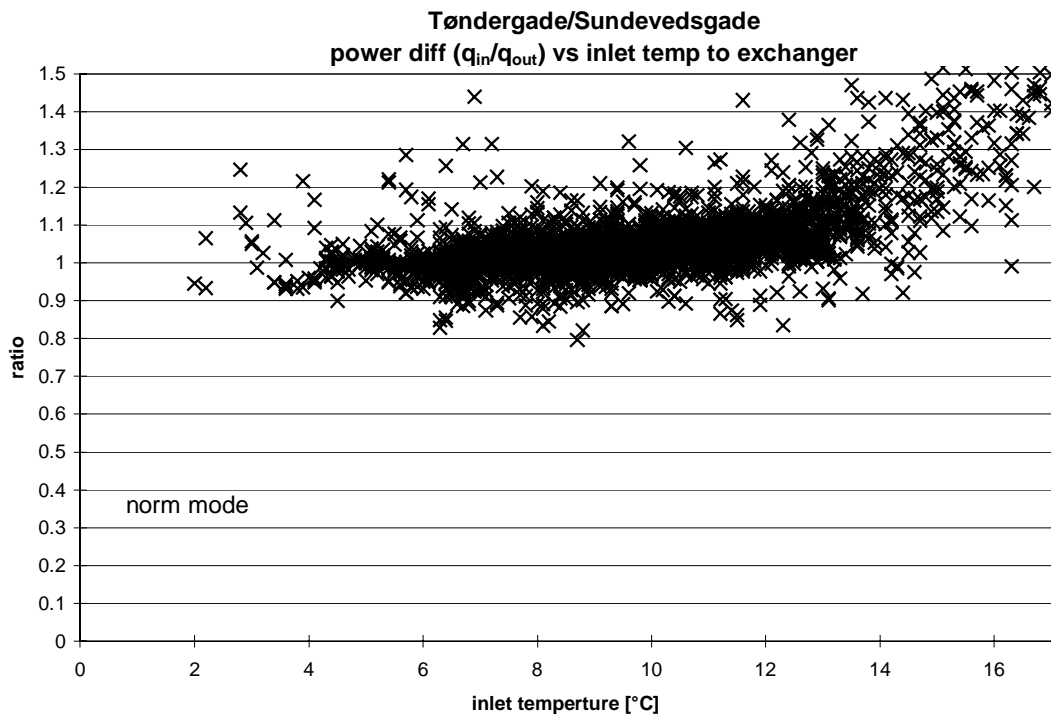


Figure 3.26. The calculated heating of the fresh air divided with the calculated cooling of the exhaust air (based on dry temperatures) in the heat exchanger for January-March 2001 at normal flow rate.

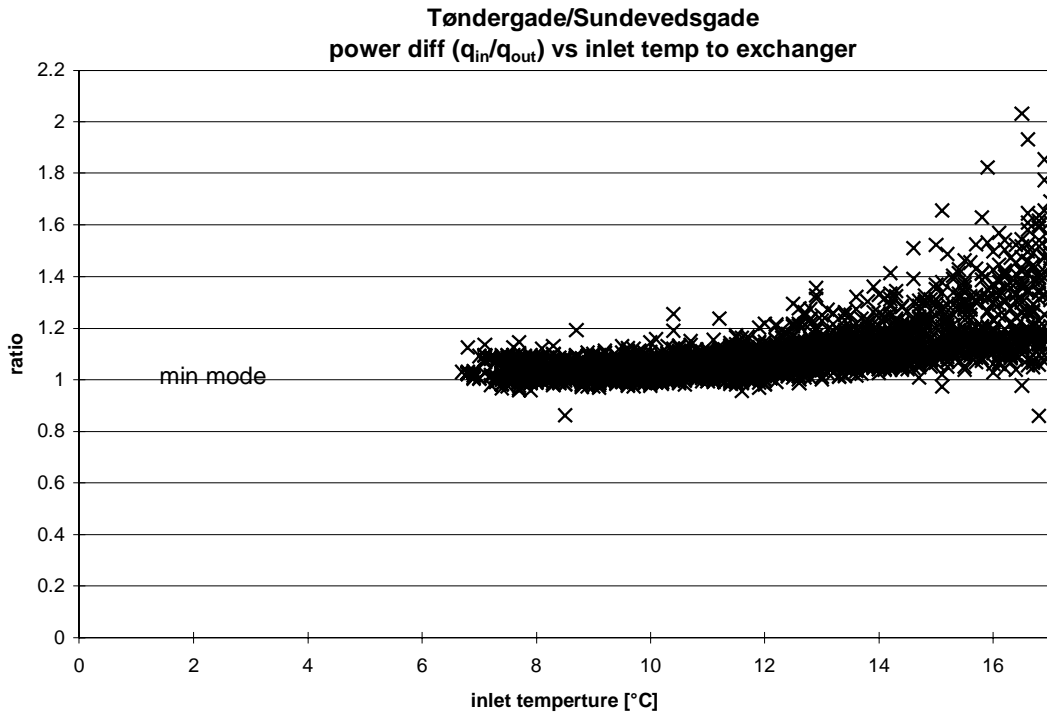


Figure 3.27. The calculated heating of the fresh air divided with the calculated cooling of the exhaust air (based on dry temperatures) in the heat exchanger for year 2000 at min. flow rate.

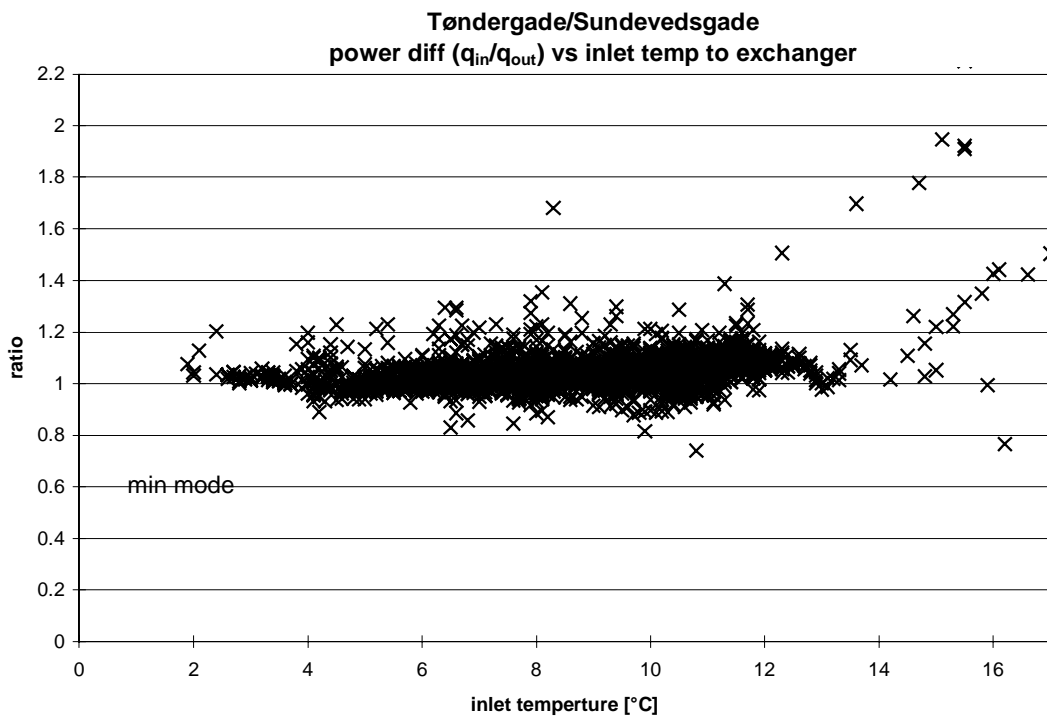


Figure 3.28. The calculated heating of the fresh air divided with the calculated cooling of the exhaust air (based on dry temperatures) in the heat exchanger for January-March 2001 at min. flow rate.

*Normal flow mode*

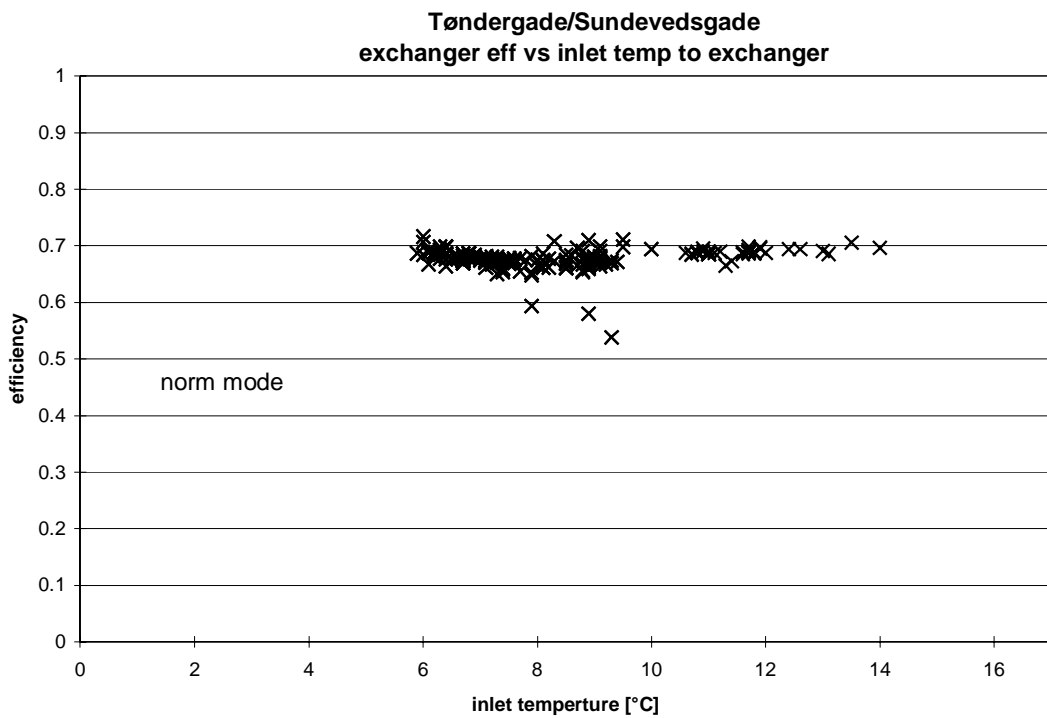


Figure 3.29. The calculated efficiency of the heat exchanger excl. the fan power (the “real” efficiency) for year 2000 at normal flow rate.

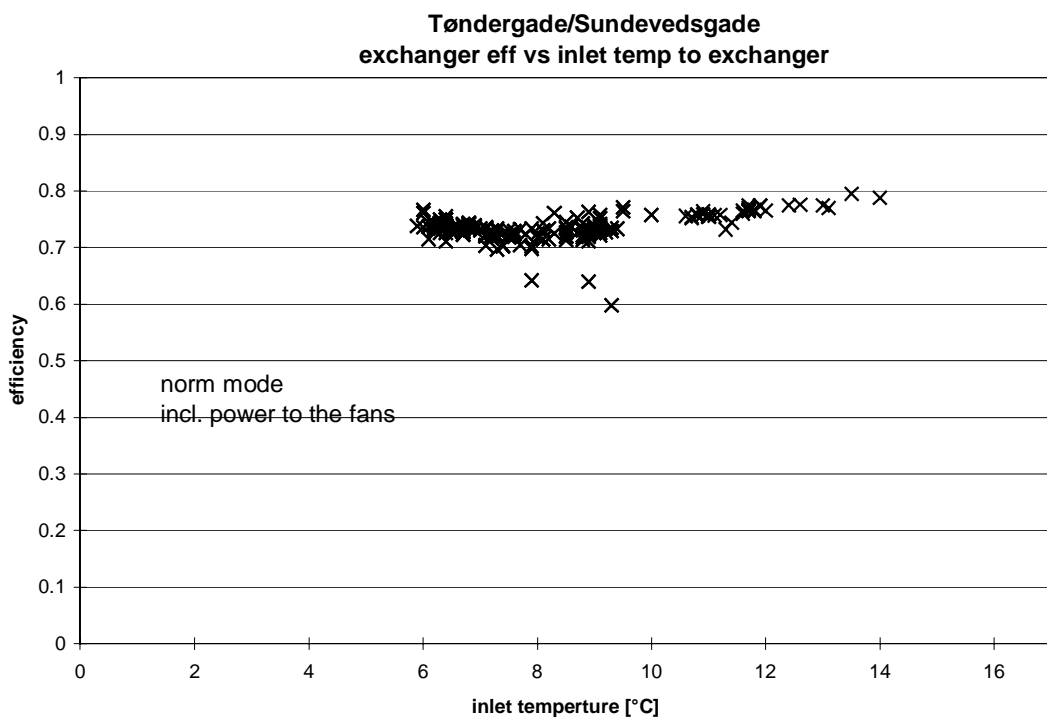


Figure 3.30. The calculated efficiency of the heat exchanger incl. the fan power for year 2000 at normal flow rate.

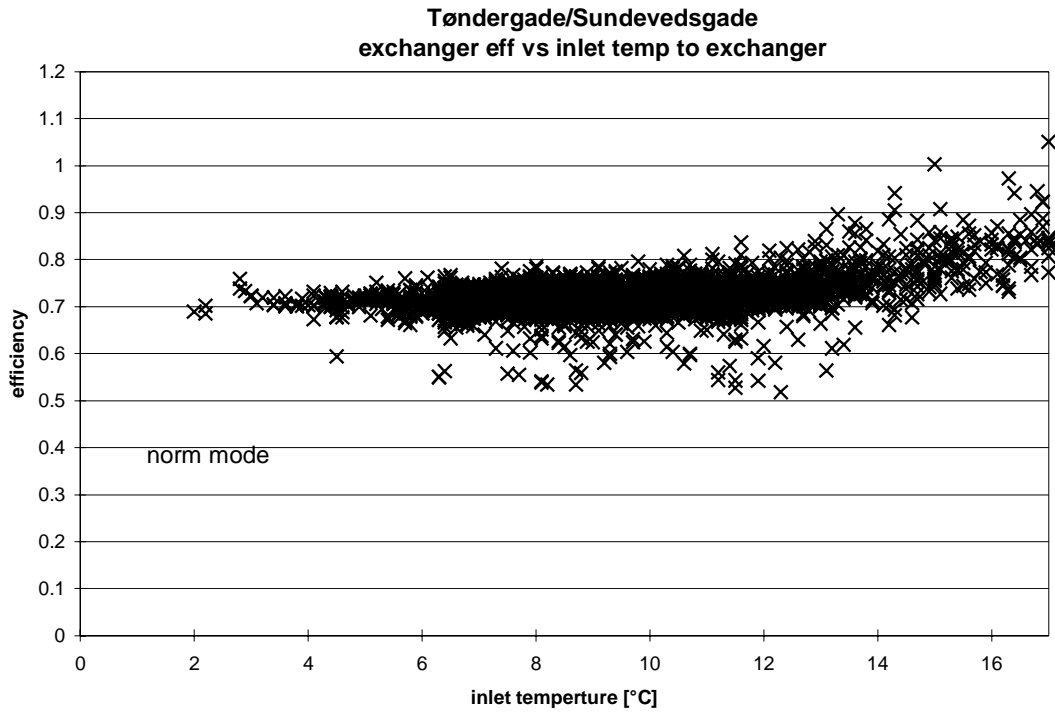


Figure 3.31. The calculated efficiency of the heat exchanger excl. the fan power (the “real” efficiency) for January-March 2001 at normal flow rate.

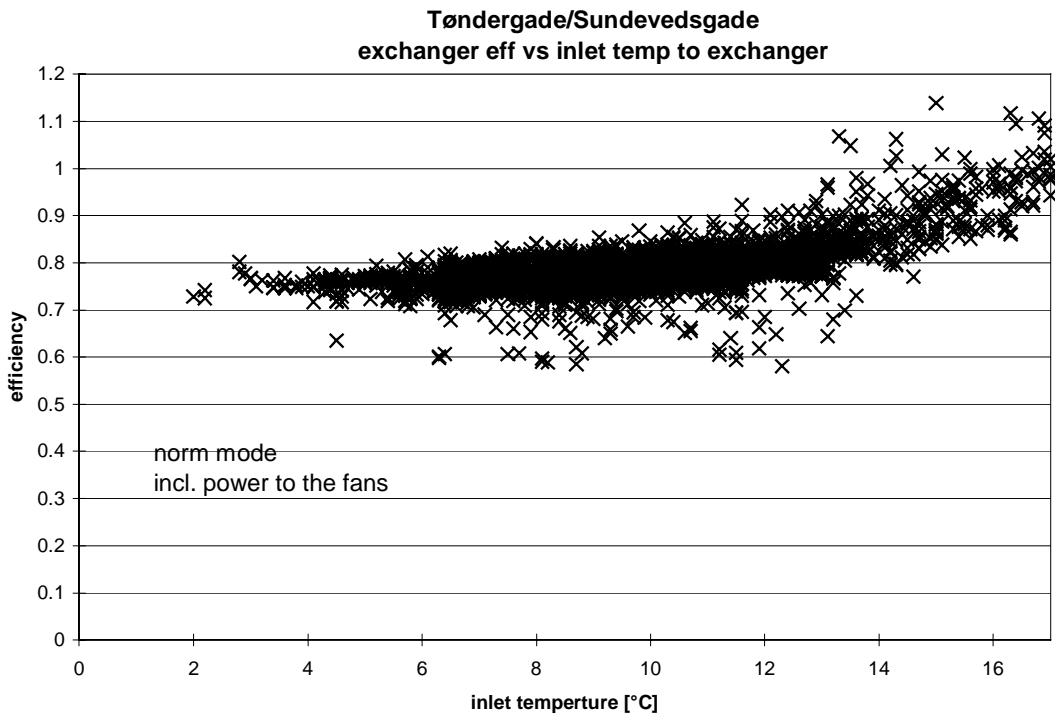


Figure 3.32. The calculated efficiency of the heat exchanger incl. the fan power for January-March 2001 at normal flow rate.

*Min. flow mode*

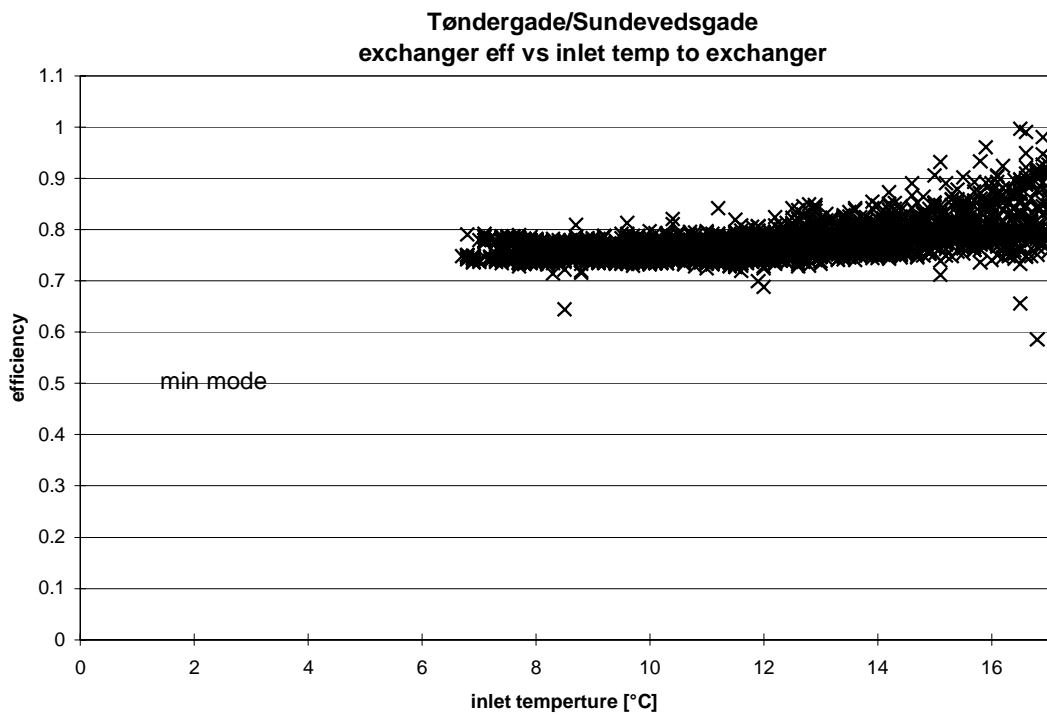


Figure 3.33. The calculated efficiency of the heat exchanger excl. the fan power (the “real” efficiency) for year 2000 at min. flow rate.

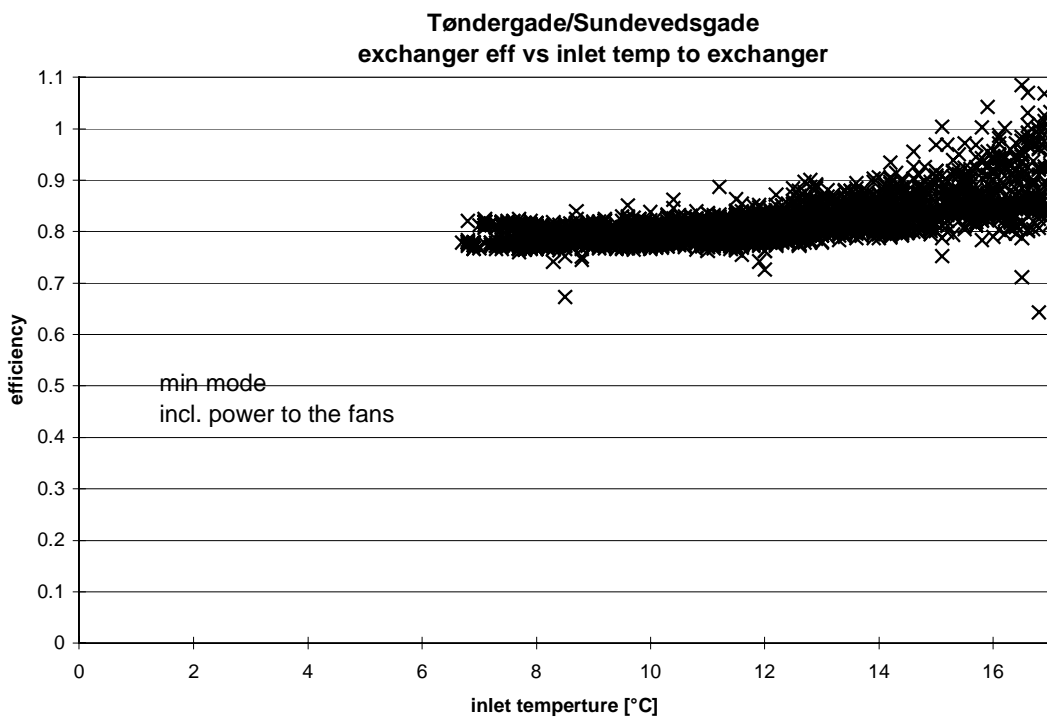


Figure 3.34. The calculated efficiency of the heat exchanger incl. the fan power for year 2000 at min. flow rate.



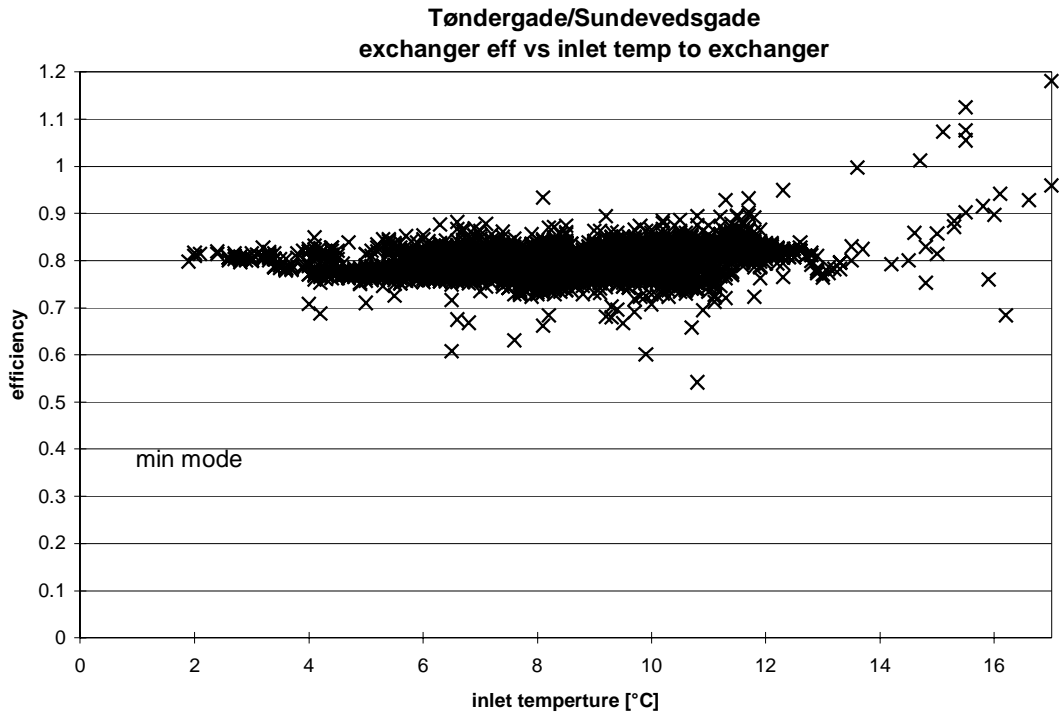


Figure 3.35. The calculated efficiency of the heat exchanger excl. the fan power (the “real” efficiency) for January-March 2001 at min. flow rate.

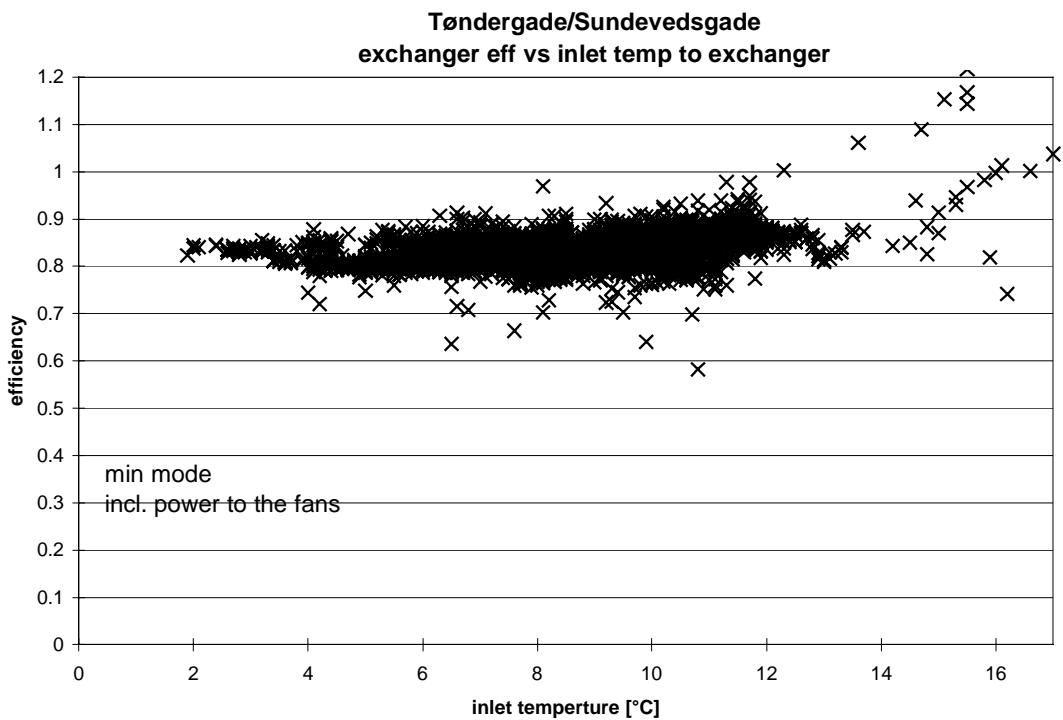


Figure 3.36. The calculated efficiency of the heat exchanger incl. the fan power for January-March 2001 at min. flow rate.

Table 3.1 shows a strange pattern – the efficiency increases with decreasing air flow rate – it should be opposite. However, the values in table 3.1 cannot be compared directly, as the two flow rates are different – except for min. mode 2000, where the two air flow rates were almost identical. The efficiency at min. mode 2001 is quite much higher than min. mode 2000, because the flow rate of fresh air here was higher than the flow rate of exhaust air.

In order to compare the efficiencies it is necessary to bring them on a form where the two air flow rates are identical, as this is the way which normally is used when comparing efficiencies of air to air heat exchangers.

### *Normalized efficiency of the heat exchanger*

It can be shown (Hansen, Kjerulf-Jensen and Stampe, 1997) that the exchanger efficiency at identical flow rates equal to the lowest flow rate is identical to the temperature efficiency for the smallest flow rate. The temperature efficiency is calculated based on the actual measured temperatures in the system.

$$\eta_{1t} = (T_{1o} - T_{1i}) / (T_{2i} - T_{1i}) \quad (3.4)$$

where:  $\eta_{1t}$  is the temperature efficiency at the smallest flow rate

$T_{1i}$  is the inlet temperature to the exchanger for the air with the smallest flow rate

$T_{1o}$  is the outlet temperature from the exchanger for the air with the smallest flow rate

$T_{2i}$  is the inlet temperature to the exchanger for the air with the largest flow rate

Figures 3.37-3.40 shows the result from applying equation 3.4 on the values from normal and min air flow rates for 2000 and 2001, while excluding the power from the fans – i.e. the efficiency of the heat exchanger alone.

In order to compensate for condensation and the heat loss the efficiency of the heat exchanger should be found at the axis to the right in the graphs. Figure 3.38 shows an unrealistic increase of the efficiency at inlet temperatures above 13°C, however, not as much as figure 3.31 and the values in figures 3.37 and 3.39-40 don't go as far as 17°C. Further figure 3.39 contains less values as figure 3.34 – this is because values where the flow rate of fresh air is higher than the flow rate of exhaust air have been rejected (although the difference between the two flow rates is small). The efficiencies and flow rates are found by extrapolation a regression lines for the values between inlet temperatures of 6 and 13°C to the axis to the right of the graphs. Doing this the figure 3.41 is obtained – however, the shown efficiencies are although less uncertain than the efficiencies in table 3.1 still a bit uncertain.

Figure 3.41 shows that the efficiency of this type of heat exchanger is between 75 and 77 % and that this efficiency is higher than measured in laboratory. The exchangers in Sundevedsgade/Tøndergade have been changed a bit compared to the exchanger tested in laboratory in order to increase the efficiency (Pedersen, 2001). The measured efficiency is rather high but a bit lower than the aim of the project – an efficiency between 80 and 90 %. This is because the heat transferring area of the heat exchangers is less than optimal in order to obtain a slim heat exchanger, which may fit into the solar walls. The heat exchangers in the type 2 systems has a larger heat transferring area and has in the Lundebjerg project (Jensen, 2001) been measured to have an efficiency of between 75 and 85%.

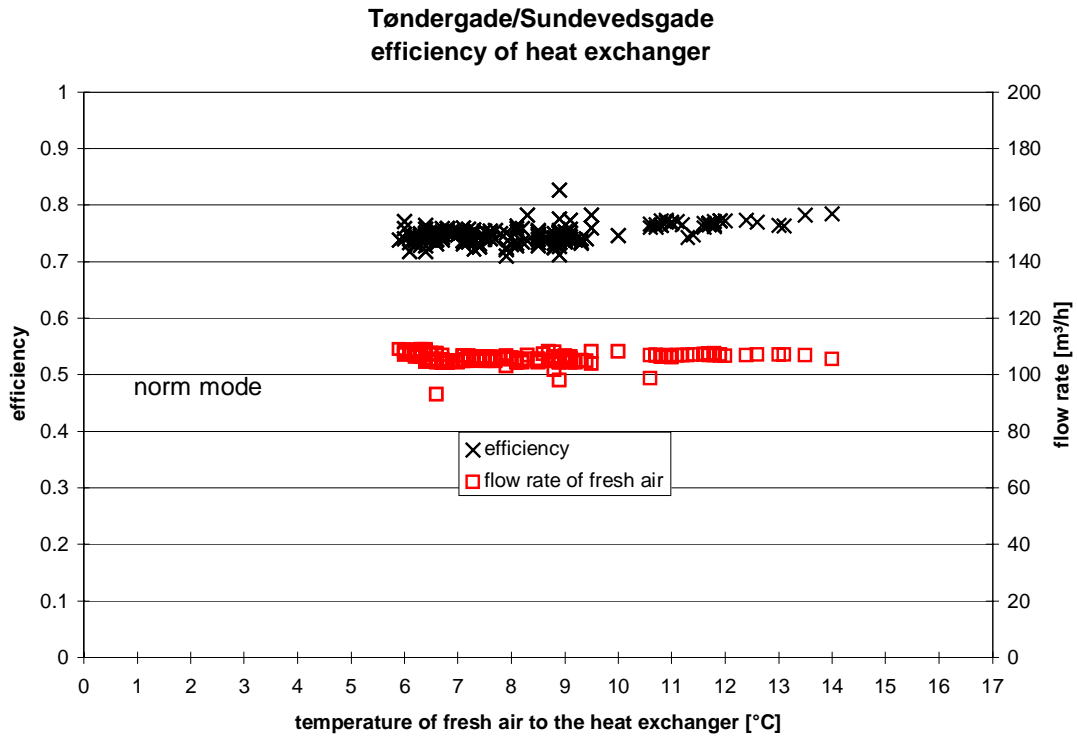


Figure 3.37. The calculated (normalized) efficiency of the heat exchanger excl. the fan power for 2000 at normal flow rate.

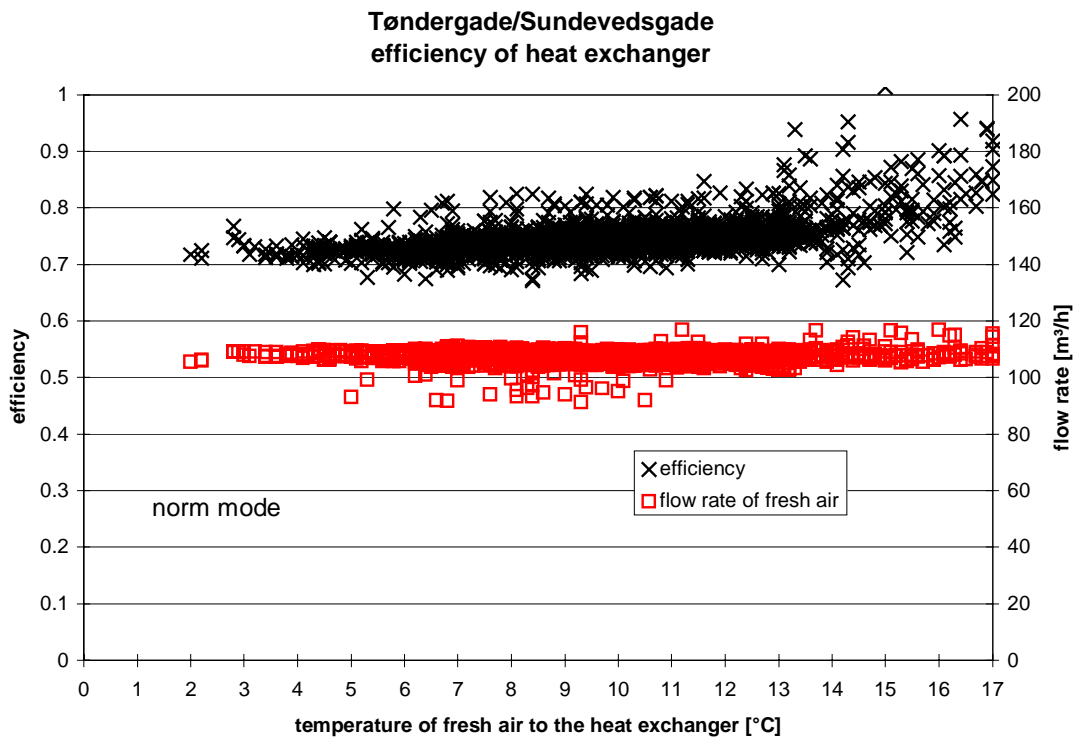


Figure 3.38. The calculated (normalized) efficiency of the heat exchanger excl. the fan power for January-March 2001 at normal flow rate.

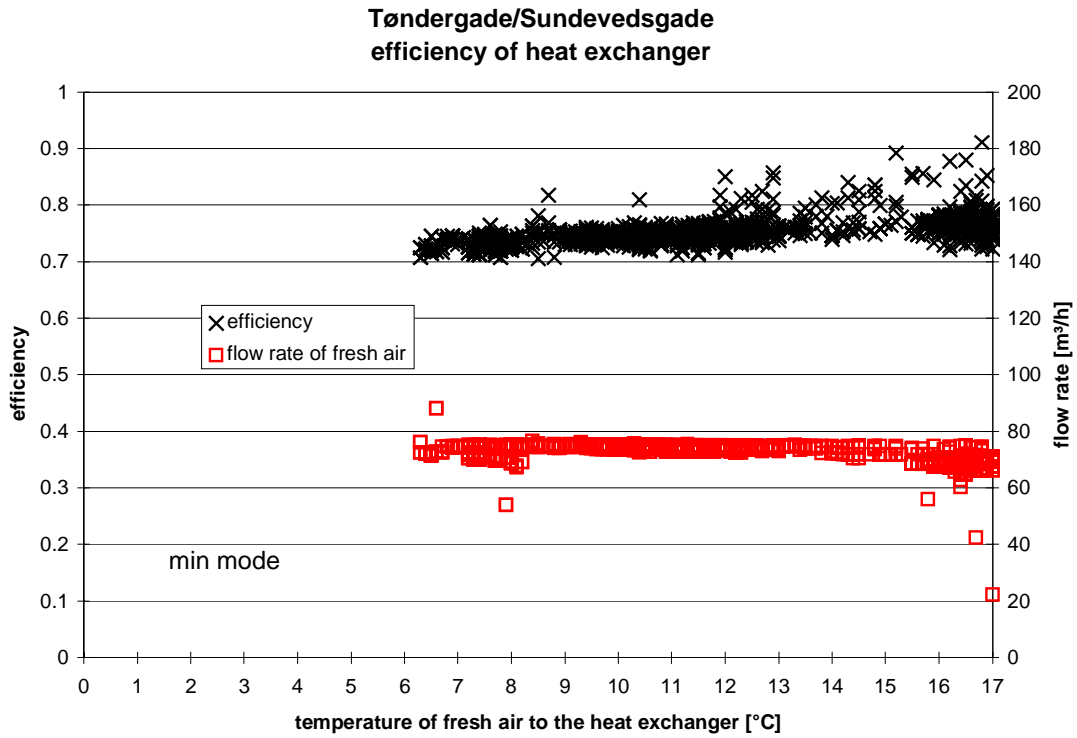


Figure 3.39. The calculated (normalized) efficiency of the heat exchanger excl. the fan power for 2000 at min. flow rate.

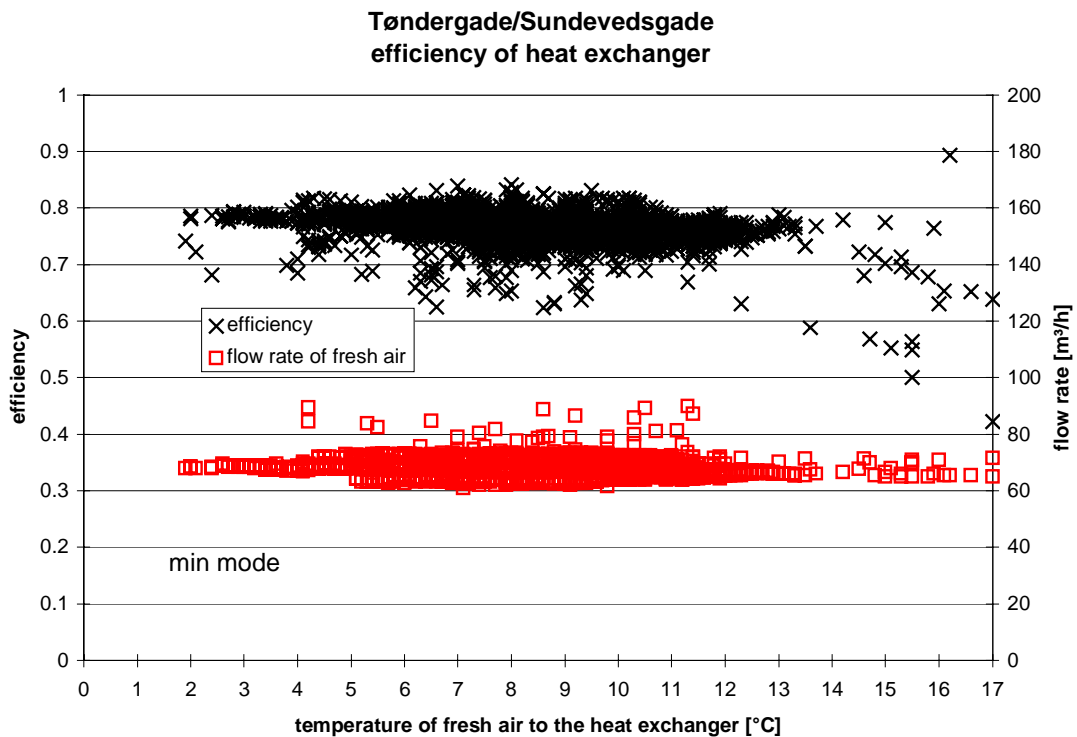


Figure 3.40. The calculated (normalized) efficiency of the heat exchanger excl. the fan power for January-March 2001 at min. flow rate.

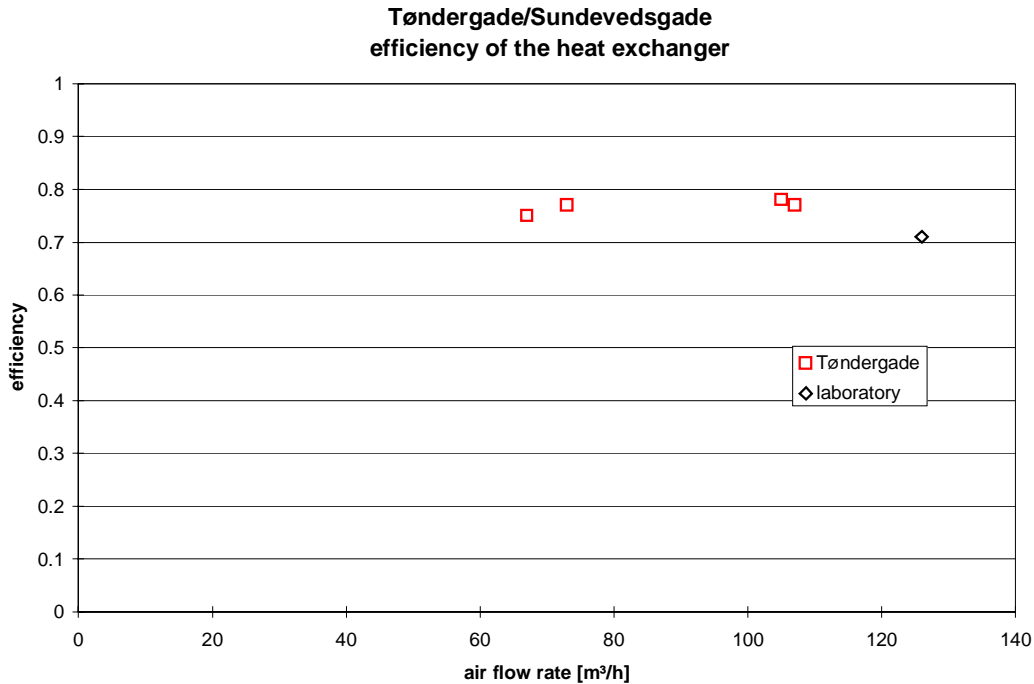


Figure 3.41. The calculated temperature efficiency found at an inlet temperature of 17°C different flow rates together with the efficiencies measured in laboratory on an earlier version of the exchanger.

### 3.3.2. Fan power

The power to the fans of the ventilation system was measured during February and March 2001. Figure 3.42 shows the dependency of the fan power on the total flow rate through the system. The total flow rate is the sum of the flow rate of fresh air and exhaust air.

The equation for the regression line shown in figure 3.42 to which the values fits very nicely is:

$$\text{fan power} = 0.00000223 \cdot \text{flow}^3 + 0.000169 \cdot \text{flow}^2 + 0.0213 \cdot \text{flow} \text{ [W]} \quad (3.5)$$

where flow is the total flow rate – i.e. the sum of fresh air and exhaust air

From figure 3.42 and equation (3.5) it is seen that the fan power at the flow rates given in the Danish building code (126 + 113 = 239 m³/h) is 45 W. This is very much lower than the max. power given in the Danish building code – 87 W. However, to the 45 W the power loss of the ac/dc converter has to be added. The power loss of the ac/dc converter is:

$$\text{power loss} = 5.6 + 0.0278 \cdot P \text{ [W]} \quad (3.6)$$

where P is the total power consumption from the grid of the fans incl. the loss of the ac/dc converter

The total power consumption of the ventilation system at a flow rate of in total 239 m³/h is then 45 + 7 = 52 W, which still is 40 % lower than required by the Danish Building code. The

fan powers in figures 3.42 should be divided with 0.96 (efficiency of the PV-mixer in grid mode – see later) when then the power is delivered entirely from the grid.

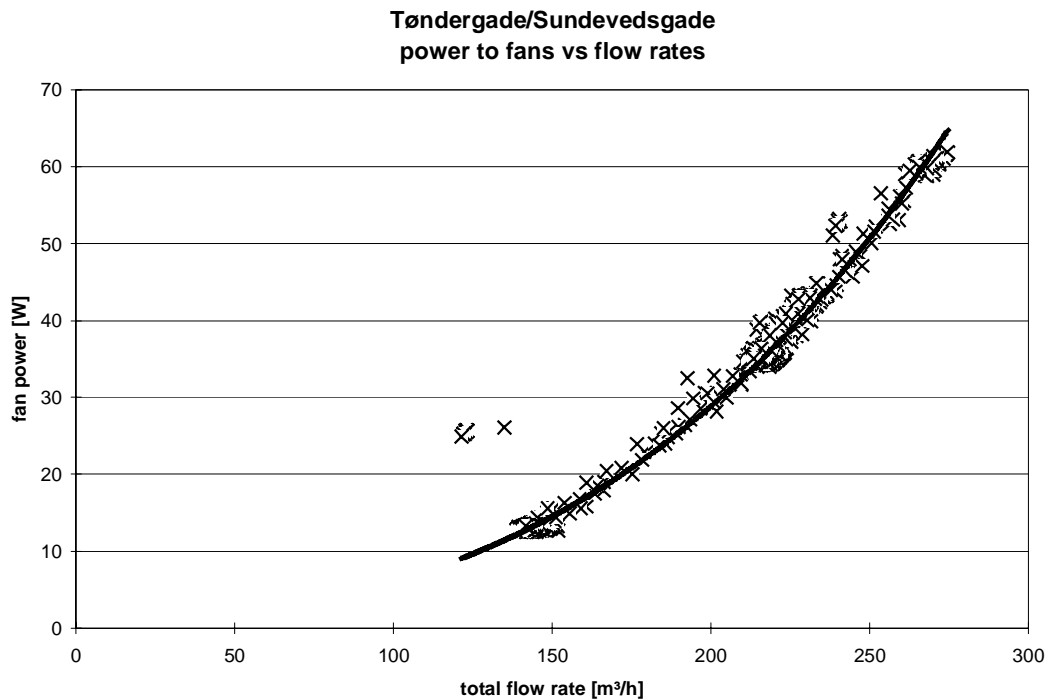


Figure 3.42. The dependency of the fan power on the total flow rate.

### 3.3.3. Temperatures in the solar wall

The evaluation of the temperatures in the solar wall during sunshine is rather difficult as the solar walls are situated on the walls facing a courtyard as seen in figure 1.1. The sun will especially during winter time first hit the solar wall at Tøndergade just before noon – and then at full power, while the sun will start to shine on the solar wall on Sundevedsgade also around noon. It is further not possible to characterize the solar wall in the same way as solar air collectors as done for Lundebjerg (Jensen, 2001) as only one flow rate has been measured. Even if all flow rates had been measured the characterization as solar air collector would still have been very difficult as the air leaves the solar wall at different levels/floors.

Figures 3.43-45 show an evaluation of the temperatures in the solar wall at Tøndergade using data from 2000 and January-March 2001. Figure 3.43 shows the temperature increase compared to ambient when air is taken from the solar wall to the apartment Tøndergade 1, 4 to the right, while figure 3.44 shows values during situations without this air flow rate. Only data from after 12:00 has been used in order to give a clearer picture of the pattern of the temperature – i.e. the rapid heating up as seen in figure 3.46 has been excluded. In this way it will further be possible to transfer the findings to other situations without shading. Figures 3.43-45 show the inlet temperature (T4 in figure 2.2) minus ambient temperature and PV-panel temperature minus ambient temperature at the fourth floor – the inlet temperatures at the lower floors will be lower as seen in figures 3.47, while the PV-temperature of the lower panels won't be very different from the PV-temperature shown in figure 3.43-45 due to the very low air speed in the solar wall – below 0.5 m/s, which is in the same order of magnitude as for buoyancy driven air flows. The equations for the regression lines are enclosed in the figures.

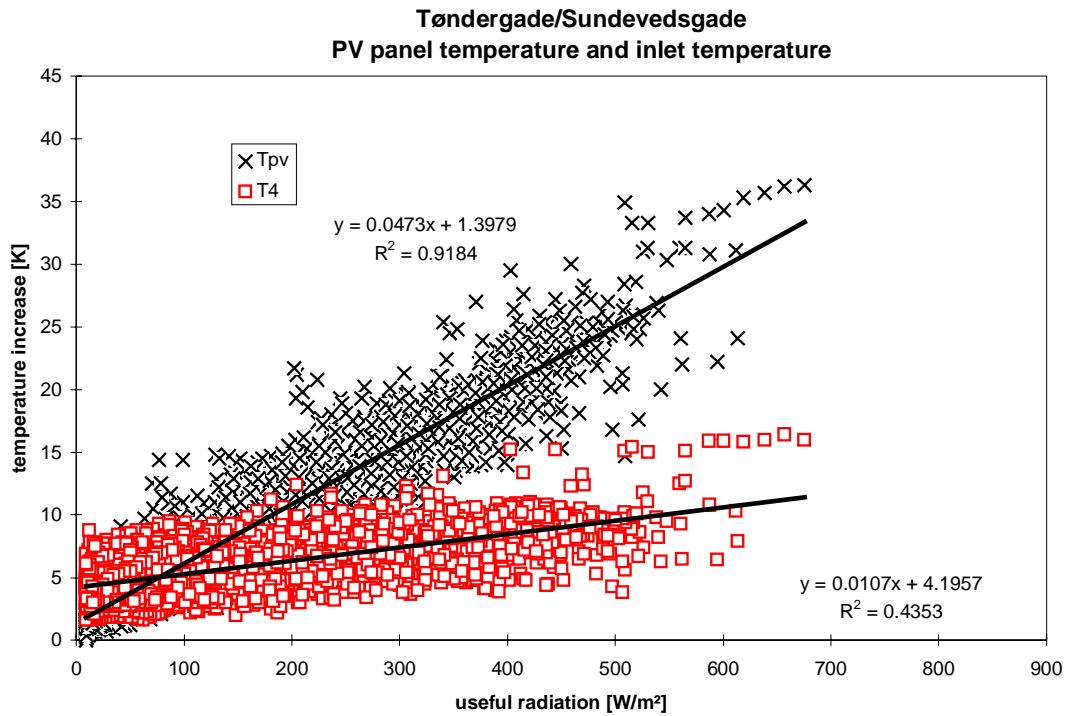


Figure 3.43. The dependency of the temperatures in the solar wall on the useful solar radiation during periods in 2000 **with** air flow to the apartment Tøndergade 1, 4 to the right. The shown temperature differences are T4 and Tpv minus the ambient temperature.

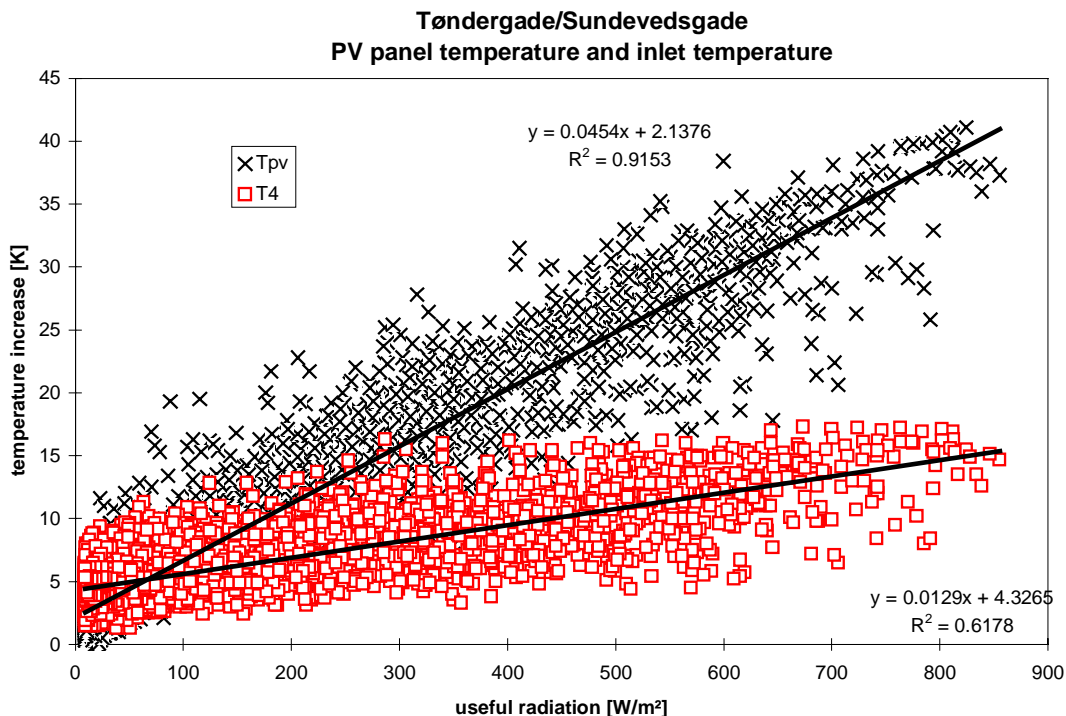


Figure 3.44. The dependency of the temperatures in the solar wall on the useful solar radiation during periods in 2000 **without** air flow to the apartment Tøndergade 1, 4 to the right. The shown temperature differences are T4 and Tpv minus the ambient temperature.

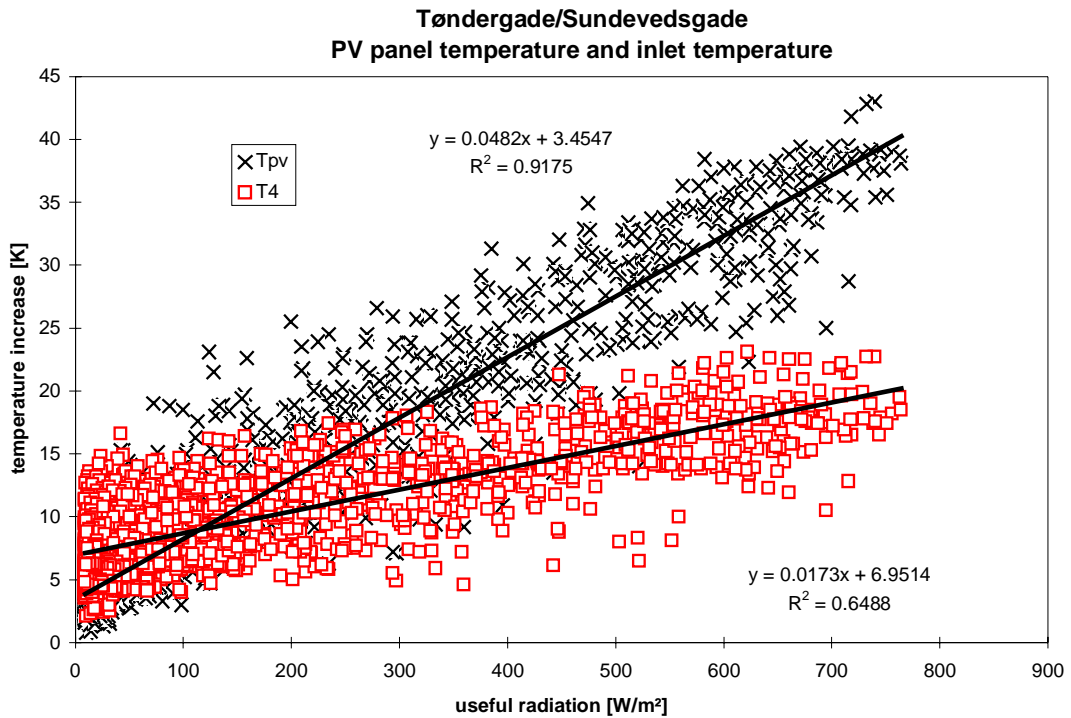


Figure 3.45. The dependency of the temperatures in the solar wall on the useful solar radiation during January-March 2001 **with** air flow to the apartment Tøndergade 1, 4 to the right. The shown temperature differences are T4 and Tpv minus the ambient temperature.

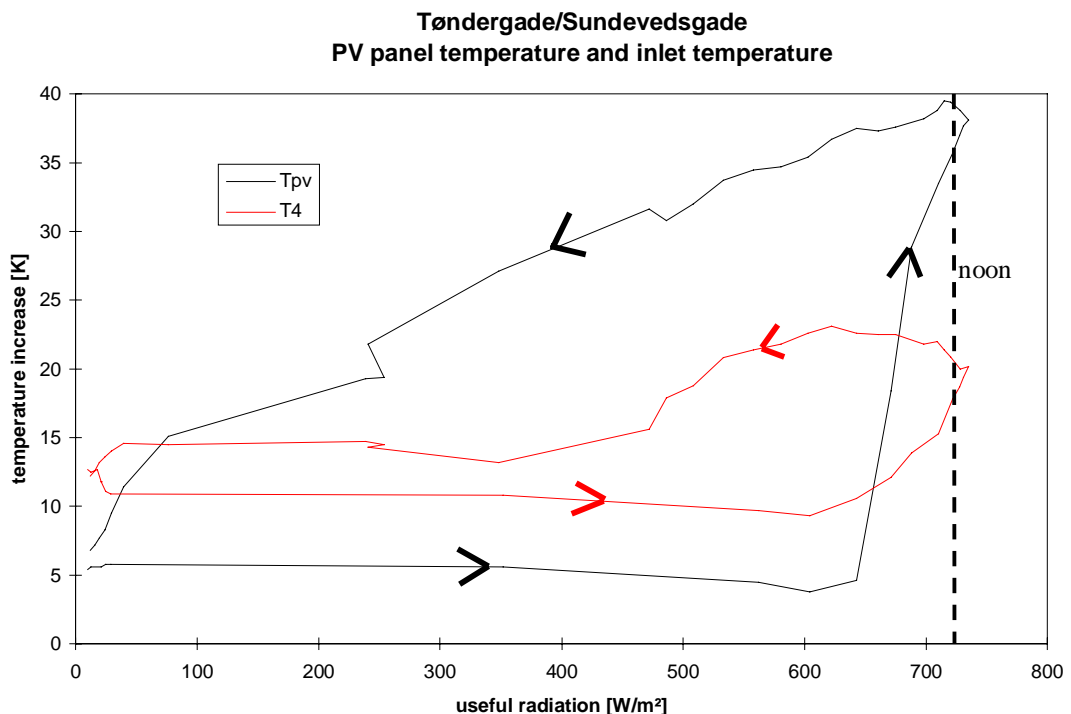


Figure 3.46. The progress during daytime of the temperature difference at T4 and the PV-panel for February 3, 2001.



The scattering of the values in figure 3.43-45 is partly due to the wind and partly due to the thermal capacity of the solar wall. The wind induces different heat losses depending on the wind speed, while the thermal mass brings the temperatures out of phase with the sun at changing radiation levels.

Figures 3.43-35 show as expected that the temperature of the PV-panel is lower than the air temperature in the solar wall during low or no solar radiation while being increasingly higher at increasing solar radiation ending at being more than 20 K higher than the air temperature in the solar wall. This indicates that the cooling of the PV-panel by the air flow in the solar wall is not efficient, which is explained by the very low air speed of the air in the solar wall – in the same order of magnitude as for buoyancy driven air flows.

Figures 3.43-45 shows identical pattern during summer and winter (2000 covers both summer and winter) and with and without air flow in the solar wall (well actually only with and without air flow to Tøndergade 1, 4 to the right). This indicates that the regression lines may be used more general to evaluate the savings of the solar wall on a more general basis – this will be done in section 3.4.

Figure 3.47 shows the inlet temperatures to the heat exchangers minus the ambient temperature at all floors. The figure shows only little difference in the inlet temperature to the 2<sup>nd</sup>, 3<sup>rd</sup> and 4<sup>th</sup> floor, while the inlet temperature to the 1<sup>st</sup> floor is considerably lower due to the close location to the air inlet to the solar wall as shown in figure 2.2.

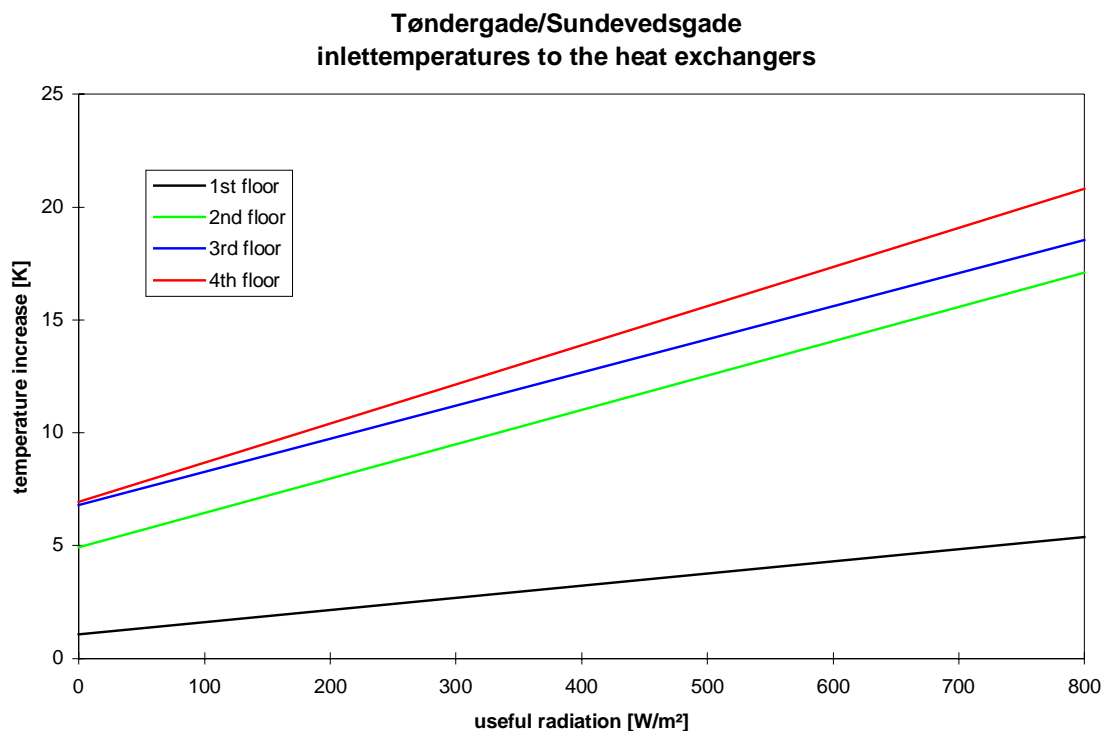


Figure 3.47. The inlet temperature to the heat exchangers in the solar wall minus the ambient temperature at different floor levels dependent on the useful radiation.

Figures 3.43-45 indicate that the temperature of the air at no solar radiation stays 5-7 K above the ambient temperature. This is further evaluated in figures 3.48-49. These figures show the

absolute temperature at T4 and the temperature difference between T4 and ambient as a function of the ambient temperature. The temperatures are found during night-time and are from October-November 2000 and January-February 2001. The equations for the regression lines as given in the figures. The scattering of the values in figure 3.48-49 is partly due to the wind and partly due to different air flows through the solar wall. The wind induces different heat losses depending on the wind speed, while the temperature difference between the air in the solar wall and the ambient is directly dependent on the air flow rate of fresh air to the solar wall.

Figures 3.48-49 show that the temperature difference between the air in the solar wall and ambient increases with decreasing ambient temperature. This is due to the heat loss from the shaft behind the solar wall which as seen in figures 3.9-10 is held at a rather high temperature level. The wall between the shaft and the solar wall is further a non insulated half stone brick wall with an U-value of approx. 4 W/Km<sup>2</sup>. The area of this wall is about 3 m<sup>2</sup>. The maintenance door (see figure 1.10) to the solar wall is also facing heated floor area. The U-value of this door is estimated to be about 3 W/Km<sup>2</sup> and has an area of approx. 0.4 m<sup>2</sup>. The heat loss from the dwelling is thus considerable. It is, therefore, no wonder that the air temperature in the solar wall is so high during periods with no solar radiation. Part of the heat loss is recovered due to the intake of fresh air from the solar wall. However, it is only a smaller part which is recovered due to the low air flow rates which especially occurs during the night as the tenants tends to run the ventilation systems at min. mode or shut down the fresh air fan completely. This will further be evaluated in section 3.4.

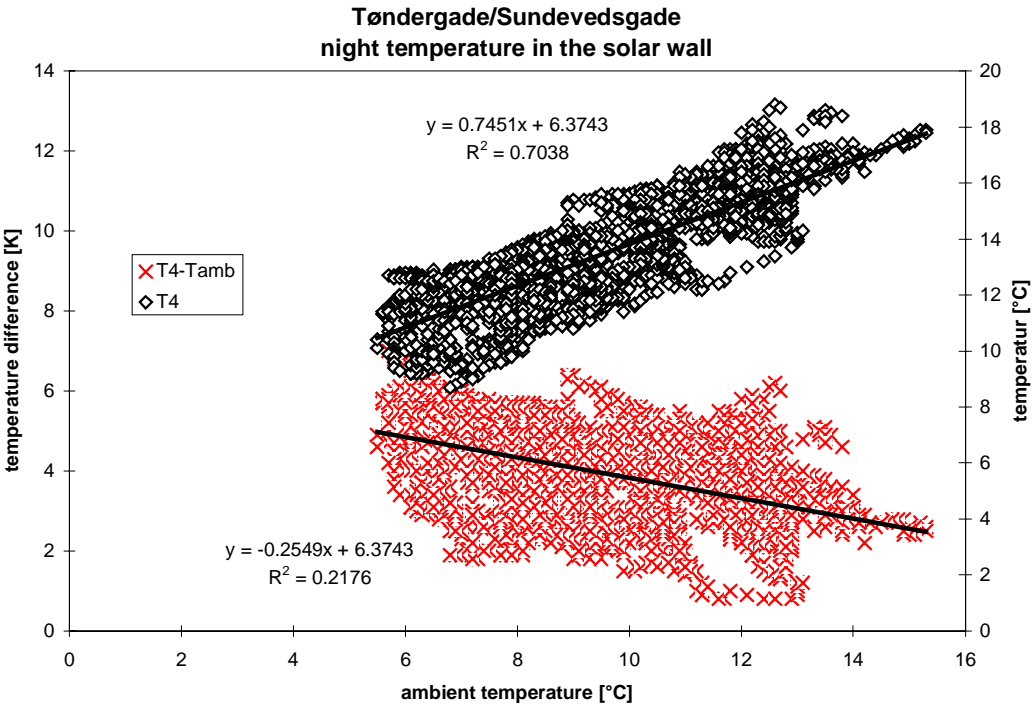


Figure 3.48. Nighttime temperatures in the solar wall – from October-November 2000.

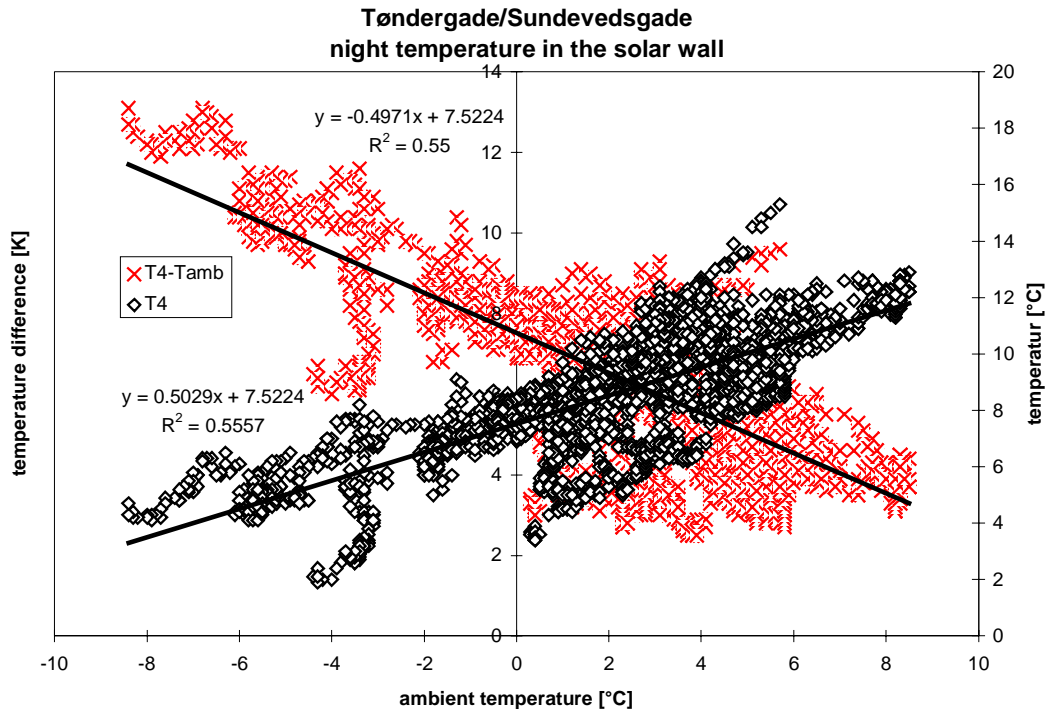


Figure 3.49. Nighttime temperatures in the solar wall – from January-February 2001.

### 3.3.4. The PV-mixer

The PV-mixer was one of the new features of the PV-VENT systems. It is therefore of special interest to evaluate this component. The objective of the PV-mixer is that it should be able to maintain the desired power to the fans while utilizing as much PV-power as possible.

The actual operation is shown in figures 3.15-20. The chosen concept of the PV-mixer does that it cannot utilize excess power from the PV-panel above the actual demand. The size of the PV-panel should therefore carefully be dimensioned in accordance with the actual power demand in order not to waste PV-power. If the power from the PV-panel is larger than the demand an inverter feeding the grid with the PV-power will most properly be a better solution.

The efficiency of the PV-mixer is evaluated in the following.

#### *Grid mode*

Table 1.3 shows the efficiency of the PV-mixer in pure grid mode. As the switch mode technology is utilized in the PV-mixer the shown efficiency of the PV-mixer of 96 % is constant.

#### *PV mode*

Table 1.4 shows the efficiency of the PV-mixer in pure PV mode. Table 1.4 indicates that the efficiency in pure PV mode is dependent on the actually power demand. Figure 3.50 shows the measured efficiency of the PV-mixer in the systems at pure PV-mode. In figure 3.51 these

values are shown together with the values from table 1.4 and values from Lundebjerg (Jensen, 2001). The equation for the regression line is further shown in the figure.

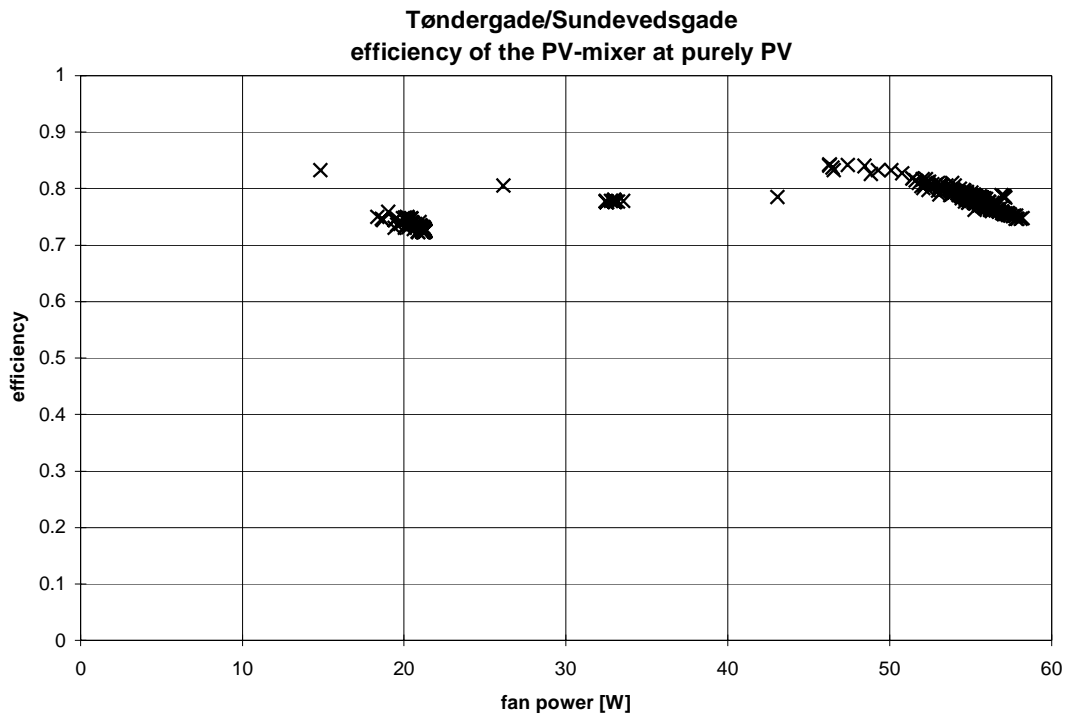


Figure 3.50. The efficiency of the PV-mixer at pure PV-mode as a function of the demand measured in Sundevedsgade/Tøndergade.

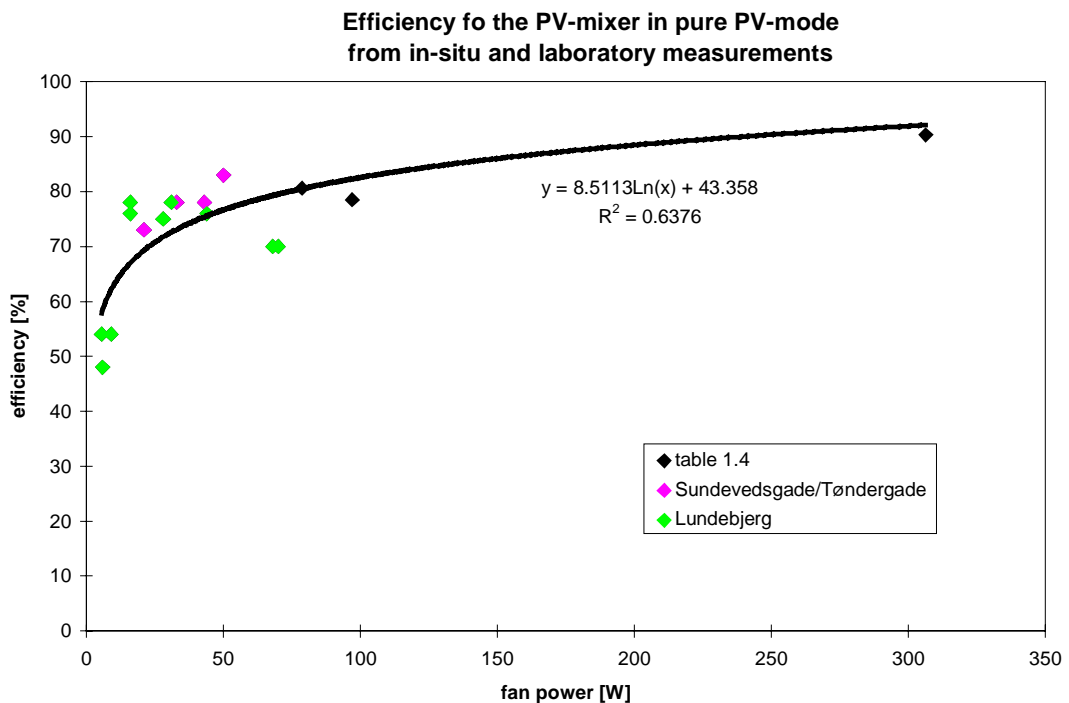


Figure 3.51. The efficiency of the PV-mixer at pure PV-mode as a function of the demand measured in Sundevedsgade/Tøndergade, Lundebjerg (Jensen, 2001) and in laboratory (table 1.4).

The max. power which the PV-mixer can deliver to the fans is 300 W. This means that the max. efficiency of the PV-mixer in pure PV-mode is 90 %, while slowly decreasing to 80 % at a demand of about 50 W. At lower demands figure 3.51 indicates that the decrease of the efficiency will be much faster – however, the measured values are rather scattered in this area indicating a large uncertainty.

### ***Mixed PV and grid mode***

The efficiency of the PV-mixer in mixed mode is rather difficult to obtain. The efficiency of the grid part will always be 96 %. Based on this the efficiency can be found based on the measured inputs from the grid and the PV-panels and the measured output to the fans. However, the measured values are too scattered to give an answer. In order to give an impression of the efficiency of the PV part during mixed mode operation the values from table 1.2 and test 3 from table 1.3 has been used in the following way:

$$\eta_{PV} = (P_{fan} - P_{grid} * 0.96) / P_{PV} \quad (3.7)$$

where  $\eta_{PV}$  is the efficiency of the PV part in mixed mode

$P_{fan}$  is the measured consumption of the fan

$P_{grid}$  is the measured power from the grid:  $U_{grid} * I_{grid}$

$P_{PV}$  is the measured power form PV:  $U_{pv} * I_{pv}$

0.96 is the efficiency of the grid part of the PV-mixer

The results are shown in figure 3.52. The values are for a demand of about 276 W and the value on the x-axis is the PV-power divided with the demand in order to obtain a normalized expression which may be used in other situation – e.g. the simulations in the next section.

Figure 3.52 indicate that the efficiency of the PV-mixer is linear dependent on the ratio between the power for PV and the power demand of the fans. At zero PV power the efficiency is about the efficiency of the PV-mixer at pure grid mode – 0.96, while it when going towards pure PV-mode decreases linearly towards the efficiency in pure PV-mode as shown in figure 3.51.

This means that the efficiency for the PV part of the PV-mixer for other fan powers may be found as a linearly function based on two points: 0.96 at no PV-power and a value found in figure 3.51 for pure PV-mode dependent on the actual power demand of the fans. When combining the information from figures 3.50 and 3.51 the following equation appears:

$$\eta = a*(PV \text{ power} / \text{fan power}) + 0.96 \quad (3.8)$$

where:  $\eta$  is the efficiency of the PV-part at mixed PV/grid mode

$a = (b + c*\text{fan power} + d*\text{fan power}^2)/(1 + e*\text{fan power} + f*\text{fan power}^2 + g*\text{fan power}^3)$

$b = -0.2405$

$c = -0.00593$

$d = 1.36*10^{-5}$

$e = 0.04232$

$f = 1.1646*10^{-4}$

$g = -1.1374*10^{-7}$

0.96 is the efficiency of the grid part

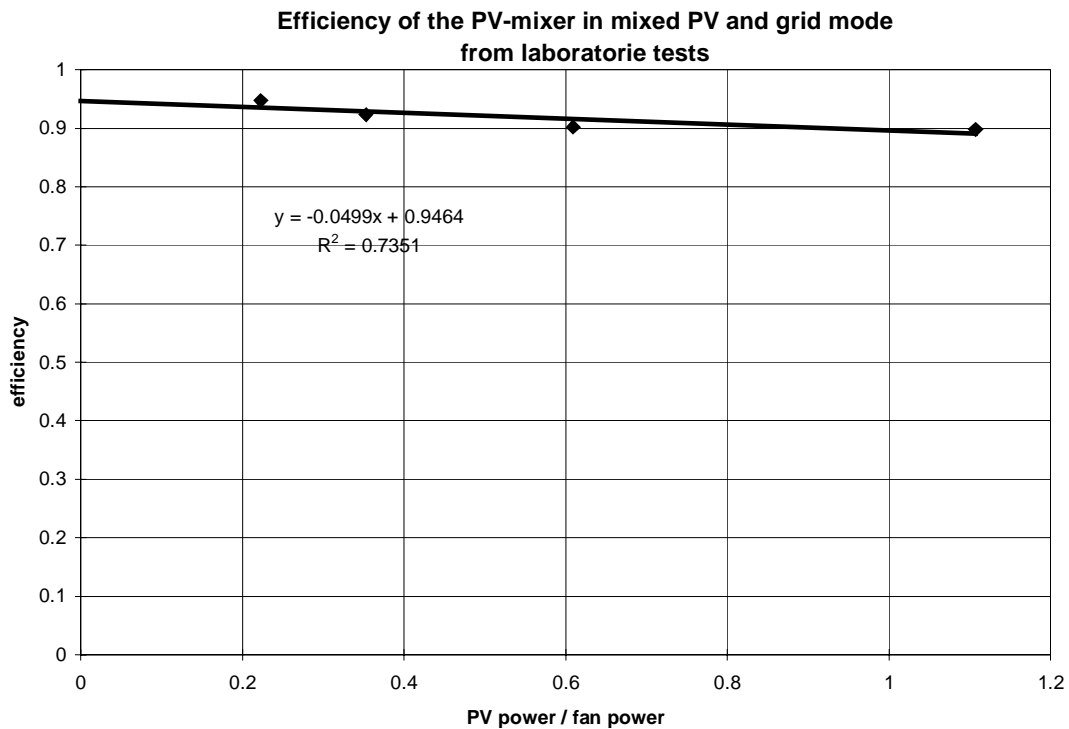


Figure 3.52. The efficiency of the PV-mixer at mixed PV and grid mode as a function of the PV power divided with the fan power - measured in laboratory (table 1.2).

It is not possible to prove that the above conclusion is correct, however, it is believed that the relationship is sufficiently correct in order to allow for the calculations in the next section.

### 3.4. Obtained and obtainable savings of the system

This section deals with the actual savings from the system as it has been run during the measuring period. The section further contains calculations regarding the savings if the system has been more optimal – i.e. being run in normal flow mode, no shading on the solar wall, etc.

For both sub-sections the following has been calculated:

- saving in ventilation losses due to the heat exchanger
- savings due to the pre-heating of the air in the solar wall
- heat loss from the apartment to the solar wall
- savings in electricity consumption due to the PV-panels
- waste of PV-energy due to a lower demand than the peak power of the PV-panels

#### 3.4.1. Obtained savings

Using the measurements it is possible to calculate the yearly performance of the system from April 1, 2000 – March 31, 2001 for the actual running of the system. It is further possible to estimate the savings of the heat exchanger if the fresh air had not been taken from the solar wall but directly from ambient. Measurements for the PV part of the system are only available

for part of the year – the energy flows thus have to be calculated based on the findings in section 3.3.4.

A computer program, which partly calculates the energy flows directly based on the measurements partly, simulated the PV performance and thermal performance of the heat exchanger without the solar wall has been created. The features of the program are listed below.

### ***Computer program***

The thermal calculations have only been carried out if the fresh air fan had been switched on and when the ambient temperature was below 17°C in order to exclude periods without heating demand. The model does not include a thermal model of the building – i.e. calculations of the actual heating demand of the building. This is why the above restrictions have been applied.

### Pre-heating

The actual heat flow from the apartment due to the exhaust and the pre-heating of the fresh air in the solar wall and heat exchanger has been calculated directly based on the measured air flow rates and temperatures in the system.

The performance of the heat exchanger without pre-heating in the solar wall has been calculated/simulated in the following way:

The actual efficiency of the heat exchanger has been calculated using equation 3.1 (page 26). The temperature of the fresh air after the heat exchanger has been calculated in the following way:

$$T = T_{\text{amb}} + \eta \cdot (T_{\text{exh}} - T_{\text{amb}}) \cdot \rho_{\text{exh}} / \rho_{\text{fr}} \cdot c_{p_{\text{exh}}} / c_{p_{\text{fr}}} \cdot V_{\text{exh}} / V_{\text{fr}} \quad (3.9)$$

where  $\eta$  is the actual efficiency of the heat exchanger incl. the fan power (figures 3.30, 3.32, 3.34 and 3.36) in order to account for the heat delivered to the air from the fans

- $\rho$  is the density of air
- $c_p$  is the heat capacity of air
- $V$  is the flow rates of air
- subscript amb indicate ambient
- subscript exh indicate exhaust air
- subscript fr indicate fresh air

When the temperature for the fresh air after the heat exchanger (for the case of no pre-heating) has been found the pre-heating in the heat exchanger can be found. One problem with equation 3.9 is that the efficiency of the heat exchanger as shown in figures 3.29-36 is dependent on the inlet temperature. The ambient temperature has been lower than the actual inlet temperature to the heat exchanger. This means that 3.9 leads to a bit too high inlet temperature of fresh air to the dwelling, which again favour the case of no pre-heating in the solar wall a bit

When having the savings of the system with and without pre-heating of the fresh air in the solar wall the benefit of the solar wall may be evaluated.

The energy transferred to the fresh air in the solar wall has been calculated based on the actual flow rate of fresh air, the ambient temperature and the temperature in the solar wall. The calculations have been divided in day and night in order to be able to evaluate the effect the pre-heating due to the sun and due to the heat loss from the building to the solar wall.

#### Heat loss from the apartment to the solar wall

The wall between the shaft and the solar wall is as mentioned earlier a non insulated half stone brick wall with an U-value of approx. 4 W/Km<sup>2</sup>. The area of this wall is about 3 m<sup>2</sup>. The maintenance door (see figure 1.10) to the solar wall is also facing heated floor area. The U-value of this door is estimated to be about 3 W/Km<sup>2</sup> and has an area of approx. 0.4 m<sup>2</sup>.

The heat loss to the solar wall per dwelling may be calculated in the following way:

$$Q = (U_w \cdot A_w + U_d \cdot A_d) \cdot (T_{\text{shaft}} - T_{\text{solarwall}}) \quad (3.10)$$

where U is the heat loss coefficient  
A is the area of the construction facing the wall  
subscript w stands for wall  
subscript d stands for maintenance door

The calculations have as for the pre-heating in the solar wall been divided in day and night in order to be able to compare the losses with the pre-heating for the two periods.

#### Fan power and savings due to the PV-panels

The actual fan power has been calculated using equation 3.5 (page 51).

The losses due to the transformer has been calculated using equation 3.6 (page 51). Losses in the wiring are not considered, as these should be as low as 2-3% and thus far less than the uncertainty of the calculations.

The potential power from the PV-panels has been calculated using equation 3.2 (page 27). The method described on page 27 for calculating the useful radiation has also been applied.

How large part of the fan power which actually can be covered by PV has been calculated using the equation in figure 3.51 (page 58) and equation 3.7 (page 59).

Based on the above the following energy flows has been calculated: Energy to fans with and without PV, energy delivered to the PV-mixer from the PV-panels and PV energy not utilized due to too low demands.

#### ***Calculated energy flows***

The calculations have been divided in 2000 and 2001, because the system was run rather well in 2001 while it in 2000 was run improperly. Table 3.2 shows the results from the calculations.



Table 3.2 shows major differences between the two years, which of course is caused by the improper running of the system in 2000.

	2000 kWh	2001 kWh	year kWh
<b>Heat exchanger</b>			
Energy in the exhaust air	1640	1217	2857
Energy in the inlet air incl. pre-heating in the solar wall	768	1100	1868
Energy in the inlet air exc. pre-heating in the solar wall	713	993	1706
Benefit of pre-heating in the solar wall <sup>1)</sup>	55	107	162
<b>Solar wall</b>			
Energy to the air from the solar wall – day	129	246	375
Energy to the air from the solar wall – night	149	230	379
Total energy to the air from the solar wall <sup>2)</sup>	278	476	754
Losses to the solar wall – day	143	139	282
Losses to the solar wall – night	212	221	433
Total losses to the solar wall <sup>3)</sup>	355	360	715
<b>Fans and PV</b>			
Energy to the fans from the grid - without PV	159	68	227
Energy to the fans from the grid - with PV	146	60	206
Benefit of PV <sup>4)</sup>	13	8	21
PV energy delivered to the PV-mixer	18	9	27
Not utilized PV energy	23	2	25

Table 3.2. Yearly measured (and calculated) energy flows in the ventilation system.

<sup>1)</sup> energy in the inlet air with pre-heating in the solar wall minus without pre-heating.

<sup>2)</sup> energy to the air from the solar wall for both day and night

<sup>3)</sup> losses to the solar wall for both day and night

<sup>4)</sup> energy to the fans from the grid without PV minus with PV

The benefit of the pre-heating in the solar wall was for the whole year 162 kWh, which correspond to 5.7 % of the energy in the exhaust air. This percentage was 3.4 and 8.8 % for 2000 and 2001 respectively. In all (for 2000/2001) 1868 kWh was saved due to the heat exchanger and solar wall corresponding to 65 % of the energy in the exhaust air, while this was 47 % and 90 % for 2000 and 2001 respectively. The very low amount of recovered heat in 2000 is due to the malfunction of the first version of the PV-mixer as shown in figure 3.23-24. The flow rate of exhaust air was here up to three times the flow rate of fresh air leading to a very low efficiency of the heat exchanger (down to 25 %).

The pre-heating (day and night) of the fresh air was for 2000/2001 in the same order of magnitude as the losses from the apartment to the solar wall. Due to the better running of the system in 2001 the fresh air was pre-heated more than was lost to the solar wall. However, the benefit of the pre-heating of the fresh air after the heat exchanger was only 30 % ( $107/360 \cdot 100$ ) of what was lost to the solar wall. Based on this it can be stated that the wall and door

facing the solar wall should have been insulated better – in fact it could also be stated that it would have been better to insulate the installation shaft better rather than installing the solar wall.

The benefit of the PV-panels was for 2000/2001 21 kWh equal to about 9 % of the required energy to the fans. This value was 8 and 12 % for 2000 and 2001 respectively. Due to the improper running of the system 56 % of the potential PV power was not utilized during 2000, while only 18 % was not utilized during 2001. It should be remembered though that the system was not run in summer mode – i.e. only the exhaust fan running – during 2001.

The above results were obtained from the actual measurements on the system. The system was during main part of the measuring period run improperly, so in order to evaluate the system under more ideal conditions a simulation program was created. This is described in the next section.

### **3.4.2. Obtainable savings**

A simulation program has been developed in order to be able to evaluate the intended performance of the systems in Tøndergade 1. The program is based on the findings in section 3.3.

#### ***Simulation program***

The simulation program is based on the Danish Test Reference Year (TRY) (SBI, 1982) and the applied solar processor (for calculation of solar incidence angle, direct and diffuse solar radiation) is the one from (Dutr , 1985).

No thermal model of the building – i.e. calculations of the actual heating demand of the building – has been included. However, in order to exclude periods without heating demand the calculations on the thermal part of the system has been skipped outside the Danish heating season (September 22 – May 8) and when the ambient temperature was above 17°C.

A more favourable location of the building is assumed in the program: the solar wall is south facing and no obstructions cause shading on the solar wall.

#### **Pre-heating**

The flow rates of the system are day and night as defined in the Danish building code: exhaust 126 m<sup>3</sup>/h and fresh air  $126 \cdot 0.9 = 113.4$  m<sup>3</sup>/h.

The inlet temperature of fresh air to the heat exchanger is either the ambient temperature (i.e. no pre-heating before the heat exchanger) or (in the case of pre-heating in a solar wall) calculated based on figures 3.43-45 (page 53-54) as a mean value of the three figures for T4 (+ the ambient temperature) during daytime and figure 3.48 (page 56) during the night.

The efficiency of the heat exchanger for the two cases is found using a regression equation for the values in figure 3.32 (page 45). The efficiency incl. fan power has been used as the fan power transferred to the air thus already will be included.

The inlet temperature of fresh air to the apartment from the heat exchanger is calculated using equation 3.9 (page 61). As it is on page 61 for no pre-heating in a solar wall and with  $T_{amb}$

replaced with the above air temperature ( $T_4$ ) in case of pre-heating in a solar wall.  $T_{\text{exh}}$  (temperature of the exhaust air from the dwelling) is in the simulation program (based on the measurements) set to 22°C.

Based on the above the energy transferred to the fresh air in the heat exchanger and solar wall can be calculated. In this case – opposite the former calculations - the efficiency of the heat exchanger for the two cases: with and without pre-heating in a solar wall will be different as they should.

The energy transferred to the fresh air in the solar wall has been calculated based on the flow rate of fresh air, the ambient temperature and the temperature in the solar wall. The calculations have been divided in day and night in order to be able to see the effect of the pre-heating due to the sun and due to the heat loss from the building to the solar wall. The air temperature in the solar wall has been calculated based on figures 3.43-45 (page 53-54) as a mean value of the three figures for  $T_4$  (+ the ambient temperature) during daytime and figure 3.48 (page 56) during the night.

#### Heat loss from the apartment to the solar wall

The heat loss from the apartment to the solar wall has been calculated as described under the former computer program – i.e. using equation 3.10 (page 62). The air temperature in the solar wall was found in the same way as described in the above paragraph. The temperature of the shaft  $T_{\text{shaft}}$  was (based on the measurements) set to 24°C.

The calculations have as for the pre-heating in the solar wall been divided in day and night in order to be able to compare the losses with the pre-heating for these two periods.

#### Fan power and savings due to the PV-panels

The fan power and savings due to the PV-panels were calculated in the same way as described for the former program – see page 62. The temperature of the PV-panels was found using figures 3.43-45 (page 53-54) where  $T_{\text{pv}}$  was found as a mean value of the three figures for  $T_{\text{pv}}$  (+ the ambient temperature).

#### *Calculated energy flows*

Table 3.3 shows the base case results from the above-described simulation model. The peak power of the PV-panels were as in Tøndergade 1 121 W.

Table 3.3 shows far better results than table 3.2. The ventilation loss is of course higher than for 2000/2001 due to the higher constant flow rate of exhaust air.

The pre-heating in the heat exchanger and solar wall amounts to 84 % of the mechanical ventilation loss, while the benefit of the solar wall is 452 or 11 % of the mechanical ventilation loss. The benefit of the solar wall is now quite good.

The pre-heating in the solar wall is now 43 % higher than the losses from the apartment to the solar wall. However, the beneficial part of the pre-heating in the solar wall (after the heat exchanger) is only 46 % of the losses to the solar wall. This again illustrates that the wall and door facing the solar wall should have been insulated better. Better insulation of these constructions will, however, decrease the pre-heating in the solar wall – i.e. the pre-heating dur-

ing the night is in the same order of magnitude as the pre-heating during the day. Part of the pre-heating during the day is also due to the losses from the building to the solar wall. So better insulated constructions facing the solar wall will considerably decrease the pre-heating of the fresh air in the solar wall. It is judged that the benefit of the solar wall in this case will be reduced from 452 to 100-200 kWh – i.e. to below 5 % of the mechanical ventilation loss.

	year kWh
<b>Heat exchanger</b>	
Energy in the exhaust air	4129
Energy in the inlet air incl. pre-heating in the solar wall	3462
Energy in the inlet air exc. pre-heating in the solar wall	3010
Benefit of pre-heating in the solar wall <sup>1)</sup>	452
<b>Solar wall</b>	
Energy to the air from the solar wall – day	712
Energy to the air from the solar wall – night	688
Total energy to the air from the solar wall <sup>2)</sup>	1400
Losses to the solar wall – day	359
Losses to the solar wall – night	618
Total losses to the solar wall <sup>3)</sup>	977
<b>Fans and PV</b>	
Energy to the fans from the grid - without PV	314
Energy to the fans from the grid - with PV	268
Benefit of PV <sup>4)</sup>	46
PV energy delivered to the PV-mixer	55
Not utilized PV energy	13

Table 3.3. Yearly calculated energy flows in the ventilation system.

<sup>1)</sup> energy in the inlet air with pre-heating in the solar wall minus without pre-heating.

<sup>2)</sup> energy to the air from the solar wall for both day and night

<sup>3)</sup> losses to the solar wall for both day and night

<sup>4)</sup> energy to the fans from the grid without PV minus with PV

The benefit of the PV-panels is 46 kWh equal to 15 % of the required energy to the fans and as only 19 % of the PV power is not utilized this is satisfactory. So the PV-system is thus rather well dimensioned. The reason for the low part not utilized (although the peak power of the PV-panels is more than twice as high as the required fan power) is of course that the radiation level at vertical south seldom is 1000 W/m<sup>2</sup> and the temperature of the PV-panels seldom is 25°C or below.

### ***Parameter variations***

The above simulation model is rather general, which means that it is possible to perform parameter variations for some of the main parameters of the system. Parameter variations are in

the following carried out for the efficiency of the heat exchanger and the peak power of the PV-panels.

### Efficiency of the heat exchanger

The efficiency of the heat exchanger is in the following fixed values – i.e. not dependent on the inlet temperature of fresh air as this makes it much easier to display the results graphically without losing too much of the realism. The simulations are carried out in order to evaluate the influence of the efficiency of the heat exchanger on the utilized fraction of the pre-heating in the solar wall. Figure 3.53 shows the results from the simulations.

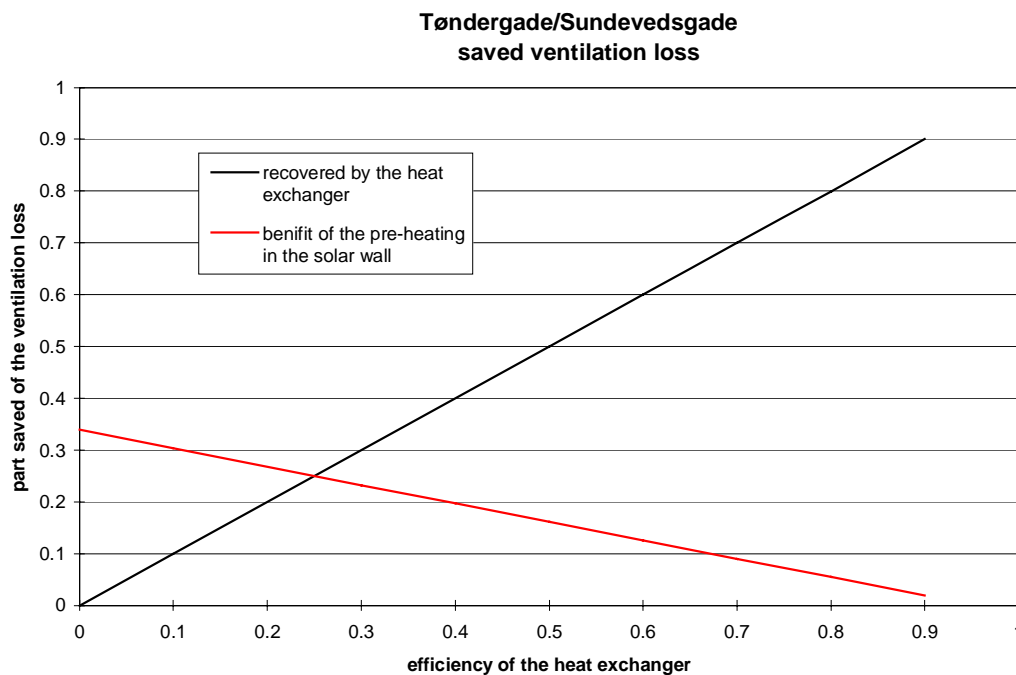


Figure 3.53. The recovered fraction of the mechanical ventilation loss and the utilized fraction of the pre-heating in the solar wall dependent on the efficiency of the heat exchanger.

Figure 3.53 shows as expected a decreasing utilization of the pre-heating in the solar wall with increasing efficiency of the heat exchanger. Due to the rather simple model without a building part, the utilized part of the pre-heating in the solar wall is at low exchanger efficiencies a bit too high, as it here compete with the direct solar gains through the windows. On the other hand - the utilized part of the pre-heating in the solar wall is a bit too low at high exchanger efficiencies as the solar energy also may cover a part of the transmission loss of the apartment.

The utilization of the pre-heating of the fresh air in the solar wall is low at high heat exchanger efficiencies and should in such cases carefully be evaluated before chosen.

## Utilized and not utilized PV power

Figure 3.54 shows the results from simulations where the peak power of the PV-panels has been varied. The necessary fan power during the heating season is in the simulations 45 W – as were the case in the former simulations.

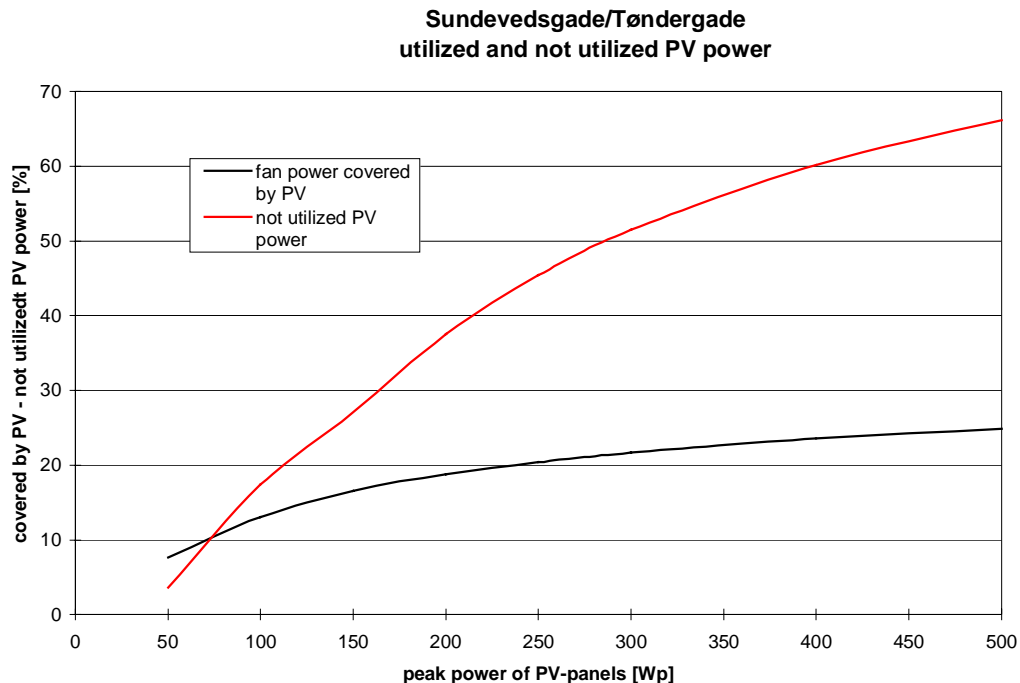


Figure 3.54. Utilized and not utilized PV power dependent on the peak power of the PV-panels.

Figure 3.54 may be used for other fan powers if the x-axis is replaced with the peak power divided with 45 (fan power in figure 3.54) as done in figure 3.55. However, the efficiency of the PV-mixer is dependent on the fan power as shown in figure 3.51 and equation 3.7. So the found values in figure 3.55 should be multiplied with the following factor:

$$f = \eta / 75.75 \quad (3.11)$$

where  $\eta$  is the efficiency of the PV-mixer at the actual fan power found in figure 3.51  
75.75 is the efficiency at a fan power of 45 W as used in figures 3.53-54

Figures 3.54-55 show that a considerable area of PV-panels is necessary to cover e.g. 25 % of the necessary fan power. The problem is, however, that the not utilized PV power increases more rapidly than the utilized part of the PV power. So if the aim is to cover a large fraction of the necessary energy to the fans it would be wise to apply an inverter rather than a PV-mixer.

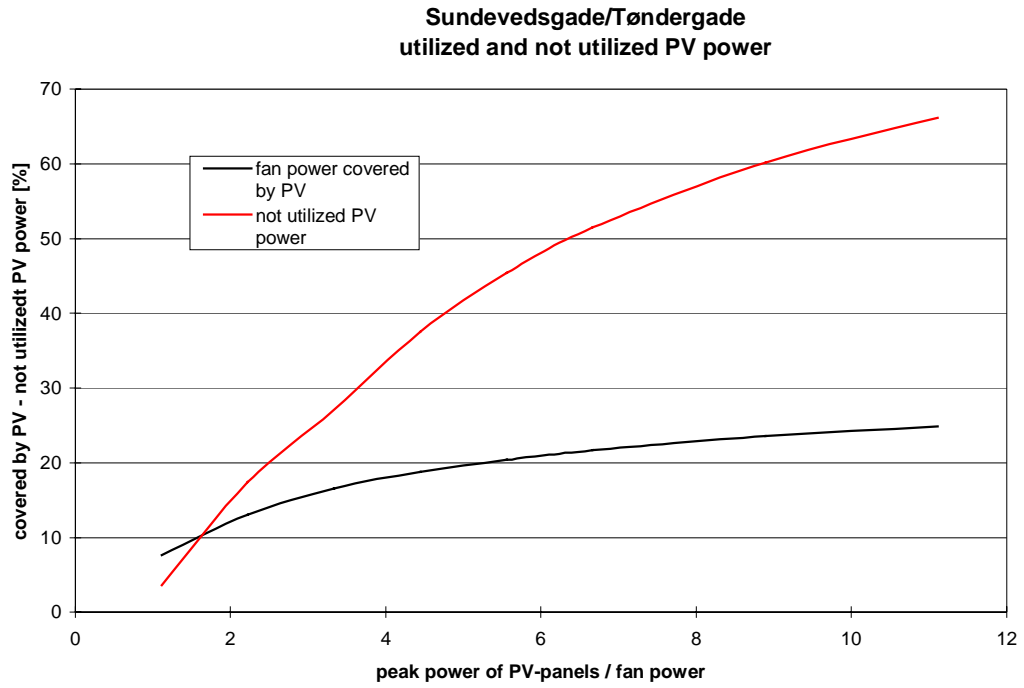


Figure 3.55. Utilized and not utilized PV power dependent on the ration between the peak power of the PV-panels and the actual fan power.

## **4. Conclusions**

The following conclusions are common for both measuring projects under PV-VENT: Lundebjerg (Jensen, 2001) and Sundevedsgade/Tøndergade.

### **4.1. Aims of the PV-VENT project**

The aims of the projects was research, development and tests in the following areas:

- develop and illustrate different ways of architectural integration of solar energy systems with combined PV power production and pre-heating of ventilation air in buildings
- investigate the potential in pre-heating fresh air to the building by cooling the PV-panels with the fresh air and further to determine how much this cooling will increase the electrical performance of the PV-panels
- develop and test air to air heat exchangers with an efficiency of 80 % or above
- develop and test fans and ventilation systems with an overall fan power demand of about 35 W
- develop and test a direct coupling of the PV-panels to the fans in order to avoid the losses in an inverter
- develop and test different ventilation systems utilizing the above-mentioned features

### **4.2. Results from the PV-VENT project**

#### **4.2.1. Architectural results**

Different ways of integrating PV-VENT systems in the building envelope has been developed and tested:

##### ***Lundebjerg***

Three different ways of integrating PV-panels with pre-heating of fresh air to the building have been demonstrated in Lundebjerg: a large PV-gable with amorphous PV-panels, a PV-facade with polycrystalline (c-Si) PV-panels and solar ventilation chimneys with polycrystalline (c-Si) PV-panels. Especially the latter feature – the solar ventilation chimney is a new and interesting concept as it allows for increased PV areas although the orientation of the building is not optimal for utilization of solar energy - as was the case in Lundebjerg.

However, the Lundebjerg project is not only interesting due to the demonstrated methods for architectural integration of PV systems in buildings. As a part of the project an architectural competition on the renovation of the building including PV-VENT systems was held in 1998 with five well known Danish architect firms. The result of the competition is seen at Lundebjerg today, but many other ways of introducing PV-VENT systems was proposed in the



not winning contributions – way of introducing PV-VENT systems that may be utilized by others in future projects.

### ***Sundevedsgade/Tøndergade***

In this building only one way of integrating PV-VENT systems is tested. The integration technique is, however, very interesting as the PV-panels are integrated in a solar wall also containing the heat exchangers. The solar wall is further integrated with a new sun space for each dwelling.

### ***General conclusions on architecture***

Several new and interesting ways of solving building integration of PV-VENT systems have been developed. Several of these have further been demonstrated in the project. It is believed that the results from the project will influence future projects in this field.

#### **4.2.2. Pre-heating of fresh air – cooling of PV-panels**

The aim of pre-heating fresh air by cooling the PV-panels is twofold: reduce the ventilation losses of the building while increasing the performance of the PV-panels.

The actual benefit of the pre-heating of the fresh air to the buildings has been low. The reasons for this are several:

- The absorber of the “solar air collectors” is the PV-panels. There is no cover in front of the absorbers as cooling of the PV-panels with ambient air is desirable in order to keep the cell temperature down and thereby the efficiency of the PV-panels up. This decreases the efficiency of the system as solar air collector – the efficiency is less than half of the efficiency of a good traditional solar air collector
- The very high efficiency of the heat exchangers in the system – see later – decreases the utilizable part of the pre-heating in the solar wall, PV-facade and solar ventilation chimneys. The projects showed that only about one third of the pre-heating by the sun actually was utilized
- It was decided that the PV-panels should be cooled on the backside by natural ventilation during the summer – in order to save fan power. This means that the air gap behind the PV-panels has to be rather wide in order to decrease the pressure loss across the PV “solar air collectors”. The air speed in forced air flow mode will then be low leading to a low heat transfer coefficient between the backside of the PV-panels and the air. This again results in a low efficiency of the solar air collectors

The solar wall at Sundevedsgade/Tøndergade showed a higher benefit of the pre-heating in the solar wall than shown at Lundebjerg. The reason for this is the high heat loss from the building to the solar wall rather than utilization of solar radiation.

The measured temperature of the PV-panels was often rather high – 50°C – due to the low air speeds behind the PV-panels. The benefit of the cooling of the PV-panels was therefore low.

Due to the low benefit of the pre-heating by the sun this feature should carefully be evaluated before chosen in future projects.

#### **4.2.3. Air to air heat exchangers**

Based on the measurements in the two projects the normalized efficiency of the air to air heat exchangers has been found. The normalized efficiency is when the two air flow rates are identical – this is the normal way to state the efficiency of air to air heat exchangers. The normalized efficiency was found to lay around 80 %. The actual efficiency was shown to be both much below or much above 80 % due to too large differences between the two air flows and due to condensation in the heat exchangers.

The aim of the project regarding efficient heat exchangers was thus fulfilled.

#### **4.2.4. Low fan power**

The necessary fan power in the balanced ventilation systems with heat recovery was shown to be 38 W per dwelling for Lundebjerg and 52 W per dwelling for Sundevedsgade/Tøndergade. The higher fan power at Sundevedsgade/Tøndergade is caused by the higher pressure loss in the heat exchanger arrangement. The high pressure loss of the heat exchangers at Sundevedsgade/Tøndergade is due to the many bendings in the duct works necessary due to the location in the solar wall.

38 W is very close to the aim of 35 W. If further the contribution from the PV-panels is subtracted (10-15 % of the necessary fan energy) the average necessary fan power is 32-34 W.

#### **4.2.5. Direct coupling of PV-panels to fans**

Electricity from PV-panels cannot be the only supply to the fans as the fans run day and night and because hardly any solar radiation is available during large part of the winter meaning that a battery bank and the area of PV-panels should be large.

Instead it was decided to develop a so-called PV-mixer, which is in charge of utilizing as much as possible of the available PV power while topping up with power from the grid when the PV power is too low or not present.

The measurements show that the developed PV-mixer works as intended. The efficiency in grid mode is 96 % but below 90 % is pure PV mode. The latter efficiency can maybe be increased by further development of the concept.

The main problem with the concept of coupling of the PV-panels to the fans via a PV-mixer rather than an inverter is that excess power from the PV-panels is not utilized – i.e. if the PV-panels are able to supply more power than the demand of the fans this excess power is lost. For this reason one should not aim at covering more than 15 % of the energy to the fans by PV via a PV-mixer. Below 15 % the waste of PV energy will stay below 20 %. If the wish is to cover a larger fraction of the energy to the fans by PV it may be wiser to apply an inverter rather than a PV-mixer.

#### **4.2.6. Total systems**

Several total ventilation system utilizing the above described features and techniques has been developed and tested in the project – both individual and common ventilation systems.

The individual systems were all equipped with a control panel in the dwellings. The tenants are thus able to change the way the systems run. The tenants are happy that they themselves can decide how the systems should run. But there is a high risk that the systems are run improperly – i.e. at too low air flow rates because e.g. the noise from the fans (although very silent) annoys the tenants.

The tenants are not allowed to control the common ventilation systems – one ventilation system per three dwelling. This has, however, not lead to a more proper running of these systems than the individual systems. Due to the low pressure drops in the systems and the thereby low speed of the fans, the systems has been very difficult to balance. There has for that reason been several complaints. This illustrates that special care should be taken when dimensioning this type of systems with low pressure losses – especially the fans should fit the actual demands.

The testing of the complete systems rather than components has revealed much valuable information on the influence of one component on the other components of the systems which in the future may lead to better systems.

#### **4.2.7. General conclusions**

It is believed that the PV-VENT project has added important information and experience to the field of combining PV and ventilation systems. Information and experience that future systems of this type may benefit from. Several of the components from the project are believed to be able to contribute to set the standards for future PV and ventilation systems. Several of the components from the project is today commercial available and are used in ordinary building projects.

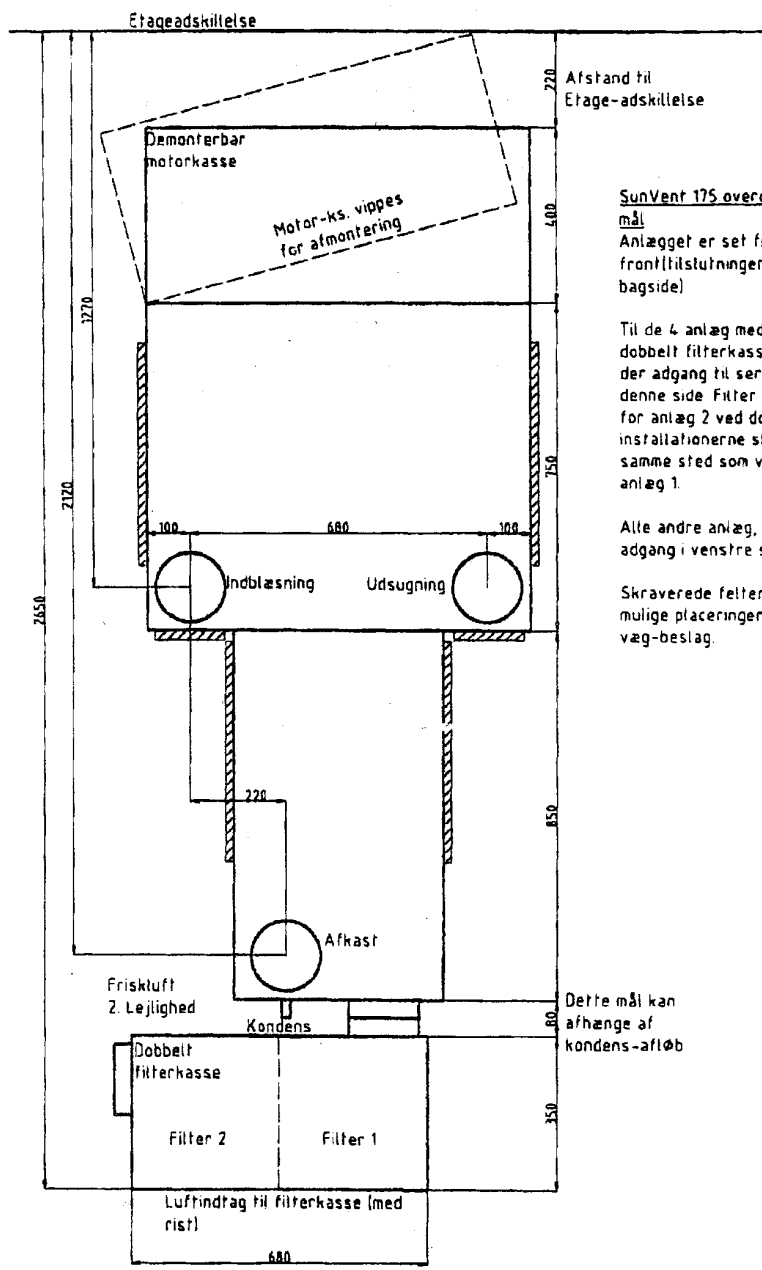
## 5. References

- Duffie, J.A. and Beckman, W.A., 1991. *Solar Engineering of Thermal Processes*. John Wiley & Sons, New York. ISBN 0-47-51056-4.
- Dutr e W.L., 1985. *A Thermal Transient Simulation Model for Thermal Solar Systems – EMGP2*. Solar Energy R&D in the European Community, series A, volume 5. D. Reidel Publishing Company. ISBN 90-277-2051-7.
- Cenergia, 1999. Technical report on renovation project in Sundevedsgade 14, T ndergade 1, Copenhagen. Cenergia Energy Consultants.
- Hansen, H.E., Kjerulf, P. and Stampe, O.B. (ed), 1997. *Heating and climate technology (in Danish)*. Danvak Aps. ISBN 87-982652-8-8.
- Jensen and Pedersen, 1999. PV-VENT, Technical Progress Report, first two years – Temovex Denmark.
- Jensen, 2000. Measuring report – PV-mixer (in Danish). Solar Energy Centre Denmark, Danish Technological Institute. August 2000.
- Jensen, 2001. Results from measurements on the PV-VENT systems at Lundebjerg. Solar Energy Centre Denmark, Danish Technological Institute. SEC-R-14. ISBN 87-7756-611-0.
- Lepp nen, 1999. PV-VENT, Technical Progress Report, first two years – Neste/NAPS.
- Lepp nen, 2000. *Solar panels Maintenance and Operation Guide*. Sundevedsgade/Tondergade, Copenhagen, Denmark. Fortum.
- Lien, A.G. and Hestness, A.G., 1999. *Architectural Integration of PV for ventilation in three buildings in Denmark – PV-VENT, Low cost energy efficient PV-Ventilation in retrofit housing*. Department of Building Technology, Norwegian University of Science and Technology.
- Mehr, 2000, Evaluation report – PV-mixer. (in Danish). Solar Energy Centre Denmark, Danish Technological Institute. January 2000.
- Nielsen, J.E., 1995. Documentation of KVIKSOL – a program for simulation of solar heating systems (in Danish). Version 5.0. Solar Energy Laboratory, Danish Technological Institute Energy.
- Olsen, H., 1998. Measuring report for heat exchangers from Temovex (in Danish). Danish Technological Institute.
- SBI, 1982. *Weather Data for HVAC and Energy – Danish Test Reference Year*. Danish Building Research Establishment. SBI Report no. 135.

# **Appendix A**

## **Drawings of the heat exchanger with fans**

(unfortunately only available in Danish)



Afstand til Etage-adskillelse

SunVent 175 overordnede mål  
 Anlægget er set fra fronttilslutninger på bagside!

Til de 4 anlæg med dobbelt filterkasse er der adgang til service fra denne side. Filter skift for anlæg 2 ved dobbelt installationerne sker samme sted som ved anlæg 1.

Alle andre anlæg, har adgang i venstre side.

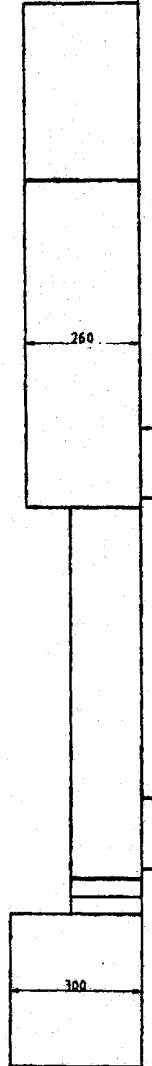
Skraverede felt er mulige placeringer af væg-beslag.

Friskluft 2. Lejlighed  
 Dette mål kan afhænge af kondens-afløb

1	Sunvent175	1	
Silh.	Genstand	Pos	Materiale
Temovæk Danmark Rudolfsgaardsvej 1b DK-2860 Viby J.		Tit: 70231077 Fax: 70232180	
Sunvent 175		A4	Konstr. smp
Mål skitse		Tegn. Nr.	18/12-98
		SUV175-4-60A	

Etageadskillelse

Ydermur på bygning

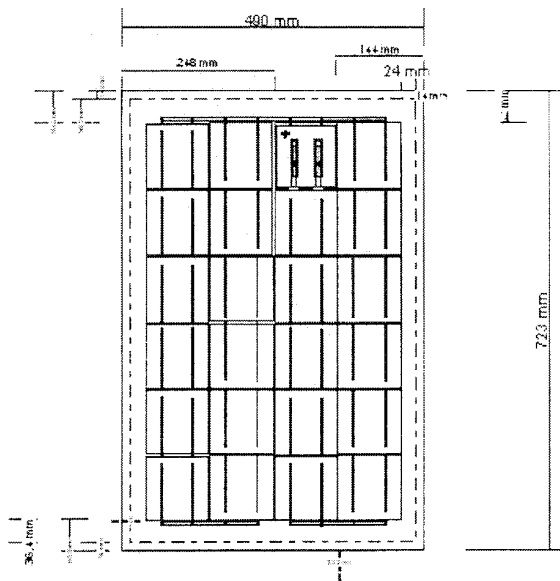


1	Sunvent175	1	Materialle	
Sik:	Gensland	Pos	Kensfr.	
TennVer Danmark		1:15	snp	
Rudolfsgaardsvej 7b		Tegn.		
DK-2860 Viby J.		A4		
Tlf: 70231077		Gaok.		
Fax: 70232180		Tegn. Nr.		
Sunvent 175		SUV75-4-61A		
Mål skitse fra siden				
			10/12-98	


# **Appendix B**

## **Data sheets for the PV-panels**






Viewed from outside



Module Type	FP33/6x4RC
Max Power (+/- 10%)	33 Watts
Typical Imp	3 Amps
Typical Vmp	11.1 Volts
Typical Isc	3.3 Amps
Typical Voc	14 Volts

Specification based on 1 kW/sq m solar irradiance  
25 deg C cell temperature, Air Mass 1.5




Maximum System Voltage 600V dc  
Potential electrical hazard,  
when exposed to sunlight

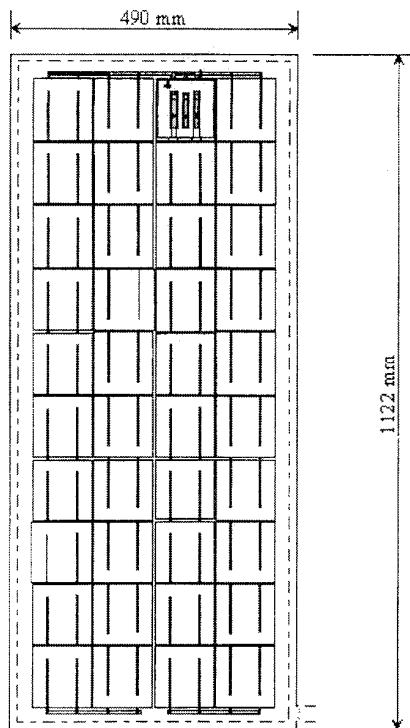
Manufactured in Finland

Serial No


Panel electrical specification label

16 modules of this type

		Description				Title	 <b>Fortum</b> <small>Advanced Energy Systems</small>
Rev.	Jan 00					Sundevedsgade & Tondergade Panel A1	Solar panels, Design




Viewed from outside



Module Type	FP55/10x4RC
Max Power (+/- 10%)	55 Watts
Typical Imp	3 Amos
Typical Vmp	18 Volt
Typical Isc	3.3 Amp
Typical Voc	24 Volt

Specification based on 1 kW/sq m solar irradiance  
25 deg C cell temperature, Air Mass 1.5




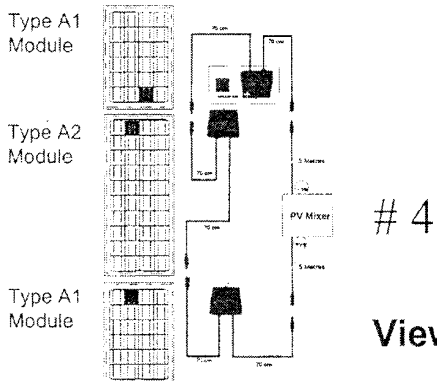
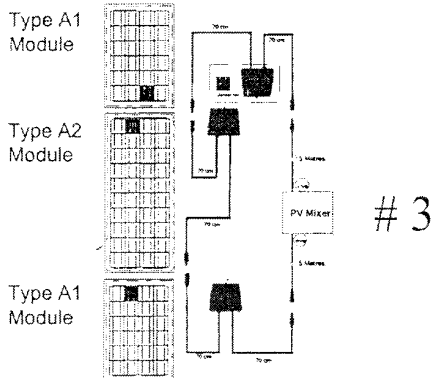
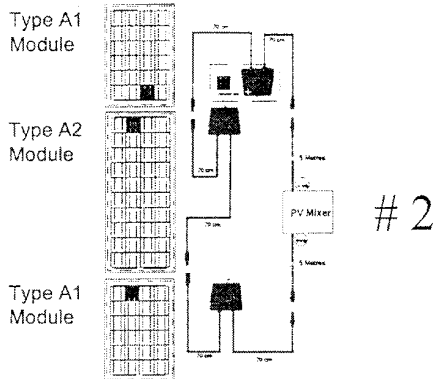
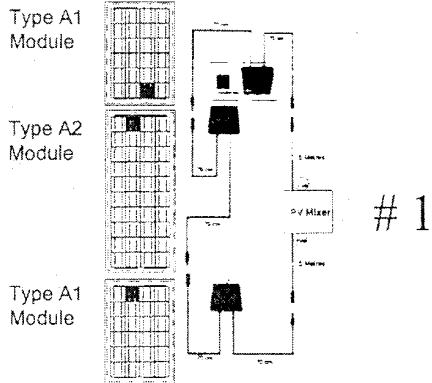
Maximum System Voltage 600V dc  
Potential electrical hazard,  
when exposed to sunlight

Manufactured in Finland


Serial No

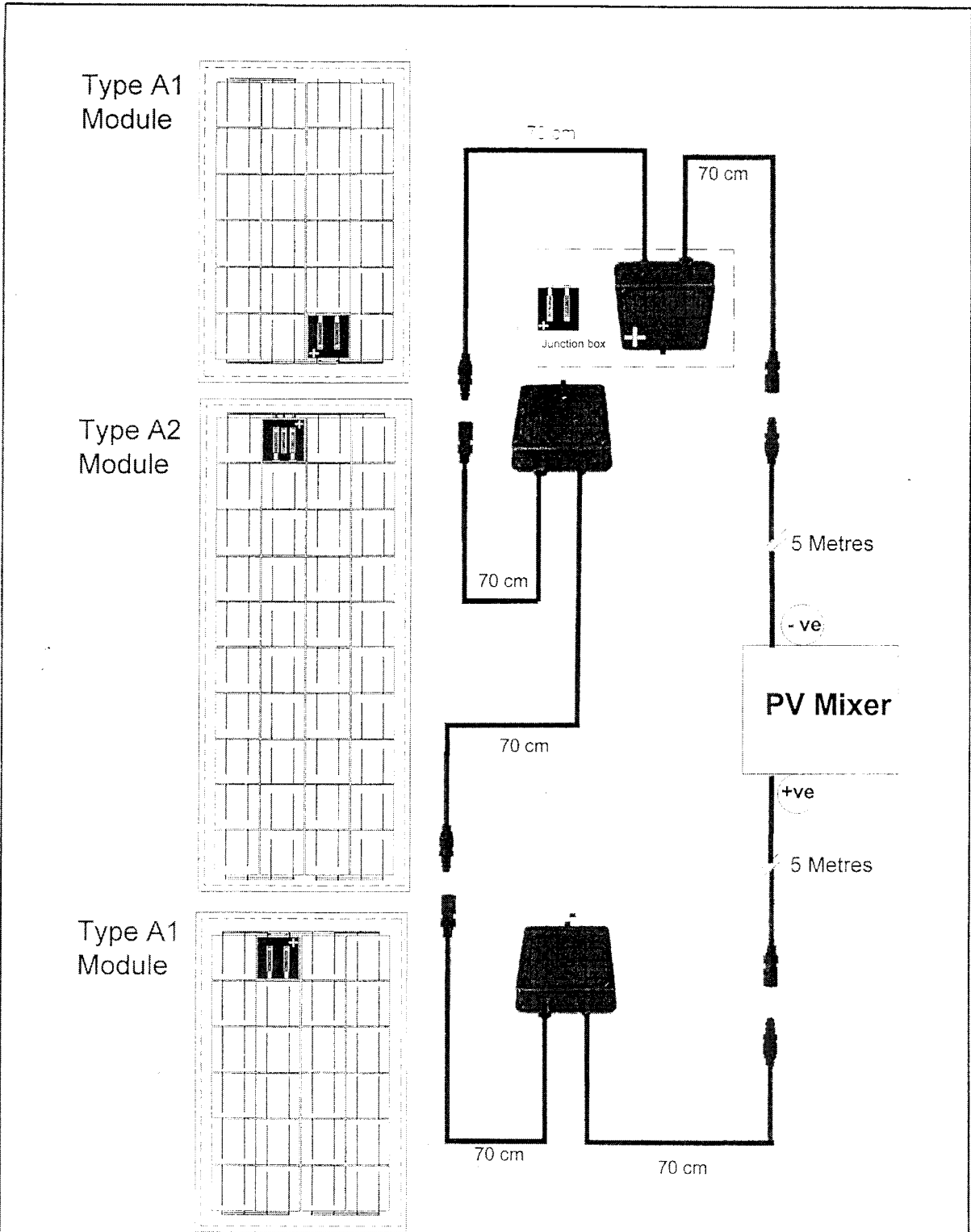
Panel electrical specification label  
8 modules of this type

		Description			Title	 <b>Fortum</b> Advanced Energy Systems Solar panels, Design
Rev.	Jan 00				Sundevedsgade & Tondergade Panel A2	




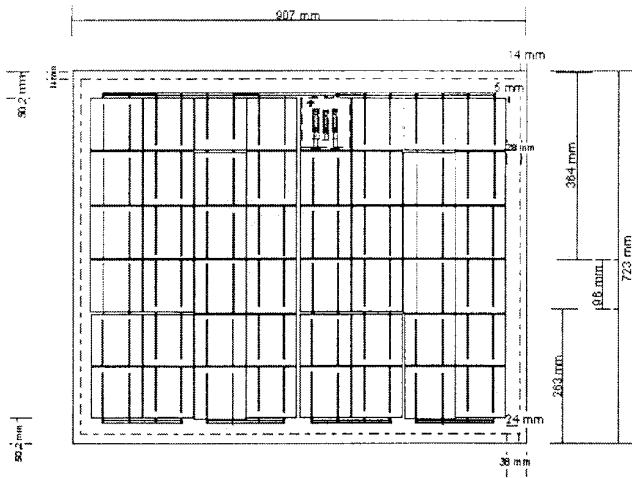
Viewed from back of the Solar panels

Rev.	Aug 99	Description	Title	 <b>Fortum</b> Advanced Energy Systems
			Sundevedsgade & Tondergade Panels A1&A2	
				Solar panels, connection




Viewed from back of the Solar panels

	Description	Title	 <b>Fortum</b> Advanced Energy Systems
Rev.	Aug 99	Sundevedsgade & Tondergade Panels A1&A2	
			Solar panels, connection




Viewed from outside



Module Type	FP6676x8RC
Max Power (+/- 10%)	66 Watts
Typical I <sub>mp</sub>	3 Amos
Typical V <sub>mp</sub>	22 Volts
Typical I <sub>sc</sub>	3.3 Amp
Typical V <sub>oc</sub>	7.8 Volts

Specification based on 1 kW/sq m solar irradiance  
25 deg C cell temperature, Air Mass 1.5




Maximum System Voltage 600V dc  
Potential electrical hazard,  
when exposed to sunlight

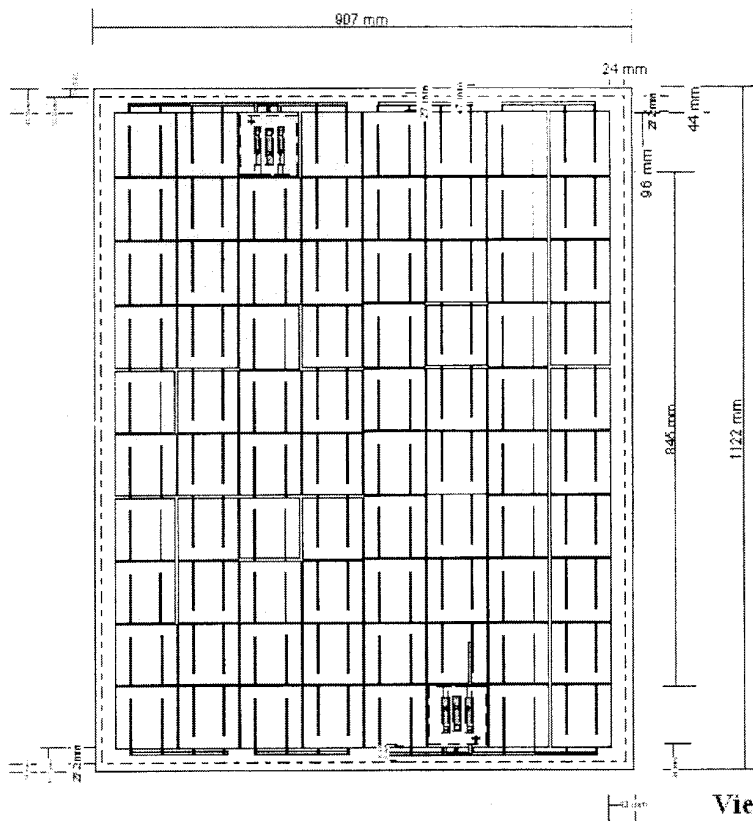
Manufactured in Finland

Serial No


Panel electrical specification label

**8 modules of this type**

		Description			Title
Rev.	Jan 00				Sundevedsgade & Tondergade Panel B1
					 Solar panels, design




Viewed from backside

 **Fortum**

Module Type	FP110/10x8RCD
Max Power (+/- 10%)	110 Watt
Typical Imp	3 Amps
Typical Vmp	37 Volt
Typical Isc	3.3 Amp
Typical Voc	48 Volt

Specification based on 1 kW/sq m solar irradiance  
25 deg C cell temperature, Air Mass 1.5

 Maximum System Voltage 600V dc  
Potential electrical hazard,  
when exposed to sunlight


Manufactured in Finland

Serial No

Panel electrical specification label

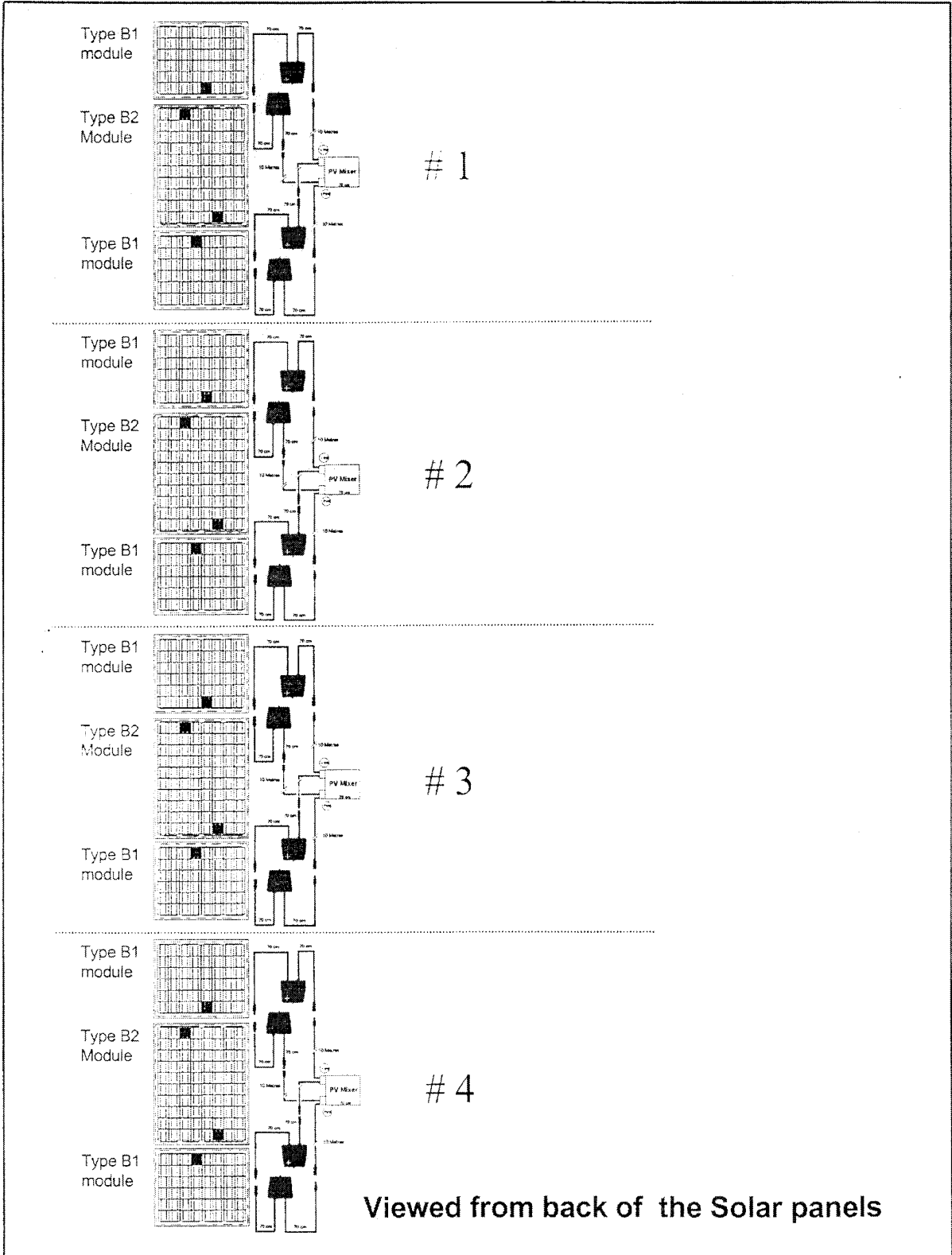
**4 modules of this type**

Rev.	Description	Title
Jan 00		Sundevedsgade & Tondergade Panel B2




**Fortum**  
Advanced Energy Systems

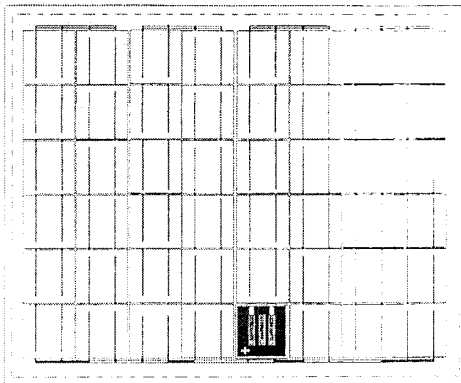
Solar panels, design



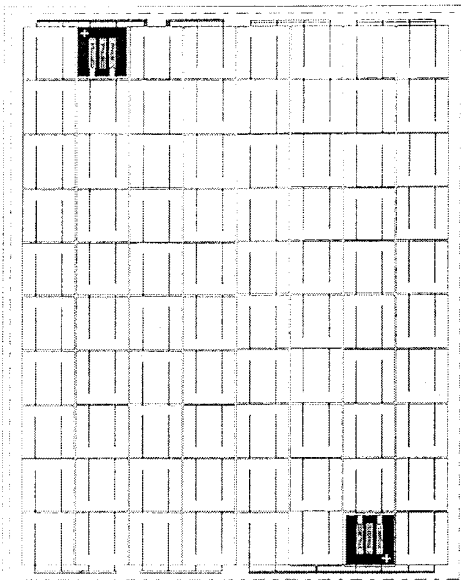
Viewed from back of the Solar panels

Description		Title Sundevedsgade & Tondergade Panels B1&B2	 <b>Fortum</b> Advanced Energy Systems
Rev.	Aug 99		

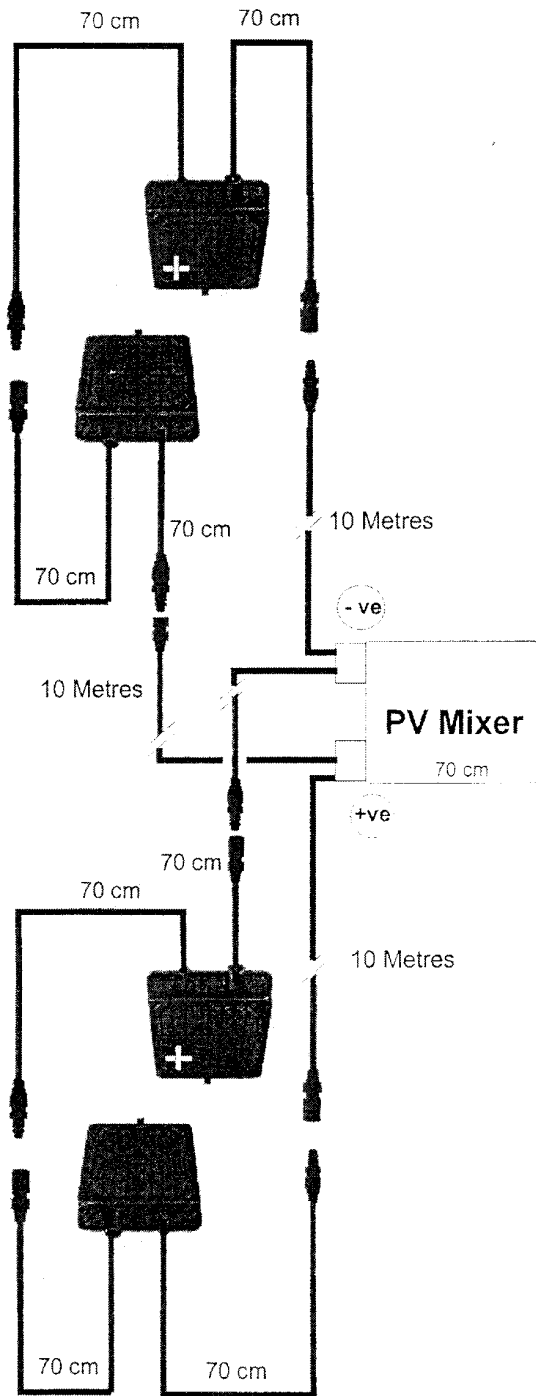
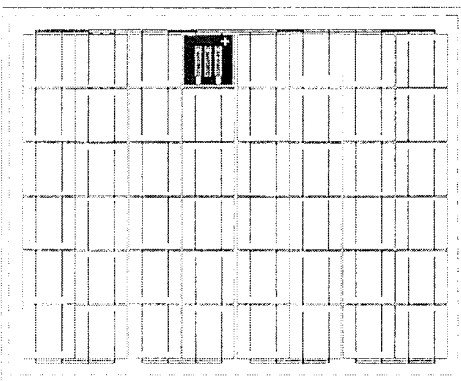
Type B1  
module




Type B2  
Module



Type B1  
module



Viewed from back of the Solar panels

	Description	Title	 <b>Fortum</b> Advanced Energy Systems
Rev.	Aug 99	Sundevedsgade & Tondergade Panels B1&B2	